博士學位 論文

# MOS 방법을 적용한 풍력터빈 발전량 예측 정확도 개선에 관한 연구

濟州大學校 大學院

機械工學科

朴 潤 鎬

2013年 6月

# MOS 방법을 적용한 풍력터빈 발전량 예측 정확도 개선에 관한 연구

指導敎授 許 鐘 哲

朴 潤 鎬

이 論文을 工學 博士學位 論文으로 提出함

2013年 6月

朴潤鎬의 工學 博士學位 論文을 認准함

審査委員長 _____

委　　員 _____

委　　員 _____

委　　員 _____

委　　員 _____

濟州大學校 大學院

2013年　6月

# A Study to Improve the Accuracy of Wind Power Forecasting for Wind Turbines by the Application of the MOS

Yunho Park
(Supervised by professor Jong-Chul Huh)

A thesis submitted in partial fulfillment of the requirement
for the degree of Doctor of Engineering

2013. 6.

This thesis has been examined and approved.

.....
Thesis director, Kyung-Nam Ko, Prof. of Multidisciplinary Graduate School Program for Wind Energy

.....
Thesis director, Il-Ju Moon, Prof. of Marine Industry and Maritime Police

.....
Thesis director, Dong-Ho Kim, Prof. of S.B Academy

.....
Thesis director, Gyoung-Bo Kim, Project Manager of Jeju Leading Industry Office

.....
Thesis director, Jong-Chul Huh, Prof. of Mechanical Engineering

.....
Date

Department of Mechanical Engineering
GRADUATE SCHOOL
CHEJU NATIONAL UNIVERSITY

# Contents

Contents of Figures

# Contents of Tables

# 요 약

본 연구는 기상 수치모델(Weather Research and Forecasting Model, WRF)로부터 생산된 수치모델 출력자료를 이용하여 제주특별자치도 성산 풍력 발전단지에 위치한 6번 풍력발전기에 대한 단기 풍속 예측 및 풍력 발전량 예측 개선에 관한 연구이다. 일반적으로 수치모델의 경우 모델의 특성이 반영된 체계적 오차를 가지고 있다. 본 연구에서는 모델 출력자료 통계(Model Output Statistics, MOS) 방법을 통해 모델의 체계적 오차가 제거된 예측자료를 생산하였다. MOS 방법을 통해 예측 자료를 생산하기 위해서는 최소 2년 이상의 수치모델 출력자료가 요구된다. 본 연구에서는 약 3년간의 모델 출력자료가 확보됨에 따라 2009년 7월부터 2011년 6월 까지의 2년간의 수치모델 출력자료와 2010년 7월부터 2011년 6월까지의 1년간의 모델 출력자료를 사용한 MOS 예보식을 통해 예측자료를 각각 생산하였다. MOS 예보식은 계절별로 특성이 달리 나타나기 때문에 전체 표본을 대상으로 하나의 예보식을 생산할 경우 예보식의 적합도가 낮아져 예보식의 성능이 떨어지게 됨에 따라 계절별(봄, 여름, 가을, 겨울)로 생산하였다. 이러한 계절별 풍속 특성을 살펴보기 위해 성산 풍력 발전단지에 인근한 기상대 관측 자료를 바탕으로 풍력발전기 허브높이 부근에서의 바람자원에 대한 평가를 수행하였다. WRF 모델에서 생산한 예측자료와 MOS 예보식을 통해 생산된 예측자료 간의 비교 검증은 풍력발전기 상단에서 관측된 풍속과 을 통해 수행하였다.

1년간의 모델 출력자료만을 사용한 실험에서는 2년간의 자료를 사용한 실험에 비해 BIAS가 크게 증가하는 특징을 보임에 따라 보다 장기간의 수치모델 출력자료가 사용된 실험을 통해 생산된 MOS 예보식이 보다 안정적임을 알 수 있었다. 2년간의 자료를 사용한 24시간 예측 실험의 결과를 살펴보면, WRF 모델에서 06UTC에 예측한 풍속으로부터 산출된 풍력 발전량은 관측된 풍속으로부터 산출된 풍력 발전량에 비해 봄, 여름, 가을 및 겨울철 예측에서 각각 7.8%, 40.4%, 53.9%의 과대 모의 및 -5.3%의 풍력발전량의 과소모의가 나타났으며, MOS 예보식을 통해 예측된 풍속으로 산출된 풍력에너지는 같은 기간의 예측에서 각각

-12.8%, -16.7%의 풍력에너지 과소모의, 32.6% 및 7.4%의 풍력에너지 과대모의가 나타났다. WRF 모델에서 18UTC에 예측한 풍속으로부터 산출된 풍력 발전량은  봄, 여름, 가을 및 겨울철 예측에서 각각 24.9%, 21.3%, 44.8% 및 59.4%의 풍력발전량의 과소모의가 나타났으며, MOS에서 예측된 풍속으로 산출된 풍력에너지는 같은 기간의 예측에서 각각 4.3%, 12.9%, 19.4%, 30.6%의 풍력에너지 과대모의가 나타났다. MOS 방법 적용을 통해 모델의 체계적 오차를 제거한 경우에도 30%(06UTC, 가을) 이상의 차이가 발생함에 따라 수치모델의 다양한 예측변수들을 적용하여 최적의 예보인자를 선택할 수 있는 단계별 선택법을 통해 선형회귀식을 산출하여 풍속 MOS 예보식을 보다 개선할 필요가 있다.

# Summary

This study is about the improvement of wind speed and wind power forecasting using weather numerical model(Weather Research and Forecasting Model, WRF) and its output data at the Sungsan wind farm in the Cheju Special Autonomous Region. Usually, numerical model has its own systemic error. In this study, I used model output statistics(MOS) method to remove the systemic error and re-calculate forecasting data through MOS method. At least two years numerical output data is needed when we apply the MOS method. In this study, I generate MOS forecasting equation using two years(July 2009 to June 2011) numerical model output data and one year data(July 2010 to June 2011) respectively, through three years archived numerical output data. In this study the seasonal MOS forecast equation(Spring, Summer, Fall and Winter) was developed, because MOS forecast equation has seasonal characteristics, so there are low efficiency when apply total population on one forecast equation. I analysis the wind resource near Sungsan wind farm with AWS observation data to analysis the seasonal wind characteristic on wind turbine hub height. Observed wind speed which was measured at wind turbine hub height was used for verification of forecasting data by WRF and MOS.

Test of one year data set using, it show the typical increasing of BIAS compare with two years data set using. It shows that MOS forecast equation is more stable when we using more numerical model output data. The result 24h forecast result using two years numerical model output data, in case of 06UTC by WRF model were over estimated during spring(7.8%), summer(40.4%) and fall(53.9%) and under estimated during winter(-5.3%) compare to wind power energy computed in the observed wind speed. And as

wind power energy by MOS were underestimated during spring(-12.8%), summer(-16.7%) and overestimated of fall(32.6%) and winter(7.4%). In case of 18UTC by WRF model wind power energy forecast were over estimated during spring(24.9%), summer(21.3%), fall(44.8%) and winter(59.4%). And as wind power energy by MOS was overestimated during spring(4.3%), summer(12.9%), fall(19.4%) and winter(30.6%). Even though apply the MOS forecast equation, over than 30%(06UTC, fall) of wind power energy difference was appear. So we are planning to improve wind speed using MOS by computing linear regression through step selection method that can select optimal predictor by applying various forecast variables of numerical model output.

# Ⅰ. Introduction

## 1.1. Background

Wind power plays an important role in the supply of electricity that is free from pollution and sustainable, and shows considerable growth for the past few years, lately electricity generated by wind power stations has become a part of various energy produced nationally [1].

If we look at the case of Germany what is leading country of generation of electricity by wind power in the world, accommodating capacity of wind power installed in Germany increased for 4.4GW in 1999 to 12.8GW in 2003. Particularly, it accounts for 4.7% of entire electricity consumption. In 2007, electricity generated by wind power accounts for 7.2% of entire power generation of Germany. As of now, total capacity of wind power generation is 22.2GW. According to German Wind Energy Association (GWE), the capacity for wind power generation is forecast to double by 2020, 45.0GW (land) and 10GW (ocean) [2].

Based of the potential for supplying electricity energy on industrial scale, EWEA and Greenpeace predict that electricity generated by wind power will account 12% of global electricity generation. In the case of Korea, it sets the target that renewable energy account for 11% by 2030 as the portion of renewable energy in the entire power production gradually increases. According to such plan, bio, wind power, solar power is forecast to account for 48% of the entire renewable energy production and of this figure, investment in wind power facilities will increase more than five times from

57.5 billion won to 307.3 billion won in 2010 [3]. Especially the Island of Cheju autonomous region is planning to increase the capacity of wind power generation from both ground and sea to 500MW by 2020 [4-6]. However, the integration and conversion of wind power energy to current electricity supply system have a few problems to be solved. Particularly, electricity suppliers and grid operators express the difficulty of stable use of wind power in terms of technology and economy as the use of wind power electricity depends on meteorological condition, which is shortcoming of wind power energy. Hence, as electricity generation from wind power energy station is determined by the speed of constant wind speed, wind power energy cannot be as conveniently used as the energy produced in the conventional power plants. As it costs considerably more for the stable and constant production of intangible fluid energy such as wind power energy, the grid operators and energy suppliers point out increase of cost due to wind power energy. As mentioned earlier, unlike conventional power plant, the generation of electricity by wind power stations entirely depends on meteorological conditions. Especially, power generation depends on the level of wind speed that cannot be altered through artificial intervention. Although such is treated as an insignificant problem, it can affect substantially on the energy development in terms of technological and economic perspectives. In order to determine the price of energy and establish the supply schedule, it is necessary to forecast production and consumption of electricity at least two days in advance. Thus, in order to stably use wind power energy, forecasted information of wind power that can be trusted and rely on in the energy market must be provided.

Economic and industrial value of wind power energy will substantially increase, if we can accurately make wind forecasting. It is the wind power forecast system that can forecast fluidity of wind speed in advance. The wind

power forecast system is designed to provide reliable forecast of power generation by each power station and subsequently will supply wind power energy stably. Generally, price in the electricity market is determined one or two days in advance. Accordingly, the wind power forecast system must be able to provide the forecast information at least before 6 hours to 48 hours. The time scale required is very crucial. The reason behind such importance is the fundamental differences existed between so-called short-term forecast for a few days and ultra short-term forecast for 0 - 3 hours time span. While for longer hours, wind speed forecast using atmosphere dynamic model can forecast, for shorter hours, better forecast outcome can be produced through purely statistical approach as wind speed in determined by archetypal meteorological conditions [1],[3].

Currently, Numerical Weather Prediction (NWP) system is mostly used in the forecast of wind speed for wind power generation [7-8]. As NWP system estimates the actual conditions of atmosphere using laws of physics based on observation data, numerical prediction within wanted time span is feasible. However, since this kind of prediction goes through various premises and parameterization, it includes errors of the model itself and the systematic errors. Therefore, the task of wind power prediction system is to convert somewhat precise raw information obtained by using NWP system to more accurate prediction values. There are basically two approach methods for the production of more accurate wind power prediction data. The first method is the production of high resolution by improving horizontal and vertical resolution through the improvement of NWP system itself. The other is the improvement of physical process and dynamic process of the model. Through this method, more accurate wind speed at the height of wind turbine can be calculated by using wind profiles within boundary layers or using parameters re forecast. However, for the improvement of the model, considerable amount

of computation time for the production of high resolution data and high capacity super computers are required and longer term research for the improvement of physical process and dynamic process required [9-10]. These are the shortcomings. The other method is to minimize wind speed prediction and systematic and meteorological errors at particular location and reduce bias though the process of Model Output Statistics (MOS). By producing correlation equation between predicted wind speed and estimated wind speed, the predicted wind speed can be closed to actual wind speed. Accordingly, in contrast to physical performance improvement, the statistical process requires long-term prediction values and long-term estimated values. In this process, the relationship between prediction values and estimated values and the evaluation of meteorological bias become crucial.

## 1.2 Objectives

In this study, I aim to develop MOS equation that can more accurately predict wind speed at the wind power generators in the Island of Cheju by using the model forecast data collected through weather forecast model and observation data collected throughout long period of time and though this I aim to improve model forecast wind speed. Furthermore, I aim to evaluate the performance capacity of wind power forecasting system through comparison and evaluation of predicted wind power calculated by using MOS, observation data and model forecast data.

# Ⅱ. Analysis of Wind Resources

## 2.1. Wind speed

The standard observation height of wind speed by AWS is about 10m above the surface. So in this study, the equation (2.1) was applied to calculate wind speed at wind turbine hub height. Usually, hub height is about 50m to 80m but it is mostly depend on its capacity. When calculate the upper level wind speed through the equation (2.1), it has to define the surface roughness. The factors that determine the length of roughness are numerous(surface type, geomorphic characteristics, building structures, etc). In this study, 0.6 length of roughness value was used to calculate wind speed at 80m of height of a hub(No.6 wind turbine of Sungsan wind farm).

$$V = V_{vef} \times \frac{\ln(Z/Z_0)}{\ln(Z_{vef}/Z_0)} \tag{2.1}$$

Here,

$V_{vef}$ : observed wind speed

$Z_0$ : length of roughness(in this study, 1.0 was applied)

$Z_{vef}$ : height of observed wind speed(in this study, 10.2m was applied)

$Z$ : wind turbine hub height

Table 2.1 show the location information of Sungsan site. The Sungsan site is located at southeastern part of Halla Mountain, it has characteristic of climate in which wind speed is relatively low when northwesterly wind occurs. Four years wind speed data was used to evaluate the wind resource near Sungsan site. In spite of the differences due to difference in equipment and manufacturers of the wind turbine, in this study, assumed that threshold wind speed of over 4.0 m/s and stop wind speed of 25.0 m/s and rated wind speed is 13.0 m/s which is minimum wind speed to generate designed power.

Table 2.1. Information of Sungsan site.

| Site(No.) | Name | Lat. | Lon. | H(m) | $H_w$(m) |
|---|---|---|---|---|---|
| 188 | Sungsan | 33°23′ | 126°53′ | 18.6 | 10.2 |

Here,

H : Height of observation field above mean sea level

$H_w$ : Height of anemometer above the ground.

Table 2.2 shows the average monthly wind speed. Through all the period, four years average wind speed was 6.1 m/s. For monthly lowest wind speed was measured at June(5.3 m/s) and Monthly highest wind speed was measured at March(7.1 m/s).


Fig. 2.1. Location of Sungsan site.

Table. 2.2. Monthly averaged wind speed at Sungsan site(m/s).

| | Jan. | Feb. | Mar. | Apr. | May | Jun | Jul. | Aug. | Sep. | Oct. | Nov. | Dec. | Ann. |
|---|---|---|---|---|---|---|---|---|---|---|---|---|---|
| 2009 | 6.6 | 6.9 | 7.8 | 6.2 | 6.6 | 5.6 | 6.7 | 6.2 | 5.8 | 5.9 | 6.4 | 6.4 | 6.4 |
| 2010 | 6.6 | 6.3 | 8.0 | 6.3 | 6.1 | 4.6 | 5.1 | 5.8 | 6.1 | 6.1 | 6.0 | 6.8 | 6.1 |
| 2011 | 6.7 | 6.3 | 6.7 | 7.1 | 6.7 | 5.3 | 6.0 | 6.8 | 6.2 | 5.6 | 5.0 | 4.5 | 6.1 |
| 2012 | 4.6 | 5.4 | 5.9 | 5.8 | 4.1 | 5.5 | 4.8 | 7.2 | 5.7 | 6.0 | 6.2 | 6.5 | 5.7 |
| Avg. | 6.1 | 6.2 | 7.1 | 6.3 | 5.9 | 5.3 | 5.7 | 6.5 | 5.9 | 5.9 | 5.9 | 6.0 | 6.1 |

Fig. 2.2 shows the hourly average wind speed. Throughout all hours, most wind speed was over than 4m/s and maximum was observed at 14h (7.8m/s). Fig 2.3 is frequency of hourly wind speed usable for generating electricity by wind turbine. It shows the similar variation with fig. 2.2 during daytime is higher than nighttime. Over 80% of wind is usable during daytime. Fig 2.4 shows the variation of monthly available wind(over than 4m/s) for power generation for each month. Most of month's available wind were over than 70%(except, June). Winter season during daytime wind speed is most usable at Sungsan site.

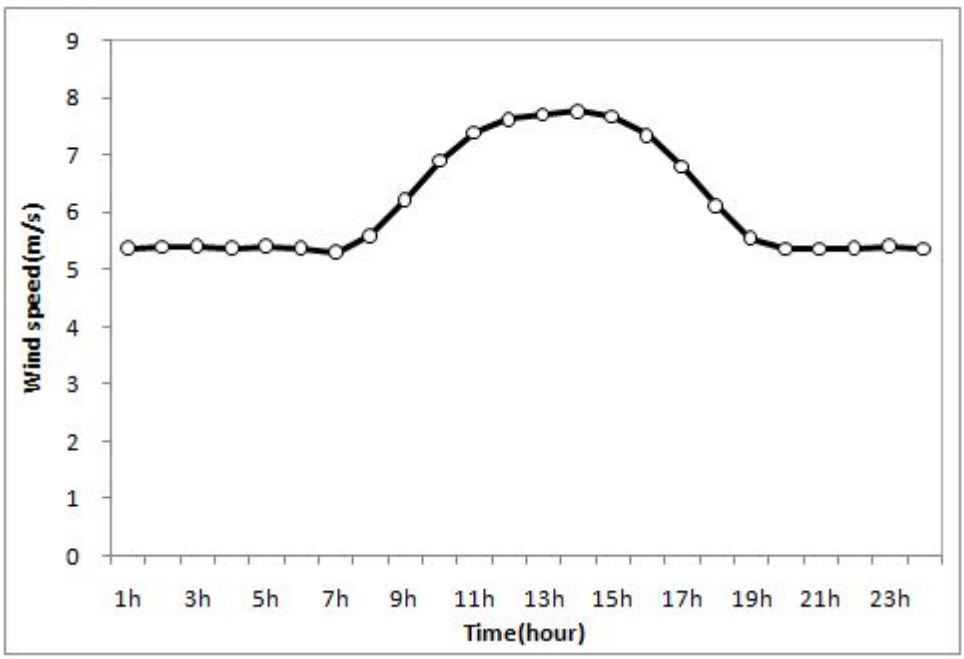


Fig. 2.2. Variation of wind speed at Sungsan site.

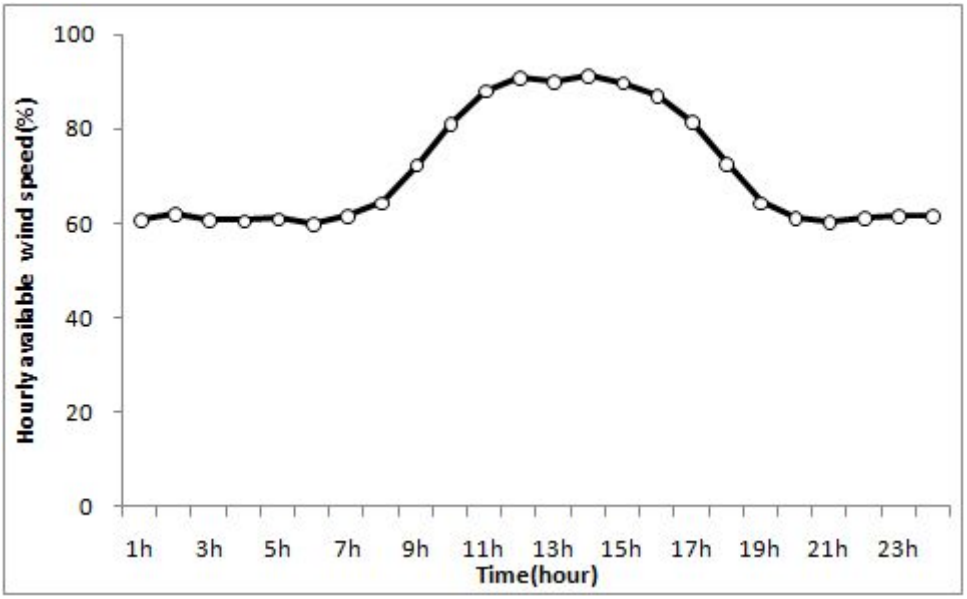


Fig. 2.3. Variation of hourly available wind speed.

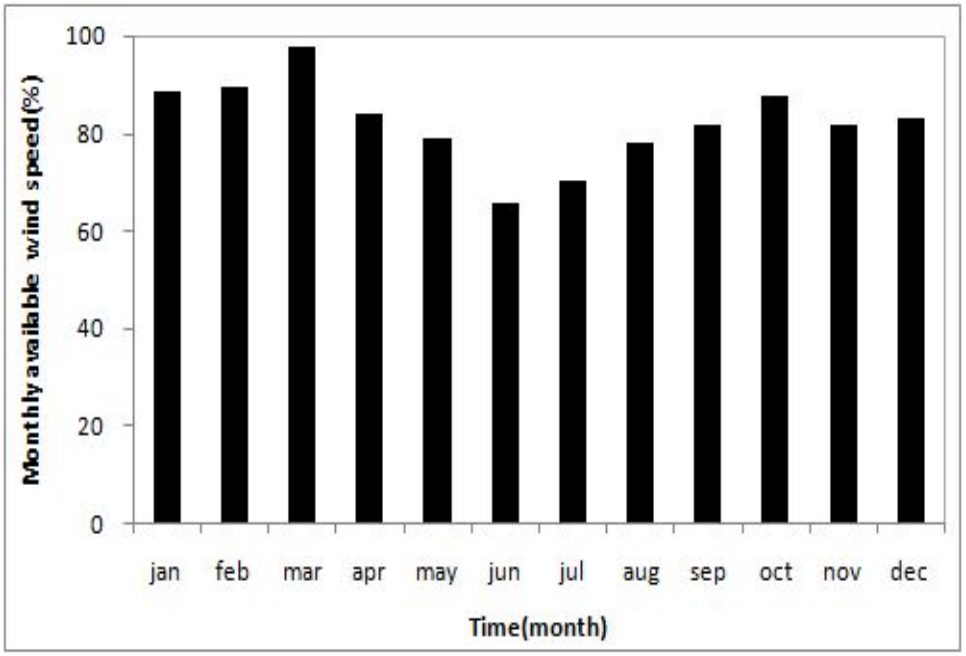


Fig. 2.4. Variation of monthly available wind speed.

2.2. Wind direction

Table 2.3 shows average wind speed by wind direction for Sungsan site. Average wind speed by wind direction for Sungsan site differs greatly due to geographic and topographical factors. Sungsan site located in east, average wind speeds by wind direction are highest at 6.0 m/s and 6.2 m/s, respectively, in the case of ENE. Due to its location at the southeast of Halla Mountain, average wind speed is relatively weak in the case of a kind of west wind and northwest wind.

Table. 2.3. Averaged wind speed of Sungsan site by wind directions.

| | Spring | Summer | Fall | Winter | Annual |
|---|---|---|---|---|---|
| N | 5.1 | 4.2 | 5.4 | 6.2 | 5.4 |
| NNE | 5.6 | 5.0 | 5.6 | 6.0 | 5.5 |
| NE | 6.1 | 5.7 | 6.4 | 6.2 | 6.1 |
| ENE | 6.1 | 5.4 | 6.6 | 7.0 | 6.2 |
| E | 5.6 | 5.2 | 6.2 | 7.0 | 5.8 |
| ESE | 5.3 | 5.4 | 5.7 | 6.2 | 5.6 |
| SE | 4.9 | 4.9 | 5.9 | 5.2 | 5.2 |
| SSE | 4.7 | 4.4 | 4.4 | 4.4 | 4.5 |
| S | 5.3 | 5.1 | 4.9 | 5.5 | 5.2 |
| SSW | 6.0 | 5.8 | 5.4 | 6.2 | 5.8 |
| SW | 6.8 | 6.1 | 5.4 | 5.7 | 6.2 |
| WSW | 4.9 | 4.3 | 3.7 | 4.6 | 4.5 |
| W | 4.4 | 3.0 | 4.0 | 4.4 | 4.1 |
| WNW | 6.2 | 3.6 | 4.9 | 5.8 | 5.5 |
| NW | 6.2 | 3.3 | 4.8 | 5.8 | 5.5 |
| NNW | 5.9 | 3.5 | 5.2 | 6.4 | 5.7 |

In this study, usable wind speeds for electricity generation by wind turbine is presumed to be from 4.0 m/s ~ 25.0 m/s. Table 2.4 show the yearly and seasonal wind speed variation. Fig 2.5 is the variation of hourly wind speed. Wind speed of 4.0 m/s ~ 13.0 m/s is highest. About 67% of annual wind is available for power generation by wind power electricity generators and the frequency is highest at 73% during winter. Also, frequency of feasible wind range of 4.0 m/s ~ 13.0 m/s during daytime occurs incessantly high.

Table. 2.4. Frequency of yearly and seasonal wind speed at Sungsan site(%).

| grade(m/s) | <4.0 | 4.0~13 | 13~25 | >25 | Sum |
|---|---|---|---|---|---|
| Annual | 33 | 65 | 2 | 0 | 100 |
| Spring | 32 | 66 | 2 | 0 | 100 |
| Summer | 41 | 58 | 1 | 0 | 100 |
| Fall | 34 | 65 | 1 | 0 | 100 |
| Winter | 27 | 71 | 2 | 0 | 100 |

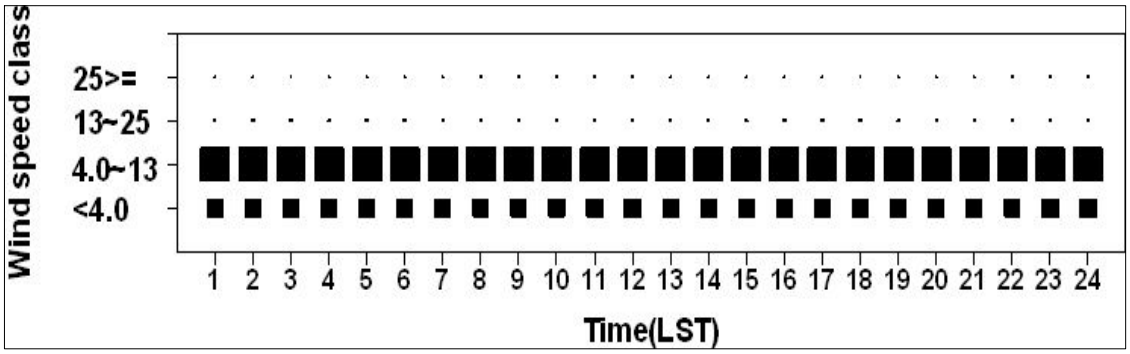


Fig. 2.5. Frequency of hourly wind speed at Sungsan site.

Fig. 2.6 shows frequencies annual and seasonal wind direction. The annual NNW wind is highest in frequency within 20% and especially in winter, frequency of NNW wind is high about over 30%.

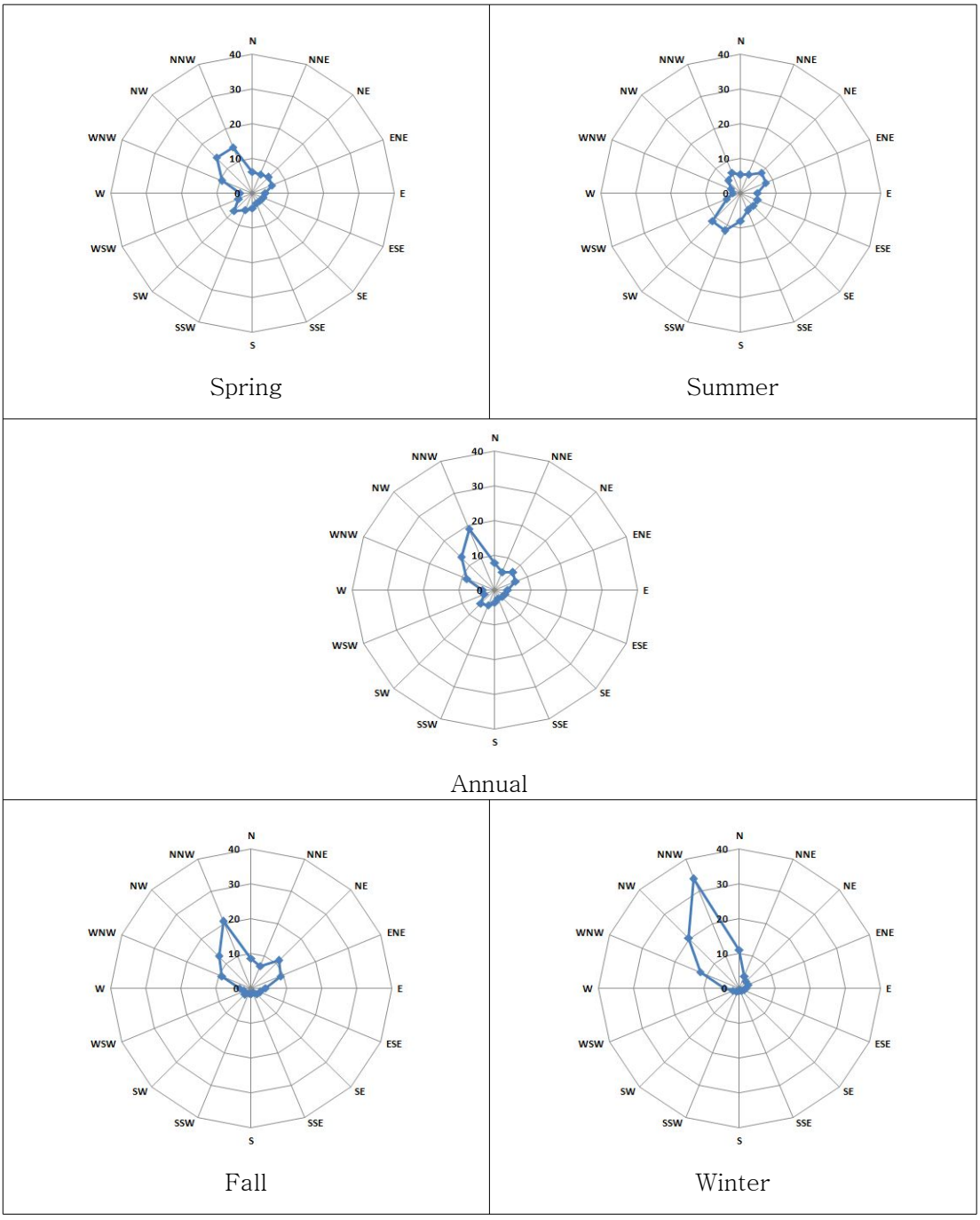


Fig. 2.6. Wind rose at Sungsan site(%).

Fig. 2.7 shows the frequency of hourly wind directions of threshold wind or higher. Hourly wind direction shows constant shape without significant change of hourly wind direction. NNW wind is predominant at Sungsan site.

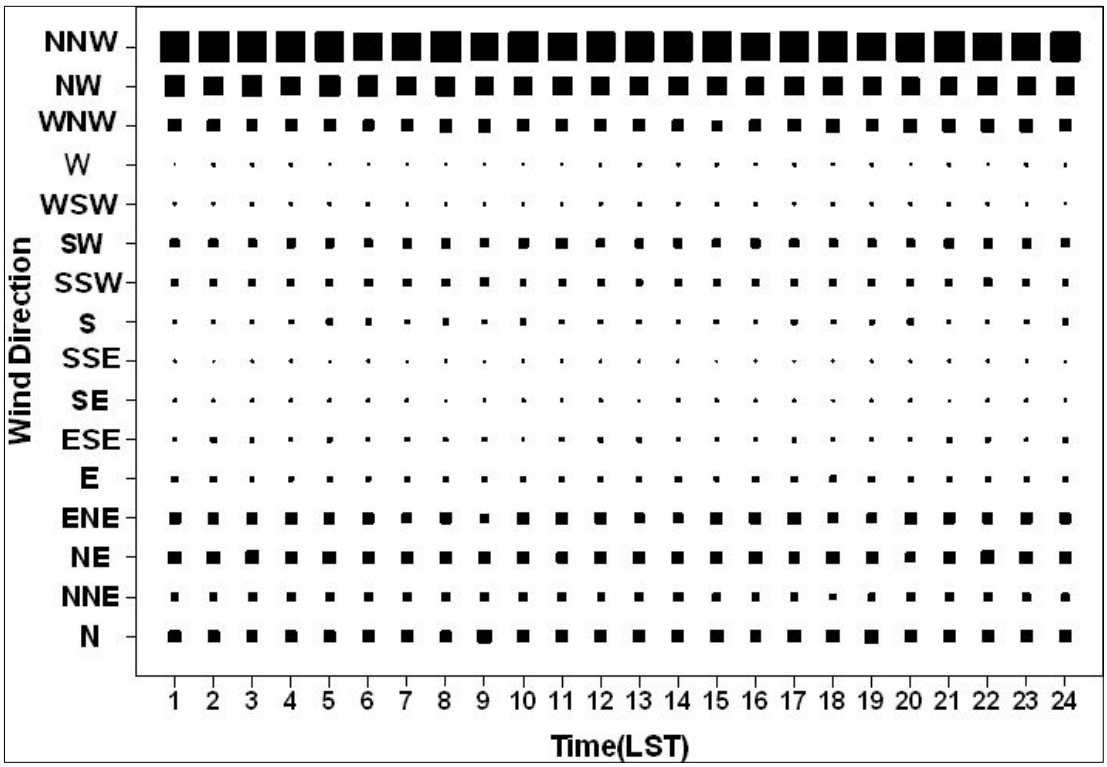


Fig. 2.7. Hourly wind direction at Sungsan site(over than 4.0 m/s).

# Ⅲ. Weather Forecasting Model

## 3.1. Forecast of wind speed

Numerical model is classified due to the size of predicted area: global scale model (approximately 1000km ~ 10km); regional scale model (approximately 10km ~ 1km); and local magnitude scale model (less than 1km). In these numerical models, by integrating nonlinear equation as to movement initiated from atmospheric conditions, the movement of atmosphere is predicted on virtual numerical grid. In global scale model, grids about whole globe can be calculated. However, because of limit on the number of numerical grids due to limited capacity of computer, it is difficult to directly implement the prediction of detailed sub-grid scale in global scale model. In the case of orographic structure that contains complex geographical features like Korea in which sub-grid process affects large scale evolution (for instance, formation of turbulence or clouds), such problem requires parameterization process for such phenomenon. Synoptic meteorological system of grid scale of approximately 100 km to grid scale of 10km is an example. In this case, the definition of finite resolution is that variations calculated at each grid point represent mean average of grid cell; thus, this prediction value cannot be optimal for the entire regions in one grid cell. If predicted value and estimated value are to be compared, caution is required. To solve such drawback, regional scale model and local magnitude scale model have been developed and using these models, prediction of wind speed at higher resolution has become possible. Regional scale model is a derivative of global scale model. For instance, in numerical model economic conditions are provided. This process is called nesting; through this process, we are able to

find out changes in wind speed as to atmospheric effects in spatially interested region in high resolution. Since nested grid domain must be two-thirds of previous higher domain, in regional scale model, 3 to 4 nestings are generally used. Regional scale model is usefully utilized in temporally and spatially heterogeneous countries such as Korea, Japan, Spain, Norway, etc. that possess complex topography. The models advantageously used for predicting wind power energy are WRF [11-13] and MM5. These two models are widely used for the prediction of wind speed. Other than these two, the Danish Predikt or model [14] and WPPT model [15], the Spanish Sipreolico model [16] and CENER's LocalPred model [17], the German Previento model [18] and ISET's WPMS model [19], the French Armines AWPPS model [20], the Greek National Technical University of Athens (NTUA) model [21] and the Aristotle University of Thessaloniki (AUTH) model [22], and the North American eWind model [23] are also used. In the case of local magnitude scale model, local magnitude scale models that have different degrees of complexity are used in order to explain floating effects on the region that is very closed to a wind power plant. Such local magnitude scale model can model somewhat complex geographical features. Yet it has a drawback: when terrain gradient is too vast, the model has the possibility to overestimate changes in horizontal wind speed. Thus, meticulous analysis is required for this drawback.

## 3.2. WRF Model

### 3.2.1. Composition of WRF Model

Using latest numerical model techniques, WRF (Advanced Research WRF : ARW) has been developed by flexible source codes in order to process vast amount of numerical data in parallel. The source codes are divided into actual work module that can be used in actual work of numerical predictions and research and development model module code that can be applied in academic research so as to make possible the application of numerous equations of physics. Moreover, more enhanced data assimilation system makes possible simultaneous executions of development of a model and test of the model. WRF has vast range of user community as to research and learning as a great number of universities participate in WRF is maintained and supported by such participation. The resolution of WRF is extensive scale from a few meters to a few thousand kilometers and has been developed to be suitable for application and utilization of , depending on the application purposes, such works as actual weather forecasting, data assimilation and parameterized physical process research, climate modeling, application of air quality model, atmosphere-oceanic in osculation, ideal prediction test, etc. The performance process of WRF model is to produce prediction data through data assimilation process of observed data which is entire process; calculation process of dynamics by initialization process required in the process of prediction, physical process, integral calculus process, etc. and after the production of prediction data, WRF model implements imagification and testing of prediction data through the process. Deduction process of dynamic values is fulfilled through ARW Solver; characteristics of dynamics can be found in the use of complete compressibility non-integer Euler Equation. This equation delineates conservation variables in the form of flux and is composed of mass

perpendicularity coordinate system that follows the surface of the Earth.

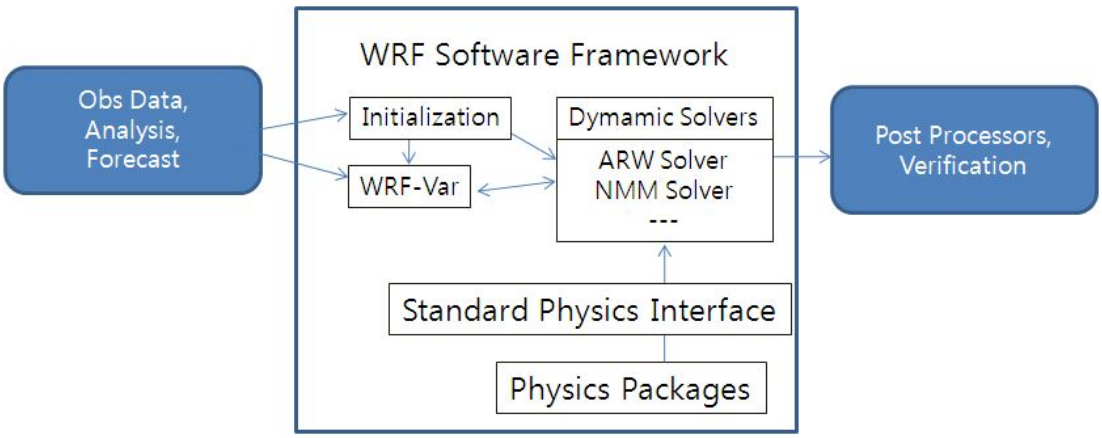


Fig. 3.1. The frame of the WRF program

The equation used in WRF (ARW) Solver, based on the statics-atmospheric pressure perpendicularity coordinate system that first follows topography, is expressed as in Equation (3.1).

$$\eta = (p_h - p_{ht})/\mu, \quad \text{where} \quad \mu = p_{hs} - p_{ht}. \tag{3.1}$$

Here, Ph is an atmospheric pressure factor; and Phs and Pht means ground surface and model top layer, respectively. Equation 1 is mostly used in statics atmosphere model; $\eta$ takes the value of ground surface (1) and the highest layer of model. Moreover, $\mu$(x,y) represents mass of column of air per unit area in model domain (x, y); variables in the appropriated form of flux are expressed as follows.

$$V = \mu v = (U, V, W),\ \Omega = \mu\dot{\eta},\quad \Theta = \mu\theta. \tag{3.2}$$

Herein, v=(U, V, W) represents horizontal and perpendicular speed components, respectively; $\omega$ represents perpendicular speed component and $\theta$ represents potential temperature. Accordingly, in ARW equation is expressed in non-conserved variables: $\Phi$=gz (geo-potential), p(atmospheric pressure), $\alpha$ =1/$\rho$ (reciprocal of density; specific volume). Oiler equation expressed in the form of flux, using the variables defined above, is as follows.

$$\partial_t U + (\nabla \cdot V_u) - \partial_x (p\phi_\eta) + \partial_\eta (p\phi_x) = F_U \tag{3.3}$$

$$\partial_t V + (\nabla \cdot V_v) - \partial_y (p\phi_\eta) + \partial_\eta (p\phi_y) = F_V \tag{3.4}$$

$$\partial_t W + (\nabla \cdot V_w) - g(\partial_\eta p - \mu) = F_W \tag{3.5}$$

$$\partial_t \Theta + (\nabla \cdot V_\theta) = F_\Theta \tag{3.6}$$

$$\partial_t \mu + (\nabla \cdot V) = 0 \tag{3.7}$$

$$\partial_t \phi + \mu^{-1}[(V \cdot \nabla\phi) - gW] = 0 \tag{3.8}$$

Herein specific volume has the relationship shown below.

$$\partial_\eta \phi = -\alpha\mu \tag{3.9}$$

State equation is expressed as follow.

$$p = p_0 (R_d \theta / p_0 \alpha)^{\gamma} \tag{3.10}$$

Equation (3.3) – Equation (3.10) is implemented, x, y, and $\eta$ are expressed in the form of differentials as in the following.

$$\nabla \cdot V_a = \partial_x (U_a) + \partial_y (V_a) + \partial_\eta (\Omega_a) \tag{3.11}$$

And finally the equation is expressed as follows.

$$\nabla \cdot \nabla_a = U\partial_x a + V\partial_y a + \Omega\partial_\eta a \tag{3.12}$$

Herein a represents a general variable; $\gamma = c_p / c_v = 1.4$ represents thermal capacity of dry air; Rd represents specific gas constant; $p_0$ represents atmospheric pressure at standard isobaric surface (1,000hpa). Herein the right hand terms of a sign of equation – $F_U$, $F_V$, $F_W$, and $F_\Theta$ represent physics formula of model, turbulent mixing, rotation projection, forced power generated by the rotation of Earth.

WRF(ARW) grid system, as shown in Fig. 3.2, uses Arakawa C grid system and normal speed is crossed over by 1/2 from thermodynamic variable and placed. Horizontal grid is expressed in (i, j) and vertical grid is expressed in (i, k); the location of variables is determined by (x, y, $\eta$)= ($i\triangle x$, $j\triangle y$, $k\triangle \eta$ ) and it is expressed in the same position as the position of mass point. $\triangle \eta$, length of vertical grid is not designated as constant value.

Therefore, a user must assign the value between ground surface (1) and top layer of model (0). Spatial grid system of ARW is defined by these grids and variables.

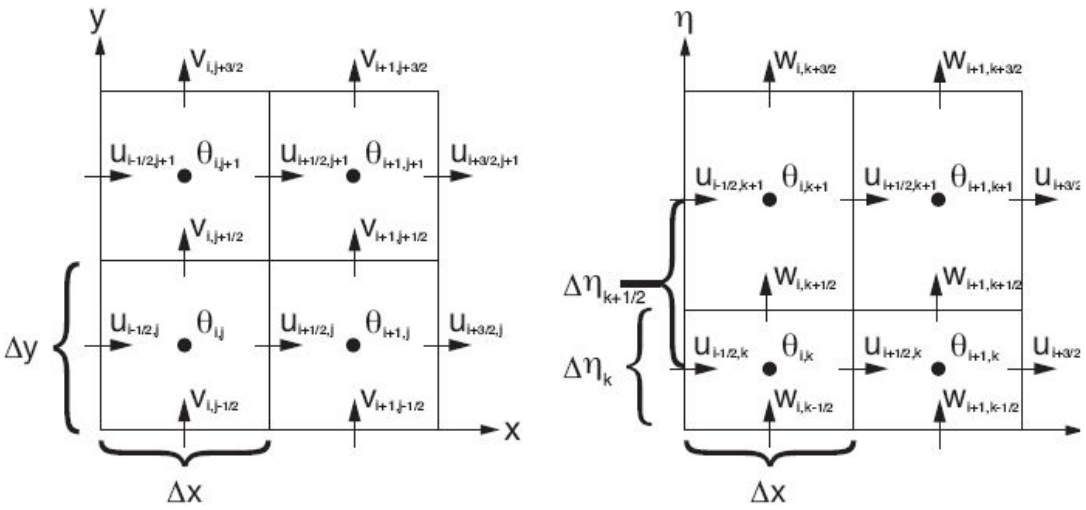


Fig. 3.2. ARW of horizontal and vertical grid structure(left: horizontal grid, right: vertical grid).

In executing WRF(ARW), a user can use two kinds of time interval. One is the model time step; the other is acoustic time step. Both are limited by the number of Courant. Time restriction of RK3 will be explained herein. Time interval of RK3 is limited by $u\Delta t/\Delta x$, advection Courant and advection schemes selected by a user. (A user can select discretization process of second order to sixth order.) When using such advection schemes, RK3 scheme's 1-dimension time interval limit on advection is given as follows.

Table. 3.1. Maximum stable Courant numbers for one-dimensional linear advection.

| Time Scheme | Spatial order | | | |
|---|---|---|---|---|
| | 3rd | 4th | 5th | 6th |
| Leapfrog | Unstable | 0.72 | Unstable | 0.62 |
| RK2 | 0.88 | Unstable | 0.30 | Unstable |
| RK3 | 1.61 | 1.26 | 1.42 | 1.08 |

In order to maintain the stability of numerical calculation, time interval used in ARW must use Courant number which is less than the theoretically proposed value; it is illustrated in the following equation.

$$\Delta t_{\max} < \frac{Cr_{theory}}{\sqrt{3}} \cdot \frac{\Delta x}{u_{\max}} \tag{3.13}$$

Herein $Cr_{theory}$ is Courant number selected in RK3 in Table 3.1; $u_{max}$is maximum speed expected in the model. In MM5 model, it has time interval of approximately 3 multiples both horizontally and vertically; yet in WRF (ARW) time interval (measured by second) must have grid distance (measured by km) of approximately 6 multiples. In WRF (ARW), it is possible to use both a few boundary conditions appropriate for idealized flow and boundary

conditions appropriate for forecasting of actual data. Such selection is made possible for a user to select boundary conditions in user specified file (name list file). Coarse grid (commonly called as parent grid) of modeling is appropriate for setting boundary conditions for a single domain. For instance, actual data use periodical, symmetric combination or lateral boundary conditions instead of the boundary condition method that depends on traditional time given by external boundary conditions. However, lateral boundary conditions that depend on time re one of idealized modeling cannot be used because outer boundaries are not generated. In a case of actual modeling, specified boundary condition is used from alleviation, nudging, boundary conditions. In WRF (ARW), a user can use two kinds of specified boundary conditions: most outer coarse grid; or time-dependant boundary conditions provided in nested grid. Lateral boundary conditions as to nest re all the detailed grids is automatically selected even though coarse grid uses symmetric, periodical combination or selectable other options.

Specified zone about coarse grid is determined by arbitrary integral calculus by external forecasting or analysis (herein they refer to analysis and forecasting provided by standard initialization; the width of the specified zone is formed in real time; the second area of lateral boundaries as to coarse grids is determined as relaxation zone.

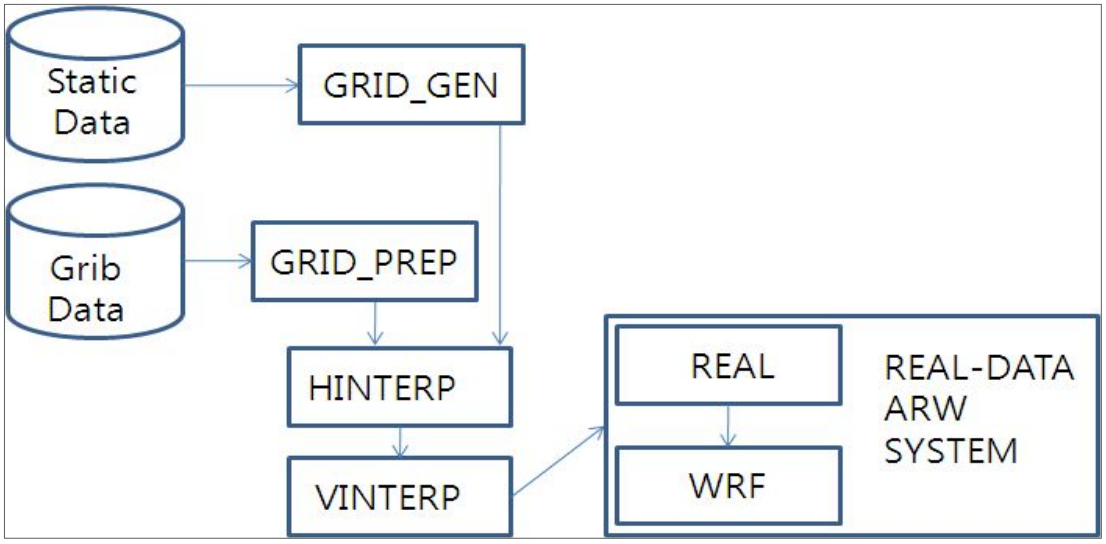


Fig. 3.3. Schematic showing the data flow and program components in the SI, and how the SI feeds initial data to the ARW. Letters in the rectangular boxes indicate program names. GRID GEN: defines the model domain and creates static files of terrestrial data. GRIB PREP: decodes GriB data. HINTERP: interpolates meteorological data to the model domain. VINTERP: vertically interpolates data to model coordinate.

WRF model, by providing additional grid in modeling, supports horizontal nested grid system that has magnified resolution of the area of interest. In current version, it is only possible for horizontal nested grid, not possible to use for vertical nested grid. Nested grid is in the form of a rectangle and located within parent grid and arbitrarily arranged within integer type space ($\Delta x_{coarse} / \Delta x_{fine}$) and parent grid. Such implementation method of nested grid is also used in other mid-scale models (MM5, ARPS, COAMPS); nested grid structure implemented in WRF (ARW), compare to these models, has advantage of more efficient calculation in a large amount of parallel process system.

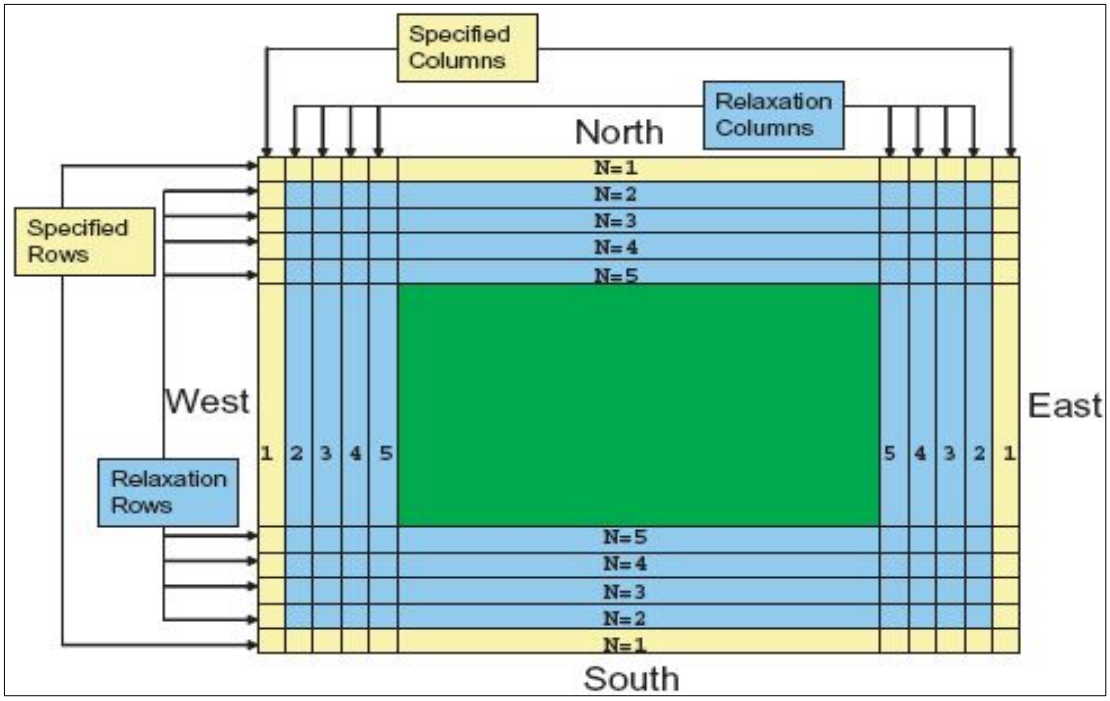


Fig. 3.4. Specified and relaxation zones for a grid with a single specified row and column, and four rows and columns for the relaxation zone. These are typical values used for a specified lateral boundary condition for a real-data case.

Explained in the followings is the method to use nested grid modeling using 1-way method and 2-way method. Options of 1-way method and 2-way method used in modeling address how coarse grid and fine grid mutually interact; boundary conditions of fine grid used in modeling that uses 1-way method and 2-way method are integrated by integral calculus from forecasting of coarse grid. Integral calculus method of 1-way nesting exchanges only information from coarse grid to fine grid, but 2-way nesting integral calculus method exchanges information between grids in bidirectional

way (from coarse grid to fine grid from fine grid to coarse grid) by the method of replacing the value of coarse grid by the value of fine grid by the method of the point of coarse grid located within fine grid. In using nested grid modeling, WRF (ARW)use the following few methods for initialization of fine grid.

- All the variables of fine grid is integrated from variables of coarse grid by integral calculus.
- All the variables of fine grid are input in external file that has high resolution meteorological model and topographic data.
- Fine grid has a few variables that are initialized to external data of high resolution; other variables are integrated from coarse grid by integral calculus.
- As to moving nested grid, external topographical files renew topography of fine grid yet not used them well.

Also, in modeling one outer grid and numerous internal nested grids can be included and in WRF (ARW) each nested grid zone must be fully included within one coarse grid and fine grid is treated as offspring grid in nested grid system. Fig. 3.5 shows the relationship between coarse grid (parent grid) and fine grid (offspring grid) and the environment that can be set.

Arakawa-C grid staggering for a portion of a parent domain and an imbedded nest domain with a 3:1 grid size ratio. The solid lines denote coarse grid cell boundaries, and the dashed lines are the boundaries for each fine grid cell. The horizontal components of speed (""U"" and ""V"") are defined along the normal cell face, and the thermodynamic variables (""Θ"") are defined at the center of the grid cell (each square). The bold typeface variables along the interface between the coarse and the fine grid define the locations where the specified lateral boundaries for the nest are in effect.

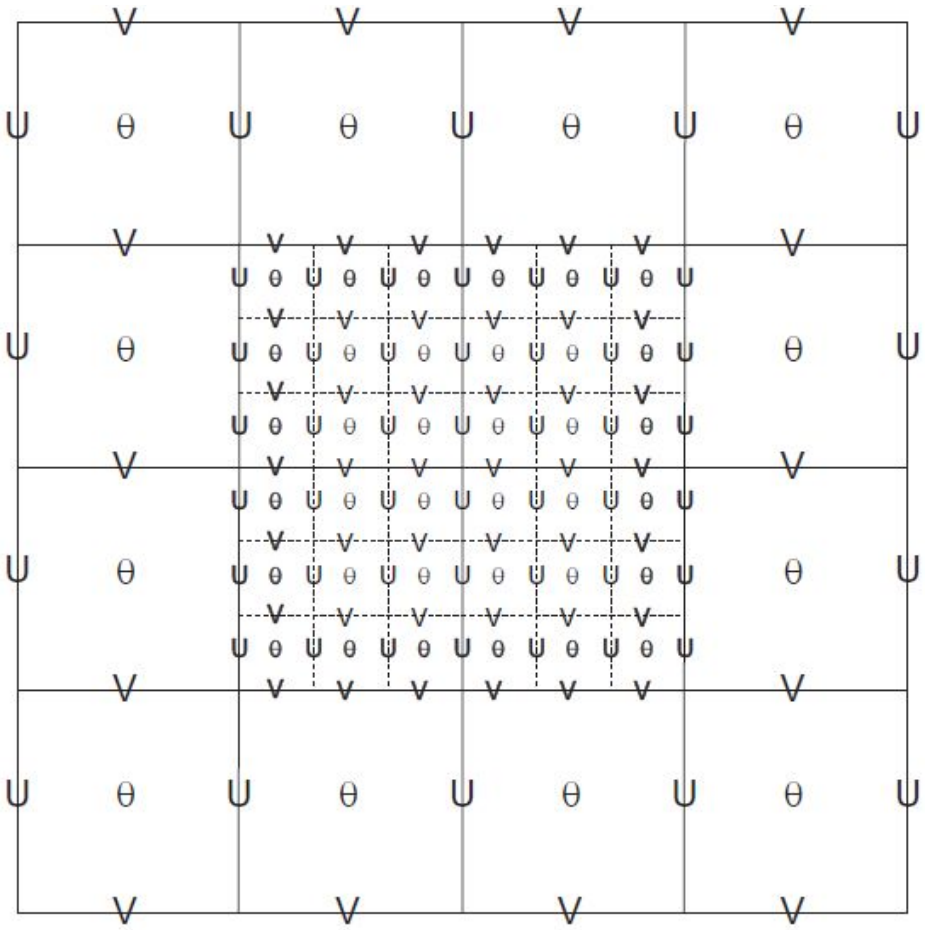

Fig. 3.5. Possible grid configurations.

Only the concurrent 1-way nest option or the 2-way nest option are considered in this section. The 1-way nest option (using two consecutive ARW simulations) is functionally similar to two separate, single-grid simulations and does not fit the following description. For a multiple grid simulation within a single model run, there are some additional infrastructure steps that are required. While the following text details a simulation with a single coarse-grid and a single fine-grid, this implies no lack of generality when handling multiple grid levels or multiple grids on the same level

```
Integrate Parent Grid One Time Step
   If Nest Grid Start Time
     (1) Horizontally Interpolate Parent to Child Grid
     (2) Optionally Input High-Resolution Child Data
     (3) Compute Child Reference State
     (4) Feedback Child Initial Data to Parent Grid
     (5) Re-Compute Parent Reference State
   End If Nest Grid Start Time
   Solve Time Step for Parent Grid
   While Existing Nest Grids to Integrate
     (1) Lateral Forcing from Parent Grid to Child
     (2) Integrate Child Grid to Current Time of Parent Grid
     (3) Feedback Child Grid Information to Parent Grid
   End While Existing Nest Grids to Integrate
End Grid Integrate
```

Fig. 3.6. Nest grid integration sequence.

Physics of WRF model uses various categories of physics options such as microphysics, cumulus parameterization, planetary boundary layer (PBL), land surface model, and radiation; diffusion is treated as a part of radiation physics. In this study, detailed explanations of options of physics were omitted.

① Microphysics

Suitable for mesoscale modeling; feasible to use bulk schemes that lead to meticulous combination physics suitable for cloud modeling in simplified physics and possible for specific selection as shown in the following table 3.2.

Table. 3.2. Microphysics Options

| Scheme | Number of variables | Ice-Phase Processes | Mixed-Phase Processes |
|---|---|---|---|
| Kessler | 3 | N | N |
| Purdue Lin | 6 | Y | Y |
| WSM3 | 3 | Y | N |
| WSM5 | 5 | Y | N |
| WSM6 | 6 | Y | Y |
| Eta GCP | 2 | Y | Y |
| Thompson | 7 | Y | Y |

② Cumulus parameterization

These schemes are responsible for the sub-grid-scale effects of convective and/or shallow clouds. The schemes are intended to represent vertical fluxes due to unresolved updrafts and downdrafts and compensating motion outside the clouds. They operate only on individual columns where the scheme is triggered and provide vertical heating and moistening profiles. Some schemes additionally provide cloud and precipitation field tendencies in the column, and future schemes may provide momentum tendencies due to convective transport of momentum. The schemes all provide the convective component of surface rainfall. Cumulus parameterizations are theoretically only valid for coarser grid sizes, (e.g., greater than 10 km), where they are necessary to properly release latent heat on a realistic time scale in the convective

columns. While the assumptions about the convective eddies being entirely sub-grid-scale break down for finer grid sizes, sometimes these schemes have been found to be helpful in triggering convection in 5~10 km grid applications. Generally, they should not be used when the model can resolve the convective eddies itself (e.g., 5 km grid). Table 3.3. summarizes the basic characteristics of the available cumulus parameterization options in the ARW.

Table. 3.3. Cumulus Parameterization Options

| Scheme | Cloud Detrainment | Type of scheme | Closure |
|---|---|---|---|
| Kain-Fritsch | Y | Mass flux | Cape removal |
| Betts-Miller-Janjic | N | Adjustment | Sounding adjustment |
| Grell-Devenyi ensemble | Y | Mass flux | Various |

Land surface models (LSMs) use atmosphere information in land surface scheme, radiative forcing in radiation scheme, precipitation forcing in microphysics and cloud scheme, land surface state variables in land surface characteristics, and heat flux and humidity flux at land and sea-ice point. These flux terms provide low layer boundary conditions re vertical transport within PBL. Moreover, LSMs have various elaborate tools such as controlling thermal and humidity fluxes in multiplex soil layers and controlling vegetation, trees, and canopy effects and feasible to select the following options.

Table. 3.4. Land Surface Options

| Scheme | Vegetation Processes | Soil Variables(Layers) | Snow Scheme |
|---|---|---|---|
| 5-layer | N | Temperature(5) | none |
| Noah | Y | Temperature, Water_Ice, Water(4) | 1-layer, fractional |
| RUC | Y | Temperature, Ice, Water+Ice(6) | multi-layer |

③ Boundary layer physics

Planetary boundary layer process processes subgrid-scale eddy diffusivity scale fluxes due to eddy transport at the entire atmosphere column: they are not processed separately in boundary layers. Therefore, if PBL schemes become invigorated, under the assumption that PBL schemes manage this process explicit vertical diffusion becomes deactivated; selective options for most suitable horizontal diffusion are constant $K_h$ value in which horizontal, vertical combination occurs independently or horizontal variation values. PBL schemes determine vertical flux profile at well mixed boundary layer and stable layer and provide atmospheric temperature, humidity including clouds, and trend of horizontal momentum in the entire column. Most of PBL schemes consider dry mixing but include saturation effect at vertical stability that determines mixing. In WRF (ARW), horizontal and vertical fluxes within PBL are determined by using the following schemes shown in Table 3.5; Table 3.5 shows profiles used in each scheme and the method of treating diffusion at top layer of the model.

Table. 3.5. Option of planetary boundary layer.

| Scheme | Unstable PBL Mixing | Enrarinment treatment | PBL Top |
|---|---|---|---|
| MRF | K profile+ countergradient term | part of PBL mixing | from critical bulk $R_i$ |
| YSU | K profile+ countergradient term | explicit term | from buoyancy profile |
| MYJ | K from prognostic TKE | part of PBL mixing | from TKE |

④ Atmospheric radiative physics

Radiation scheme provides the information about atmosphere heating due to radiation flux and long and short wave radiation toward the face of the earth heat budget. Long wave radiation includes thermal radiation that is absorbed into atmosphere and land surface or released and infrared ray radiation; long wave radiation flux that is going upward from land surface is determined by land surface release rate that depends on land surface temperature and form. Short wave radiation includes visible ray wavelength that generates solar spectrum and such processes as absorption, reflection, scattering that occur at the atmosphere and on land surface. Also, the flux that point upward is determined by reflectivity due to land surface albedo. Radiation in the atmosphere reacts not only to clouds, moisture distribution, carbon and ozone generated in the model but also to a minute amount of gas concentration. As radiation scheme of WRF (ARW) is presently one dimensional scheme, each column is treated independently and fluxes are horizontally infinite and identified as the same as columns in a particular planes. This becomes good approximation when vertical layer is not greater than the length of horizontal grid; however, such assumption result in drop in accuracy when horizontal resolution is high. The followings illustrate option for basic radiation schemes used in WRF (ARW).

Table. 3.6. Physics Interactions. Columns correspond to model physical processes: radiation (Rad), microphysics (MP), cumulus parameterization (CP), planetary boundary layer/vertical diffusion (PBL), and surface physics (Sfc). Rows corresponds to model variables where i and o indicate whether a variable is input or output (updated) by a physical process.

| Scheme | physical processes | Rad | MP | CP | PBL | Sfc |
|---|---|---|---|---|---|---|
| Atmospheric State or Tendencies | Momentum | | | i | io | |
| | Pot. Temp. | io | io | io | io | |
| | Water Vapor | i | io | io | io | |
| | Cloud | i | io | o | io | |
| | Precip. | i | io | o | | |
| Surface Fluxes | Longwave Up | i | | | | o |
| | Longwave Down | o | | | | i |
| | Shortwave Up | i | | | | o |
| | Shortwave Down | o | | | | i |
| | Sfc Convective Rain | | | o | | i |
| | Sfc Resolved Rain | | o | | | i |
| | Heat Flux | | | | i | o |
| | Moisture Flux | | | | i | o |
| | Surface Stress | | | | i | o |

⑤ Execution process of WRF

WRF modeling system, after first specifying domain of modeling that should be numerically computed, generates initial field by using gridded meteorological data and based on this, calculation of main model is implemented and the composition consists of the following crucial programs. Fig. 3.7 is overall modeling flow of WRF model.

- The WRF Preprocessing System(WPS)
- WRF-Var
- ARW solver
- Post-processing graphics tools

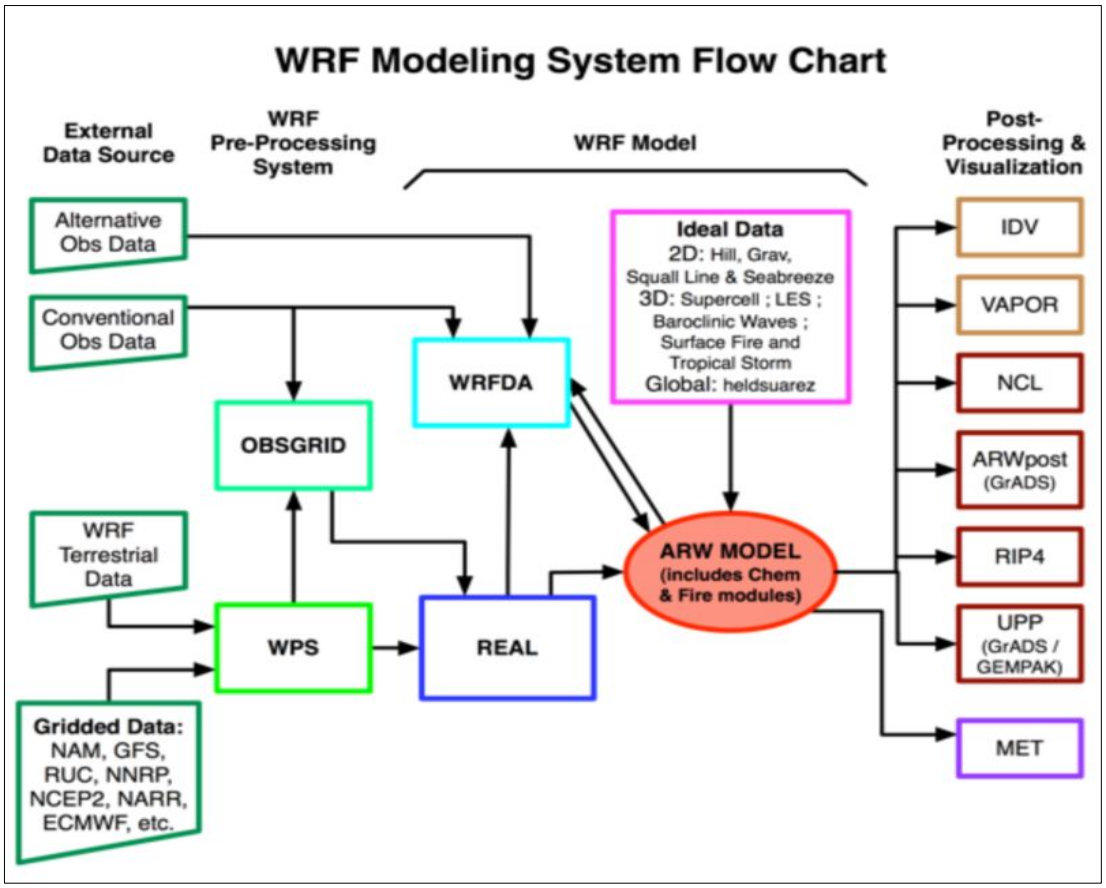


Fig. 3.7 Flow chart of WRF(ARW) modeling system.

### 3.3. Domain Setting

In this study, wind power forecasting system has been established so as to produce forecast data for real-time wind power in the region of the Island of Cheju. Wind power forecasting system using GFS(Global Forecast System) model entire globe analysis place as boundary data to execute generation of initial field twice a day (06 UTC and 18 UTC) and model forecasting in the region of the Island of Cheju through WRF(Weather Research Forecasting).By using topographical data on initial field and boundary data in execution of 3 dimensional meteorological modeling for the forecast of wind field, forecast of wind speed at target area can be more accurate. In this study, to predict wind field more specifically in the wind power complex, high resolution grid system (horizontal resolution 1km) has been established and for this establishment, nesting method (1-way nesting) is employed in order to generate external boundary conditions of nested grid model. In general, a 3 dimensional meteorological model executes the model by using nesting method. Nesting method is used for more accurate calculation by generating boundary conditions of ultimate forecast domain. In this method, domain greater than ultimate domain is firstly calculated and then, using the computation outcome, calculation of smaller domain is executed. In order to accurately predict wind at the wind power complexes in the Cheju region through this method, the nested grid domain of the model was divided into four resolution domains and modeling was executed. The size and the number of grid for each domain are shown in Table 3.7.

Table 3.7. WRF Domain design.

| Domains | Resolution | Grid number | | Area |
|---|---|---|---|---|
| | | X | Y | |
| Domain 1 | 27㎞ | 60 | 60 | 1,620㎞ × 1,620㎞ |
| Domain 2 | 9㎞ | 61 | 61 | 549㎞ × 549㎞ |
| Domain 3 | 3㎞ | 67 | 64 | 201㎞ × 201㎞ |
| Domain 4 | 1㎞ | 85 | 61 | 85㎞ × 61㎞ |

Most coarse grid domain (Domain 1) was horizontally set for the 1620㎞ ×1620㎞ domain, including the Korean Peninsular, with grid interval of 27 km; second coarse grid domain (Domain 2) was horizontally set for the 549㎞×549 ㎞domain, including South Korea, with grid interval of 9 km; third coarse grid domain (Domain 3) was horizontally set for the 201㎞×201㎞domain, including the south-west coasts and the Island of Cheju, with grid interval of 3 km; final domain (Domain 4) was horizontally set for the 85㎞×61㎞domain, including the Cheju region and Marado, the most southern part of Korea, with grid interval of 1 km in order to mimic the wind at sea surface near Cheju. Vertical layers are composed of15 stories for all the four domains. Based on ultimately generated initial field, the wind fields of the region of the Island of Cheju which have the resolution of 1 km interval is produced at the interval of one hour for up to 72 hours through real-time model forecast process. Fig. 3.8 represents the final forecast domain (Domain 4). In this study, domain 4 using different map data compare with domain 1 through 3. Domain 4 using high resolution topographical data which was provided by

National Geographic Information Institute. DEM(Digital Elevation map) from USGS(United States Geological Survey) was used on domain 1 through domain 3[29]. In this study, early stage of forecasting(0h to 6h) data was not used to prevent data distortion by model spin up.

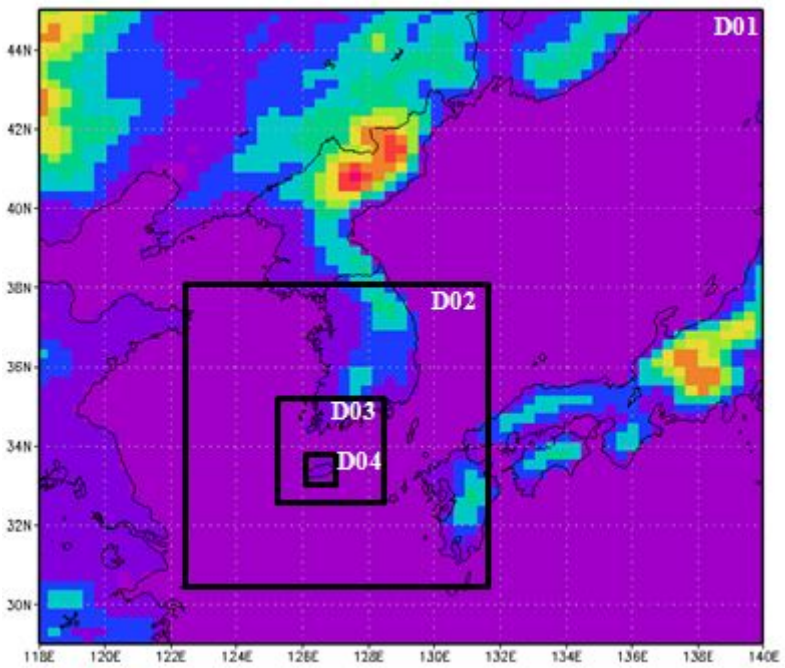


Fig. 3.8. Horizontal domains(4 horizontal domain).

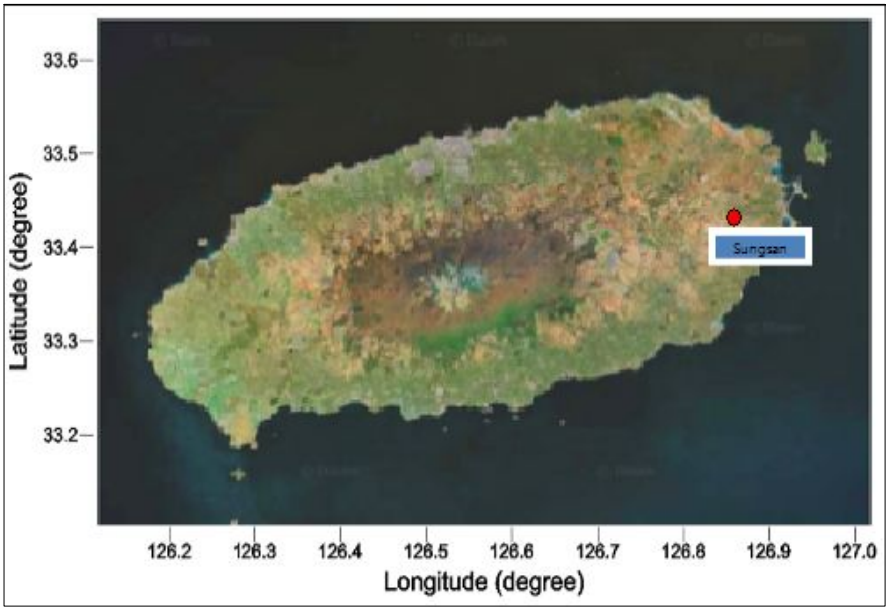


Fig. 3.9. Final forecasting domain(Domain 4).

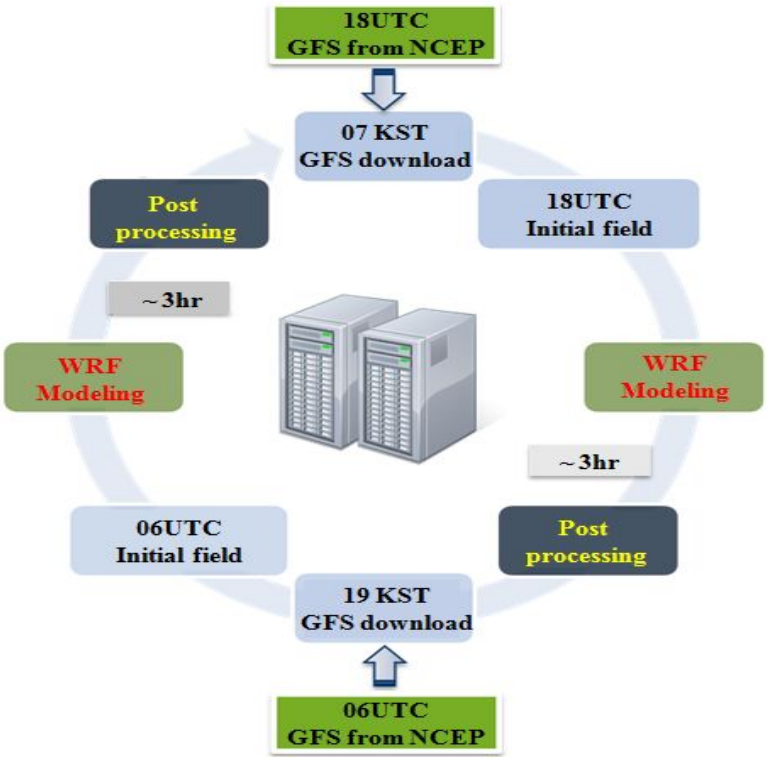


Fig. 3.10. Time schedule of real-time wind power forecasting system.

# Ⅳ. Development of MOS

## 4.1. MOS Forecast Equation

### 4.1.1 Predictors and Predictand

Numerical statistical model corrects systematic errors of numerical forecasting model and a statistical technique that can predict forecast elements that cannot be produced by numerical forecasting model and can also predict particular locations other than grid points. As error characteristics of numerical forecasting model differ at each time of forecasting, forecast errors increased as forecast time increased. To reduce such errors and improve forecast performance as to wind speed, numerical statistical model forecast equations for each forecast time has been developed. For the development of numerical statistical model, numerical forecast data must be accumulated for sufficient period without alternation of numerical forecasting model because numerical statistical model develops relational expression between forecast data of numerical forecasting model and forecast elements and use it as forecasting equation and thereby reflects characteristics of numerical forecasting model itself in the computation of forecasting equation. Generally, in order to produce stable Numerical Statistical Model Forecast Equation, sample data of 300 are known to be most stable sample size. However, in this study data for one year was used and approximately 90 samples were used seasonally and thereby developed numerical statistical model equation. Basic form of Numerical Statistical Model Forecast Equation can be seen in Equation (4.1).

$$\hat{Y}_t = \sum_{i=1}^{n} \alpha_{i,t} X_{i,t} \qquad (4.1)$$

Herein Y is forecast element or predictand and is the value actually observed. X is called predictor and is the value calculated from numerical model data and composed of variables that explain Y best. t is regression coefficient of multiple linear regression equation that represents relationship between $Y_t$ and $X_t$.

- Y: defined as wind speed at 80m above the ground in this study
- X: In this study, it is predictor. forecast variables of various numerical models that can be used as explanatory variables; yet, as an initial stage, simple linear regression equation was calculated by using forecast value of wind speed in numerical model.

Forecast element (Y) should be defined by feasible quantitative element that fits the purpose of forecasting; in this study, wind speed 80m above the ground at the locations of Sungsan is defined as forecast element. Since predictor (X) differs in accordance with location and forecasting time of various forecast variables, all of the possible predictors that can be considered to affect forecast element are calculated; these are called potential predictors. In general, predictors that have the capacity to affect differ in line with location of forecast and time of forecast. In this case, statistical method called stepwise selection is used for the method of selecting optimal predictors among possible potential predictors.

In this study, to figure out degree of fundamental improvement of MOS before using various potential predictors, wind speed predicted in numerical

model is used as sole predictor. Therefore, in this study regression equation was calculated using sole predictor without going through stepwise selection.

As forecast errors of wind speed in numerical forecast model has seasonal differences, forecasting equation was calculated by separating it seasonally: Spring (March to May); Summer (June to August); Fall (September to November); Winter (December, January to February).

4.1.2 Observation data for verification

Observation wind speed which was measured on top of the wind turbine(WT6, Sungsan wind farm) was used for verifying WRF forecasting and MOS forecasting data. Normally, the observation wind speed was not much different (±2.5%) with met-mast wind speed which was measured in front of wind turbine[30]. Generally, wind speed is distorted by another wind turbine when operate several wind turbine at wind farm. In this study, between 215° to 280° wind speed data was removed to reduce the wind speed distortion by another wind turbine(Fig. 4.1).

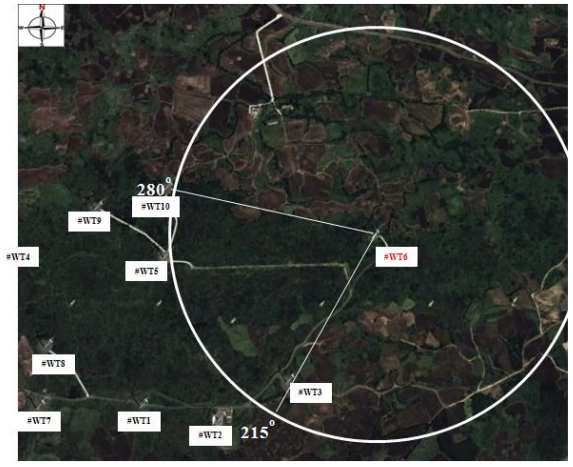


Fig. 4.1. Location of wind turbines and distortion degree(215° to 280°)

Fig. 4.2. show the power curve of wind turbine(WT #6 of Sungsan wind farm). Wind turbines produce power over a wide range of wind speeds. They cut in at between 3 and 4 m/s, reach their rated output at about 13 m/s and are regulated to produce their maximum output through to 25 m/s, when they typically shut down to protect the drive train, gearbox and structure from potential damage. Fig. 4.3 show the comparition of wind power from wind turbine and calculated wind power by observed wind speed. The difference of wind power output was very small($R^2$ = 0.994). Normally, wind power was calculated from equation (4.2).

$$P = \frac{1}{2}\rho A V^3 \tag{4.2}$$

Herein P is Electricity output from wind turbine, $\rho$ is air density, A is area of wind speed, and V is wind speed on nacelle height. In this study, wind power was calculated from power curve(V80-2.0MV) and wind speed of observation on nacelle height and forecasting by WRF model and MOS forecasting equation.

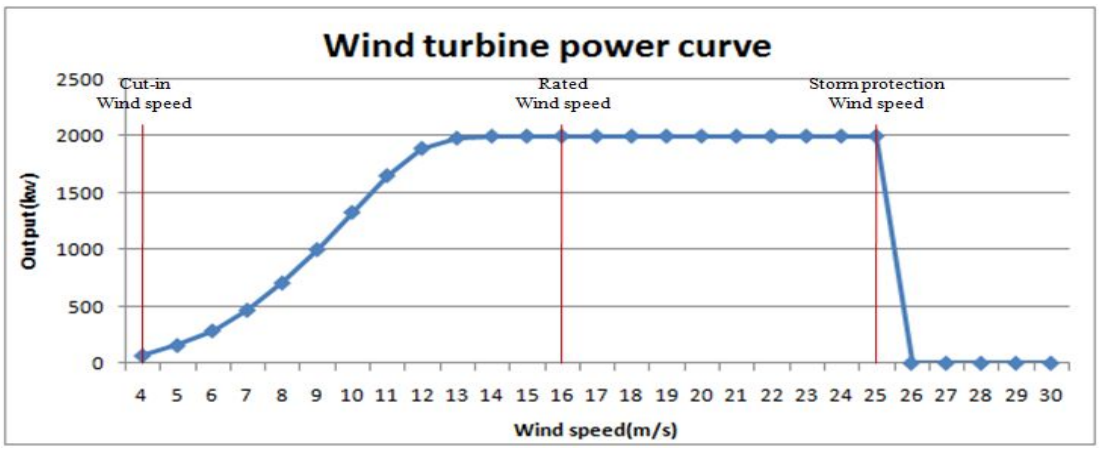


Fig. 4.2. Power curve of V80-2.0MW.

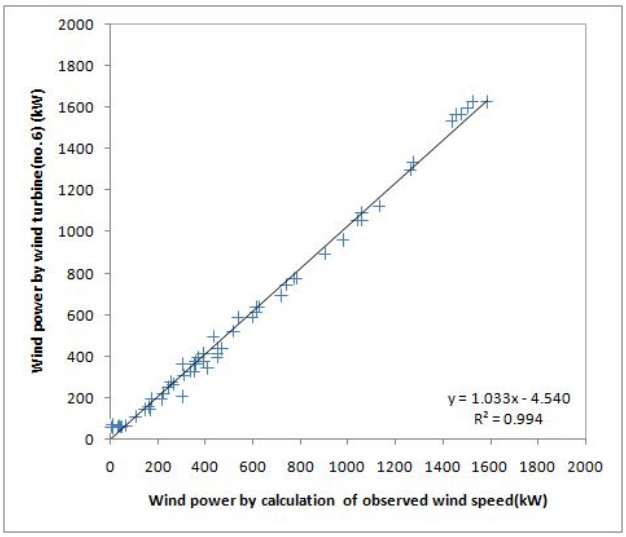


Fig. 4.3. Power output of wind turbine and calculated by observed wind speed (2012.3.1.06UTC).

4.1.3 Composition of the sample

In the composition of the sample, due to seasonality in forecast errors of wind speed of the numerical model, we divided a year into four seasons spring (March to May), summer (June ~ August), fall (September to November), and winter (December, January to February) and calculated the numerical statistics model forecast equations.

The numerical forecast model spatially calculates forecast values by the unit of grid points. It derives forecast values vertically by layers and spatially by the unit of grid points on the coordinates system of the model. Therefore, it is not capable of providing direct forecast value for a particular location and/or for a particular elevation. Moreover, the numerical model itself has systematic errors, it cannot use forecast values without modifications. There are a few objective analysis techniques for numerical forecast data for the forecast of particular locations and correction of errors using numerical model

data and those various statistical approaches are as follows: PPM(Perfect Prog. Method), MOS(Model Output Statistics), KF(Kalman Filter), etc. In PPM, the interaction formula between observation data on the ground and synoptic analysis data of the lower and middle parts of the atmosphere based on observation data and apply the formula to numerical model data. As this method assumes that numerical model is perfect and applies numerical forecast data without revision to the interaction formula of synoptic variables of the actual atmosphere and surface elements, it fails to correct errors of numerical forecast model. Unlike PPM, MOS develops interaction formula between synoptic forecast variables of numerical forecast model accumulated in the past and the surface elements observed in the past and then applies the interaction formula to numerical model data. By doing so, MOS explains systematic errors and is capable of predicting forecast elements that numerical forecast model cannot produce on particular locations other than on grid points [24-25]. In addition, by selecting different predictors at each forecast time, MOS generates forecast close to the mean average of the sample as forecast time increases and thereby provides the information about predictability of numerical forecast model and easier to approach various forecast elements [26-28]. KF corrects the differences between numerical model and observation everyday and makes management of work-site operation easier; therefore, the usability of KF at work-site operations is high. However, KF is easy to apply to such elements as temperature that has continuity and has limitation in expanding forecast elements. In general, if there is sufficient amount of numerical forecast model data accumulated for sufficient periods and if there is no change in the numerical model, MOS method is known to be most effective. Therefore, in this study MOS forecast equation for wind speed has been developed for the improvement of capability to predict wind speed and its performance has been tested and verified.

4.2. Types of forecast equations

Forecast location is the position of the 6th wind power generator in the Sungsan wind farm. Frequency of forecast is twice a day (06, 18UTC); forecast time is +00 ~ +72 hours at the interval of 1 hour; forecast equations have been generated by separating the samples by seasons. Accordingly, the total number of forecast equations is 584: 2 (frequency of forecast) x 73 (forecast time) x 4 (seasons).

Equation for calculating total errors of forecast value is shown in (4.3). Y is observation value; $\bar{Y}$ is the mean average of observation values $\hat{Y}$ is the regression estimated values. squared sum of total errors (SST) is express by squared sum of regression values (SSR) and squared sum of residual errors (SSE).

$$\underbrace{\sum(Y-\overline{Y})^2}_{SST} = \underbrace{\sum\ (\hat{Y}-\overline{Y})^2}_{SSR} + \underbrace{\sum\ (Y-\hat{Y})^2}_{} \tag{4.3}$$

The number of samples is n; the number of predictors is p; the equation of revised coefficient of determination is expressed in (4.4).

$$R_{adj}^2 = 1 - \frac{SSE/(n-p+1)}{SST/(n-1)} \tag{4.4}$$

If the regression equation is perfect, SSE becomes 0 and revised coefficient of determination becomes 1; if there is no goodness of fit by regression,

revised coefficient of determination becomes 0. Accordingly, revised coefficient of determination becomes the benchmark for judging goodness of fit. Numerical statistics model is a statistical method that corrects systematic errors of the numerical forecast model and that can generate forecast elements, which cannot be generated by the numerical forecast model, and predict at places other than grid points. Since error characteristics of the numerical forecast model differ in accordance with each forecast time, forecast errors increases in line with the increase of forecast time. Numerical statistics model forecast equations for each forecast time have been developed in order to reduce such errors and to enhance capacity to predict wind speed. For the development of numerical statistics model, numerical forecast data for sufficient periods of time must be accumulated without changes in numerical forecast model. The reason behind this is that characteristics of numerical forecast model are reflected in the generation of forecast equations as numerical statistics model develops interaction formula between forecast elements and forecast data of numerical forecast model accumulated in the past and use the formula as forecast equation. In general, the sample data of 300 are known to be the most stable sample size for the generation of stable numerical statistics model forecast equation. In this study, however, numerical statistics model equation has been developed by using approximately 180 samples per each season for usable data for the period of two years (Fig. 4.4).

Position = Sungsan(point), Ftime = + 000 h, Total freedom = 78, Radj = 43.03

| P_ID | Pname | Coefficient | STD_error | T-Value | P-Value | VIF | SD | MEAN |
|---|---|---|---|---|---|---|---|---|
| 0 | INTERCEPT | 2.92282 | | | | | | |
| 1 | WS80m | 0.61683 | 0.0797 | 7.7411 | 0.0000 | 1.0000 | 10.9561 | 7.0456 |

Position = Sungsan(point), Ftime = + 001 h, Total freedom = 79, Radj = 50.79

| P_ID | Pname | Coefficient | STD_error | T-Value | P-Value | VIF | SD | MEAN |
|---|---|---|---|---|---|---|---|---|
| 0 | INTERCEPT | 1.97446 | | | | | | |
| 1 | WS80m | 0.78345 | 0.0862 | 9.0844 | 0.0000 | 1.0000 | 10.5568 | 6.9087 |

Position = Sungsan(point), Ftime = + 002 h, Total freedom = 79, Radj = 40.74

| P_ID | Pname | Coefficient | STD_error | T-Value | P-Value | VIF | SD | MEAN |
|---|---|---|---|---|---|---|---|---|
| 0 | INTERCEPT | 2.41194 | | | | | | |
| 1 | WS80m | 0.65283 | 0.0878 | 7.4365 | 0.0000 | 1.0000 | 9.8342 | 6.5500 |

Position = Sungsan(point), Ftime = + 003 h, Total freedom = 80, Radj = 41.23

| P_ID | Pname | Coefficient | STD_error | T-Value | P-Value | VIF | SD | MEAN |
|---|---|---|---|---|---|---|---|---|
| 0 | INTERCEPT | 1.96368 | | | | | | |
| 1 | WS80m | 0.68683 | 0.0909 | 7.5574 | 0.0000 | 1.0000 | 10.6005 | 6.4444 |

Position = Sungsan(point), Ftime = + 004 h, Total freedom = 80, Radj = 40.05

| P_ID | Pname | Coefficient | STD_error | T-Value | P-Value | VIF | SD | MEAN |
|---|---|---|---|---|---|---|---|---|
| 0 | INTERCEPT | 2.31026 | | | | | | |
| 1 | WS80m | 0.62164 | 0.0842 | 7.3786 | 0.0000 | 1.0000 | 10.5790 | 6.5222 |

Position = Sungsan(point), Ftime = + 005 h, Total freedom = 80, Radj = 39.00

| P_ID | Pname | Coefficient | STD_error | T-Value | P-Value | VIF | SD | MEAN |
|---|---|---|---|---|---|---|---|---|
| 0 | INTERCEPT | 2.13695 | | | | | | |
| 1 | WS80m | 0.66278 | 0.0918 | 7.2218 | 0.0000 | 1.0000 | 9.9907 | 6.6407 |

Position = Sungsan(point), Ftime = + 006 h, Total freedom = 80, Radj = 45.18

| P_ID | Pname | Coefficient | STD_error | T-Value | P-Value | VIF | SD | MEAN |
|---|---|---|---|---|---|---|---|---|
| 0 | INTERCEPT | 1.91964 | | | | | | |
| 1 | WS80m | 0.68456 | 0.0837 | 8.1808 | 0.0000 | 1.0000 | 9.7939 | 6.5012 |

Fig. 4.4. Example of MOS equation.

Here,

- Position : the name of the point
- Ftime : forecast time
- Total freedom : the number of samples used for the generation of forecast equation (the number of data from 90 samples for each of the three month period minus missing values)
- $R^2$adj : revised coefficient of determination that denotes goodness of fit of regression equation
- Pname : the name of predictor (INTERCEPT: constant term; WS80m: forecast value of wind speed by WRF)
- Coefficient : regression coefficient for each predictor

- STD_error : standard error
- T-value : T value
- P-value : P value
- VIF : variance inflation coefficient (factor) (statistics that checks multicollinearity)
- SD : standard deviation of the samples
- MEAN : mean average of the samples

## 4.3. Variation of Coefficient and $R^2$adj

Fig. 4.5 shows the variation of coefficient and $R^2$adj at each season and each forecasting times. In this study, forecast data by WRF was normally overestimated compare with observation. So coefficient values were less than one. The maximum value of coefficient and Radj were decreased with forecasting time. This means that the goodness of fit of regression equation were getting worse with forecasting time. In this study, early stage of forecasting(0h to 6h) data was not used to prevent data distortion by model spin up.

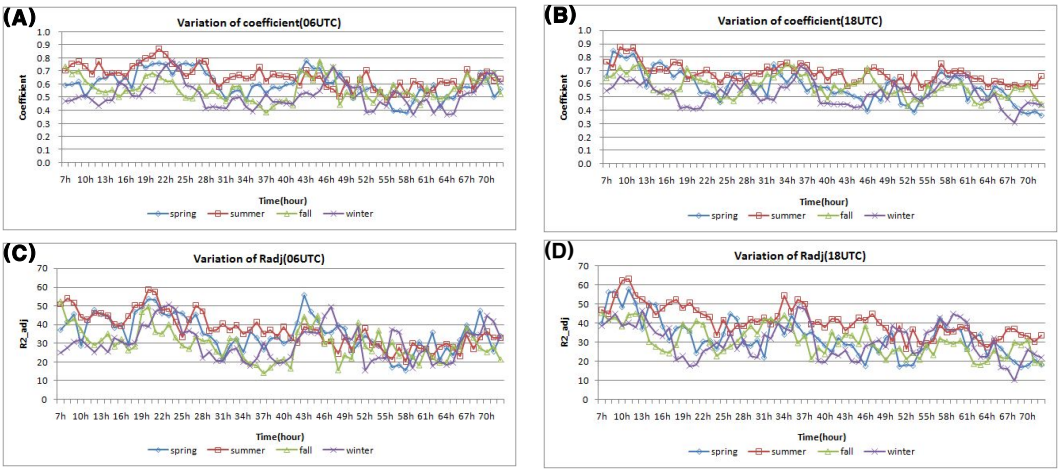


Fig. 4.5. Variation of coefficient(A:06UTC, B:18UTC) and $R^2$adj(C:06UTC, D: 18UTC).

4.4. Generation of MOS forecasting data

For the forecast of wind speed at the interval of one hour at the point of Sungsan, forecast data and observation data of WRF, a numerical forecast dynamics model, were used; WRF forecast data produce 06UTC data and 18UTC data (twice a day); these data are predicted data at the interval of one hour from +00 hour to +72 hours for each time.

The period of data used for analysis is from July 1, 2009 to June 30, 2011; data used were 06UTC and 18UTC forecast data (twice a day) and 80m wind speed forecast data from +00 hour to +72 hour at the interval of one hour for WRF model for the observed data, wind speed generated at 80m above the ground at the interval of 1 hour were used.

4.5. Independent test and verification

During the period of the study, the data from July 2009 to June 2011 were used as data for numerical model statistics; the data from July 2011 to June 2012 were used as data for independent verification. Verification of BIAS and RMSE were executed for forecast equation using data for independent verification: spring (March to May 2012); summer (July to August 2011 and June 2012); fall (September to November 2011); and winter (December 2011 and February to March 2012).

$$BIAS = \frac{1}{N}\sum_{n=1}^{N} (f_n - O_n) \tag{4.5}$$

$$RMSE = \sqrt{\frac{1}{N}\sum_{n=1}^{N} (f_n - O_n)^2} \tag{4.6}$$

Table 4.1 Sample data and verification period.

| | Period for MOS Equation | Verification for MOS Equation |
|---|---|---|
| Spring | 3~5. 2010<br>3~5. 2011 | 3~5. 2012 |
| Summer | 7~8. 2009<br>6~8. 2010, 6. 2011 | 7~8. 2011, 6. 2012 |
| Fall | 9~11. 2009 | 9~11. 2011 |
| Winter | 12. 2009, 1~2. 2010<br>1~2. 2011 | 12. 2011, 1~2. 2012 |

For the forecast of wind speed at the interval of one hour at the point of Sungsan, forecast data and observation data of WRF, a numerical forecast dynamics model, were used; WRF forecast data produce 06UTC data and 18UTC data (twice a day); these data are predicted data at the interval of one hour from +00 hour to +72 hours for each time. The period of data used for analysis is from July 1, 2009 to June 30, 2011; data used were 06UTC and 18UTC forecast data (twice a day) and 80m wind speed forecast data from +00 hour to +72 hour at the interval of one hour for WRF model; for the observed data, wind speed generated at 80m above the ground at the interval of 1 hour were used.

Table 4.2 shows average BIAS and average RMSE of 06UTC entire verification period (July, 2011 ~ June, 2012) at the Sungsan point; Table 4.3 shows average BIAS and average RMSE of 18UTC. The forecast of wind speed by WRF by and large tends to over-predict (BIAS of quantity); numerical statistics model tends to reduce errors of quantity of WRF model.

While WRF, in case of forecast errors of 06UTC, shows errors of approximately 3.0 m/s, numerical statistic model shows error of 2.7 m/s, resulting in 0.3 m/s reduction of RMSE. Especially in 18UTC forecast, we can find out that BIAS of WRF model becomes larger than BIAS of 06UTC. In the case of numerical statistics model, BIAS of large WRF model, which is similar to 06UTC, tends to be reduced. Correction effect of 18UTC RMSE errors is 0.3 m/s, which is similar to 06UTC. However, in the case of BIAS during winter, BIAS of quantity tended to be rather increased. Judging by such result, additional study is necessary through the increase of the sample size and increase of predictors.

Table 4.2. BIAS and RMSE at 06UTC during, July. 2011 to Jun. 2012.

| | MOS(BIAS) | WRF(BIAS) | MOS(RMSE) | WRF(RMSE) |
|---|---|---|---|---|
| Spring | 0.006 | 0.180 | 2.890 | 3.144 |
| Summer | -0.107 | 0.335 | 2.491 | 2.662 |
| Fall | 0.706 | 0.840 | 2.601 | 2.659 |
| Winter | 0.451 | 0.412 | 2.659 | 3.022 |

Table 4.3. BIAS and RMSE at 18UTC during, July. 2011 to Jun. 2012.

| | MOS(BIAS) | WRF(BIAS) | MOS(RMSE) | WRF(RMSE) |
|---|---|---|---|---|
| Spring | 0.031 | 0.248 | 2.959 | 3.258 |
| Summer | -0.054 | 0.467 | 2.463 | 2.622 |
| Fall | 0.698 | 0.974 | 2.649 | 3.100 |
| Winter | 0.487 | 0.438 | 2.735 | 3.176 |

Fig. 4.6 to 4.13 show the BIAS and RMSE of 06UTC and 18UTC by forecast time and by season at the point of Sungsan from July 2011 to June

2012. Overall, tendency of BIAS shows value of quantity and BIAS of MOS decreased more than BIAS of WRF. Also, RMSE of MOS decrease somewhat compare to MOS of RMSE; especially RMSE of MOS decreased after +45h.

MOS skill is usually depend on the amount of forecast output. So in this study, I was calculate the MOS equation using only one year forecast data(2010. 7 ~ 2011. 6) and calculated RMSE and BIAS of Summer and winter season with independent data(2011. 7 ~ 2012. 6). Table 4.4 show the RMSE and BIAS which was used one year data set. RMSE of MOS was increased both 06UTC and 18UTC during both summer and winter seasons, respectively. Especially, BIAS side the effectiveness was more significant. BIAS of MOS was increased almost double value compare with two years data set. It means that two years data set is more effectively work to reduce the bias of wind speed forecasting through MOS.

Table 4.4. BIAS and RMSE of one years data set using(July 2011 to Jun 2012).

| | MOS(BIAS) | WRF(BIAS) | MOS(RMSE) | WRF(RMSE) |
|---|---|---|---|---|
| Summer(06UTC) | -0.275 | 0.335 | 2.498 | 2.622 |
| Winter(06UTC) | 0.725 | 0.412 | 2.723 | 3.022 |
| Summer(18UTC) | -0.221 | 0.467 | 2.475 | 2.622 |
| Winter(18UTC) | 0.781 | 0.438 | 2.812 | 3.176 |

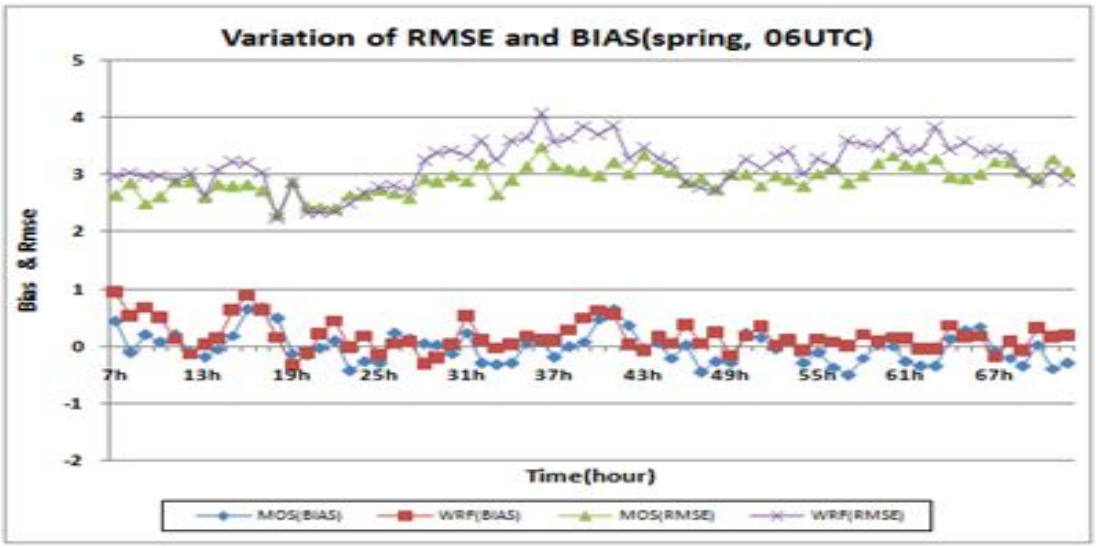


Fig. 4.6. Variation of bias and RMSE for MOS and WRF at 06UTC(spring).

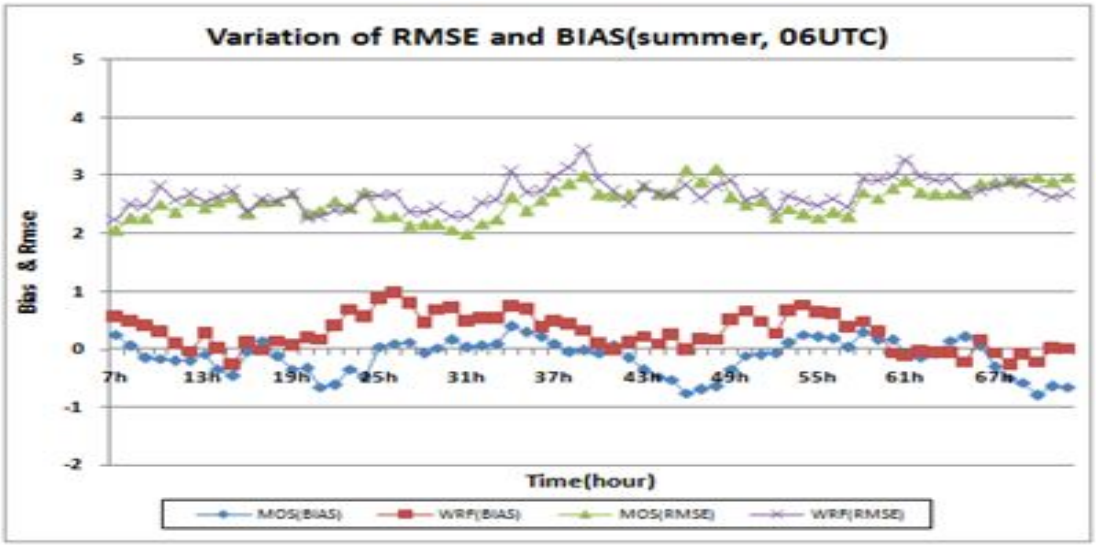


Fig. 4.7. Variation of bias and RMSE for MOS and WRF at 06UTC(summer).

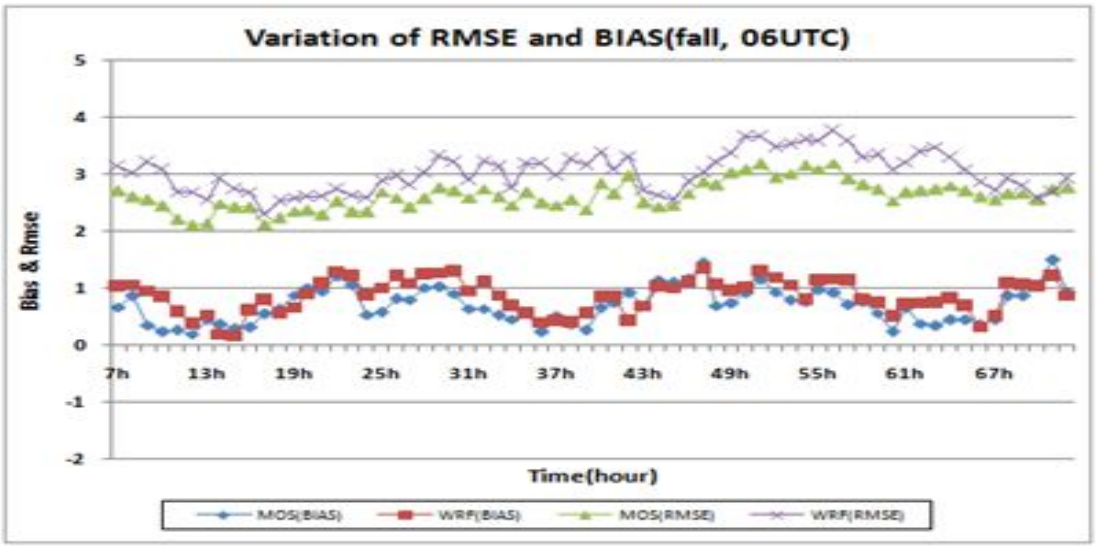


Fig. 4.8. Variation of bias and RMSE for MOS and WRF at 06UTC(fall).

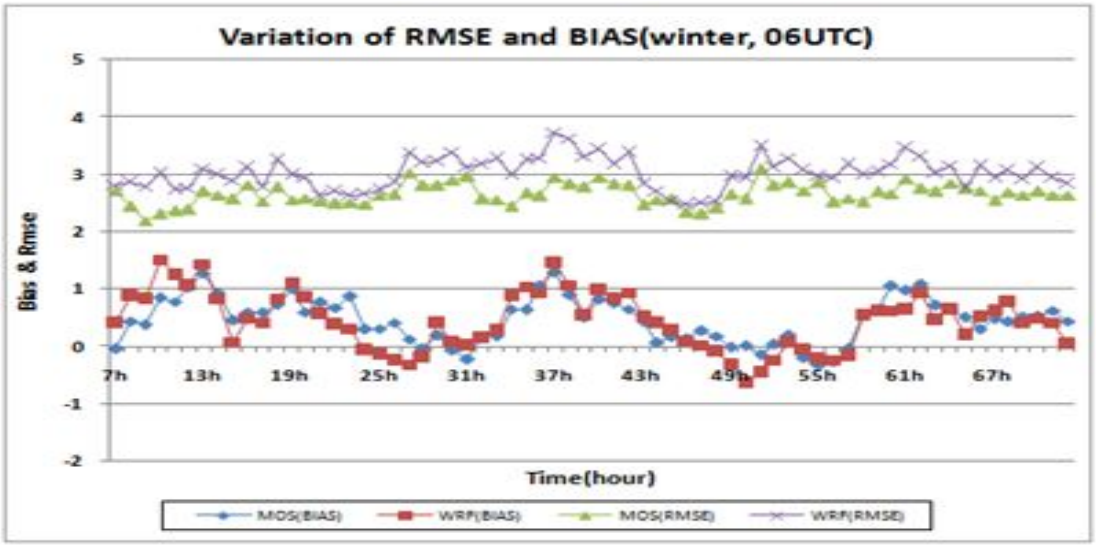


Fig. 4.9. Variation of bias and RMSE for MOS and WRF at 06UTC(winter).

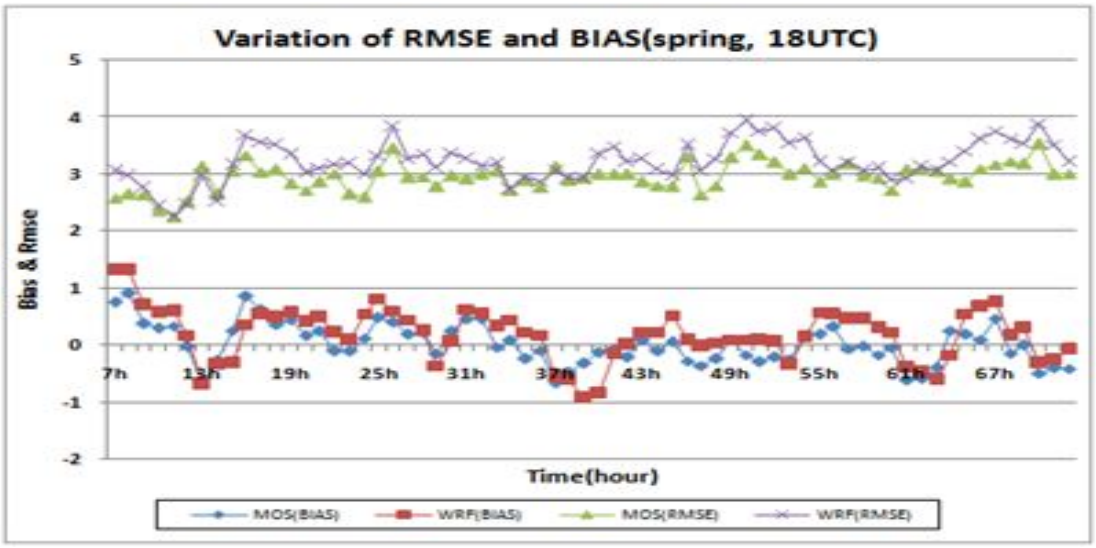


Fig. 4.10. Variation of bias and RMSE for MOS and WRF at 18UTC(spring).

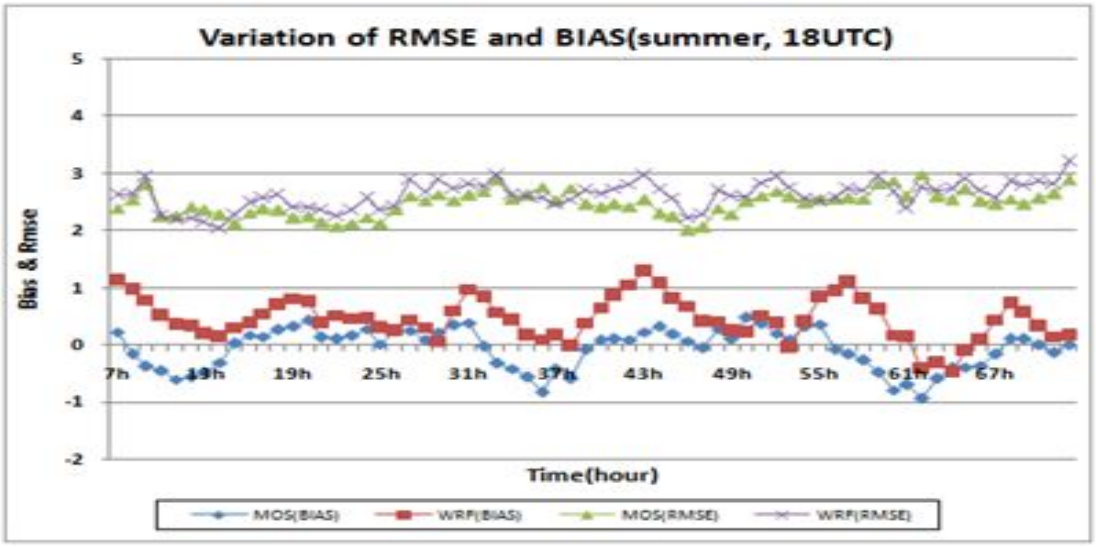


Fig. 4.11. Variation of bias and RMSE for MOS and WRF at 18UTC(summer).

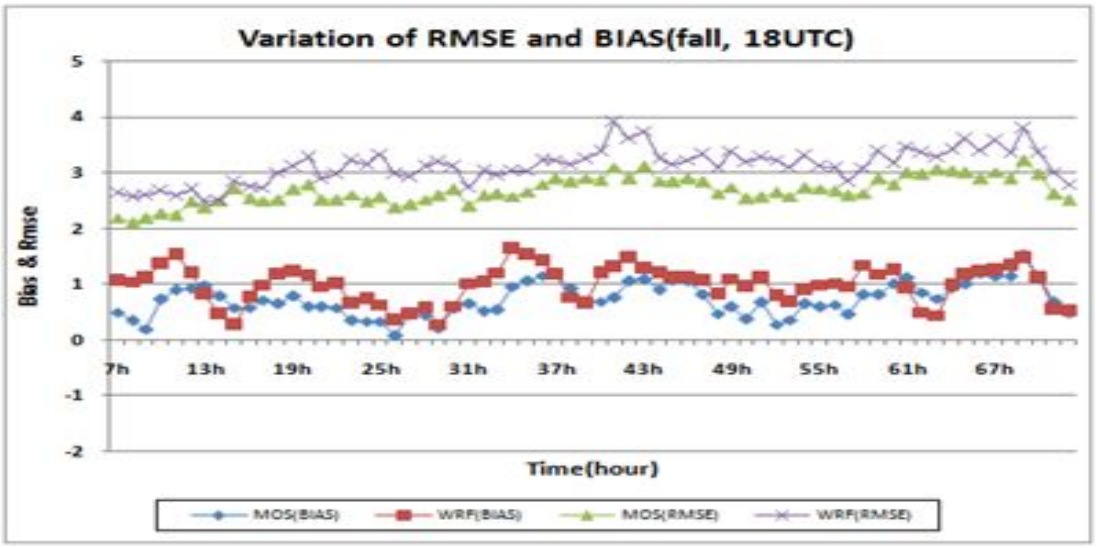


Fig. 4.12. Variation of bias and RMSE for MOS and WRF at 18UTC(fall).

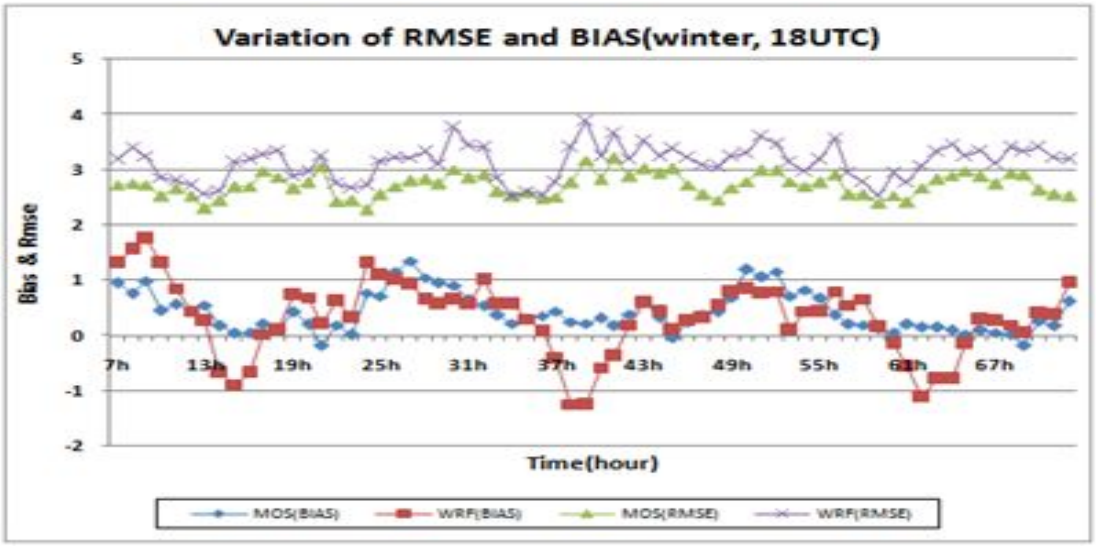


Fig. 4.13. Variation of bias and RMSE for MOS and WRF at 18UTC(winter).

Fig. 4.14. and Fig. 4.15. shows the comparison between observed wind speed and forecasted wind speed by WRF and MOS during different forecasting time. The $R^2$ from the comparison between observation and MOS was higher than WRF. But +72h forecasting of $R^2$ was little lower than WRF. The lower $R^2$ of +72h forecasting of MOS could understand from the high rmse and bias during spring to fall on 06UTC forecasting.

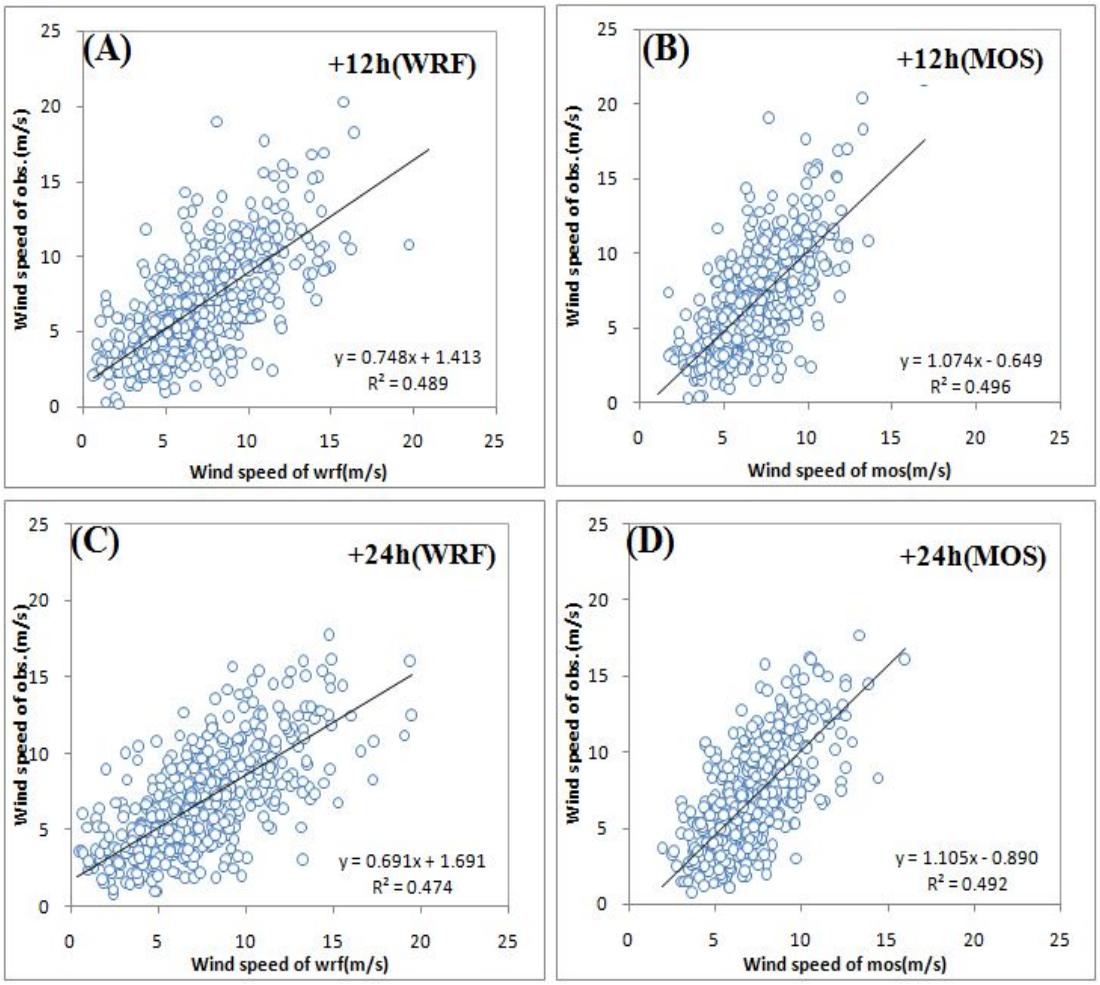


Fig. 4.14. Comparison between observed wind speed and forecasted wind speed by WRF and MOS(A: +12h WRF, B: +12h MOS, C: +24h WRF, D: +24h MOS.

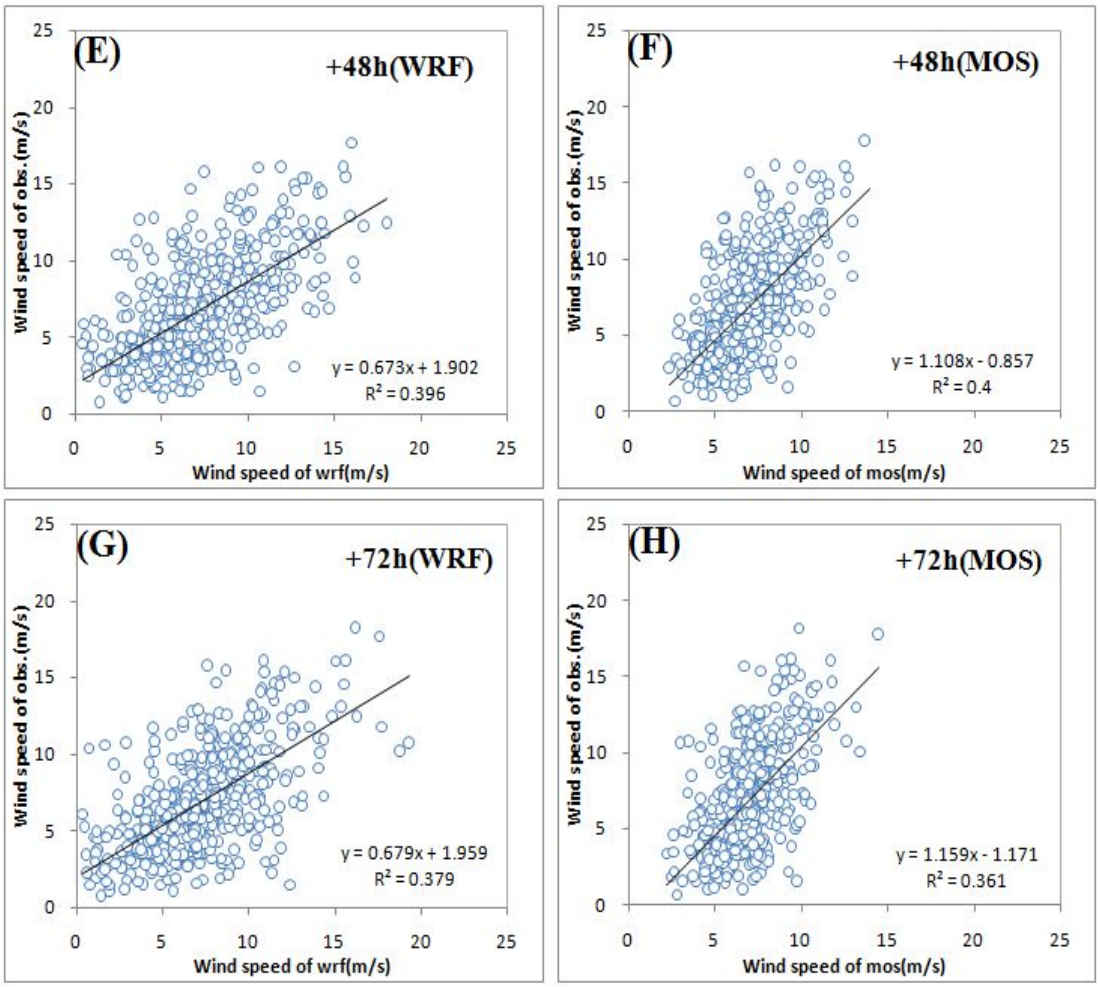


Fig. 4.15. Comparison between observed wind speed and forecasted wind speed by WRF and MOS(E: +48h WRF, F: +48h MOS, G: +72h WRF, H: +72h MOS.

4.6. Sample data analysis

In order to study fluctuations by day, the forecast data for the 6th wind power generator at Sungsan wind farm for summer (July 1 2011 06UTC & 18UTC) and for winter (December 1 2011 06UTC & 18UTC) were selected. Generated were the time series about observation data at 06UTC & 18UTC on July 1 2011 and 06UTC & 18UTC on December 1 2011 and 0h~72h forecast data predicted in the model and forecast data processed by MOS (Model Output Statistic). Predicted observation wind velocities at 06UTC & 18UTC on July 1, 2011 shows fluctuations from approximately 1 m/s to 10 m/s; though changes in predicted wind speed in line with changes in actual wind speed were well corresponded, after 48h predicted wind speed was higher than observed wind speed. (yet, in the case of 18UTC, predicted values after 62h were lower than the observed values.) This implies that in the forecast of the amount of generated electricity, the predicted amount can be smaller than actual amount. However, the fluctuations in the MOS predicted data, compare to wind speed predicted in the model, turned out to somewhat more similar to the observed wind speed. On December 1, 2011, which is winter season, the fluctuations were smaller than those in the summer, observation and forecast and MOS forecast were nearly similar.

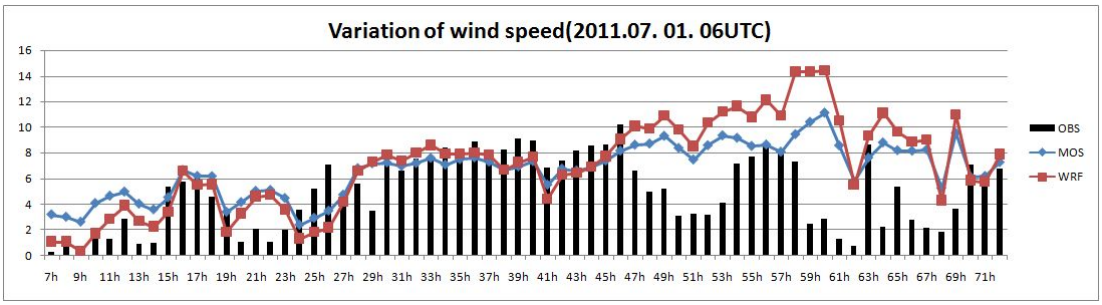


Fig. 4.16. Variation of wind speed(06UTC 1st July 2011)

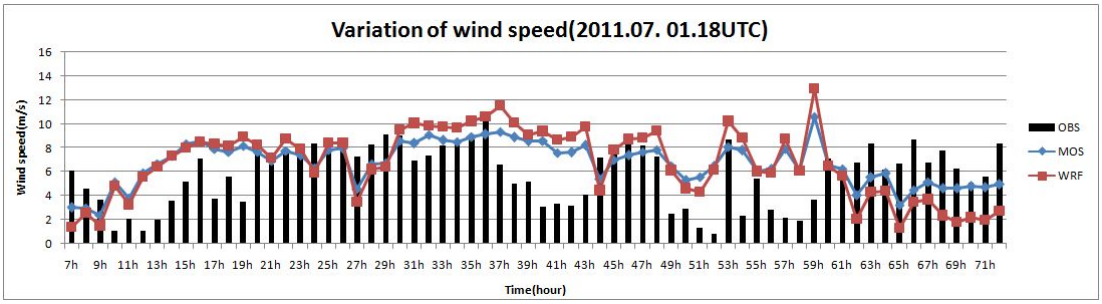


Fig. 4.17. Variation of wind speed(18UTC 1st July 2011)

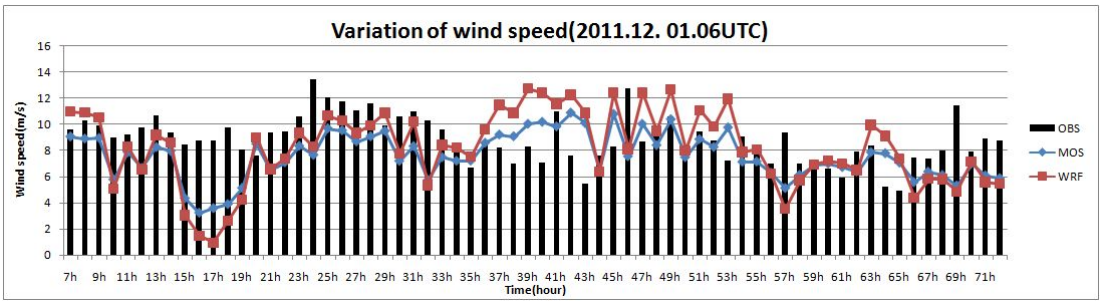


Fig. 4.18. Variation of wind speed(06UTC 1st December 2011)

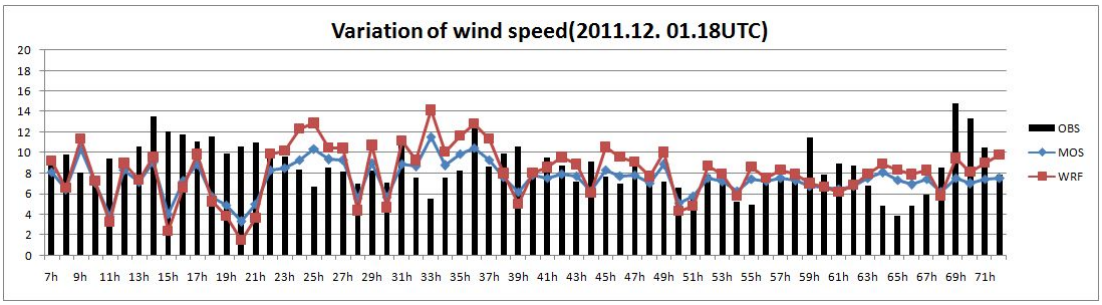


Fig. 4.19. Variation of wind speed(18UTC 1st December 2011)

## 4.7. Annual average variation of forecasting wind speed

In order to examine the long-term forecast outcomes, mean averages of changes in observed and predicted wind speed by each forecast time from July 2011 to June 2012 were analyzed(Fig. 4.20 ~ 4.22). Wind speed was in the range of 6 m/s ~ 8 m/s in both WRF model and MOS forecasting and overestimated of wind speed was appeared. In the outcome of forecast of both WRF model and MOS, wind speed during daytime was similar to observation of diurnal variation of high wind speed. Especially, in the case of WRF model predicted in 18UTC, predicted values preceded about 3 hours in the area where wind speed is high during daytime; however, such tendency was removed in the case of MOS. Moreover, in the case of both WRF model and MOS forecast, predicted wind speed in both models are higher than the observed wind speed. This suggests that if forecast data of WRF model and MOS forecast are used in the forecast of actual amount of generated electricity, the amount of generated electricity is overestimated. However, in the case of predicted wind speed of MOS compare to WRF model, the tendency of overestimation is smaller and thus the difference between actual amount of generated electricity and predicted amount by MOS forecasting is smaller.

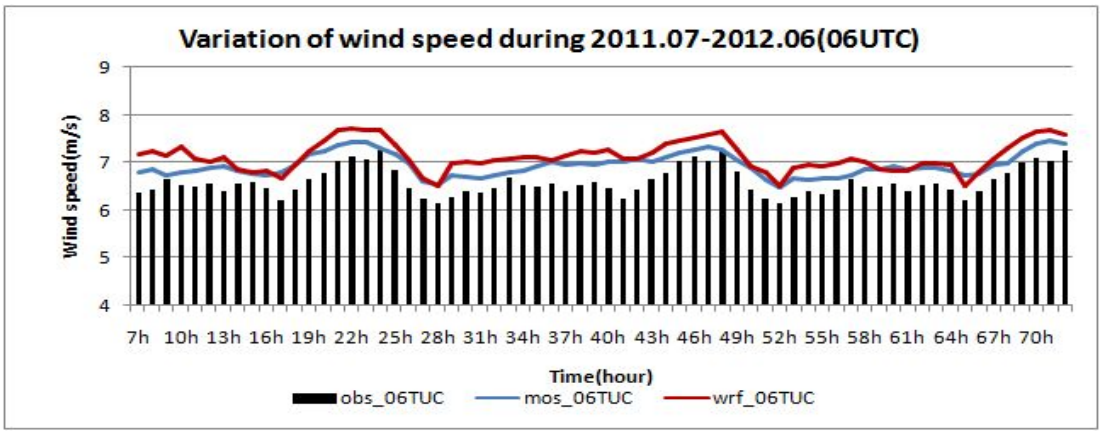


Fig. 4.20. Averaged wind speed(06UTC)

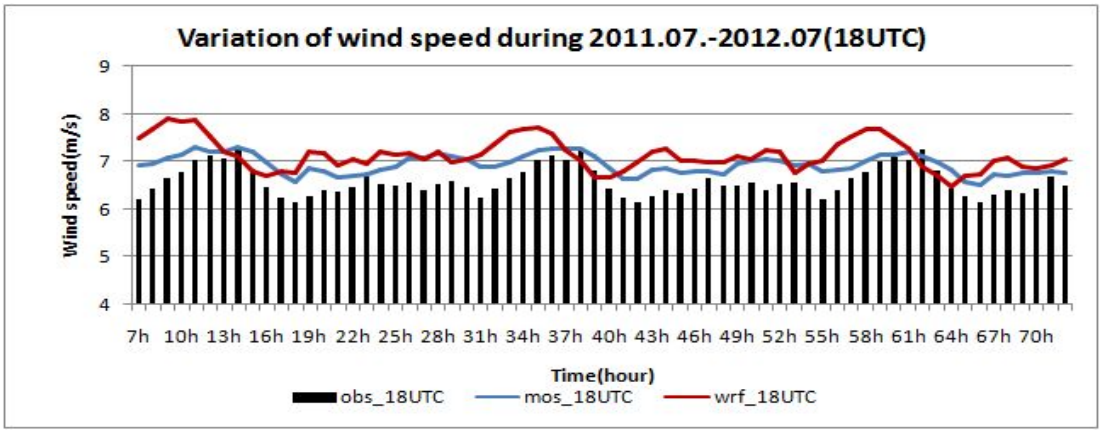


Fig. 4.21. Annual averaged variation of wind speed(18UTC)

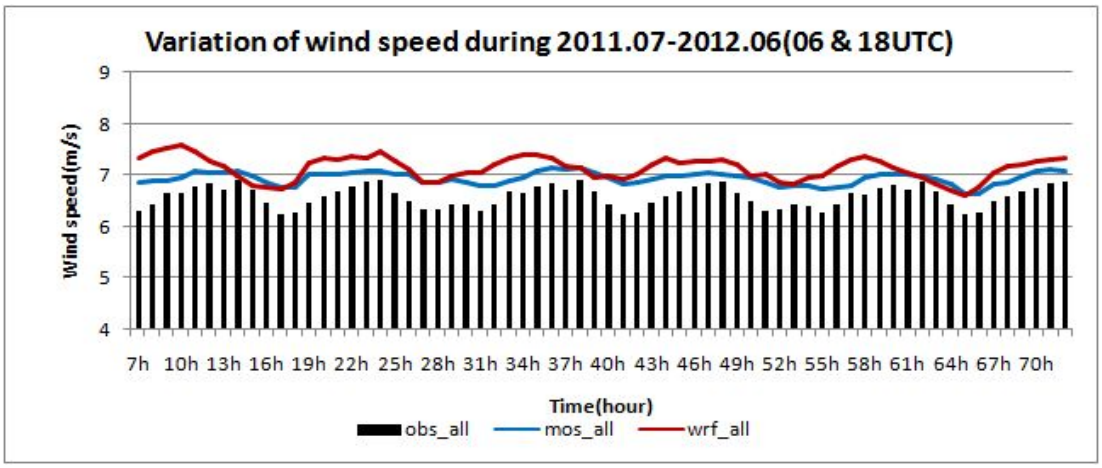


Fig. 4.22. Annual averaged variation of wind speed(all time)

4.8. Comparison of seasonal wind speed

Fig. 4.23 ~ 4.28 are ratios of seasonal average wind speed predicted in both WRF model and MOS to the observed wind speed at forecast time (24h, 48h, and 72h) and at 06UTC and 18UTC. In 06UTC 24h forecast outcomes, in spring and winter, the differences between the forecast by WRF model and MOS were less than about 5%. However, in summer and in fall, the differences between the predicted wind speed in WRF model and the observed wind speed were greater 11.4% in summer and 14.8% in fall. Especially in Fall, the forecast by MOS also showed somewhat great difference of 9.4%. 18UTC 24h forecast outcomes showed greater errors for all the four seasons than 06UTC. Especially, WRF showed great difference (5.8% ~ 16.1%) during seasons while the forecast by MOS showed smaller errors (approximately 1.3% ~ 8.9%). The outcome of WRF forecast at 06UTC 48h showed tendency to overestimate from 3.9% to 17.1% during spring to fall and underestimate -4.2% during winter. In the case of MOS forecast, in spring and summer, the forecast has tendency to underestimate compare to the observed wind speed. However, the differences were not great (less than -6.5%). In 18UTC 48h forecast, in the case of WRF, the differences are not greater in spring and winter(about 3%). However, in summer and fall, WRF forecast showed 10.5% ~ 14.5% difference. In the case of MOS forecast was less than 8.9%. In 06UTC 72h forecast outcome, WRF forecast and MOS forecast were not great(less than ±6%) except fall(about 14.1% for MOS, 12.7% for WRF). In 18UTC 72h forecast outcome, the forecast outcome of WRF model showed insignificant differences in spring. But summer, fall, winter were over than about 10%. MOS forecast outcome showed fewer errors than WRF model forecast outcome(less than 10%).

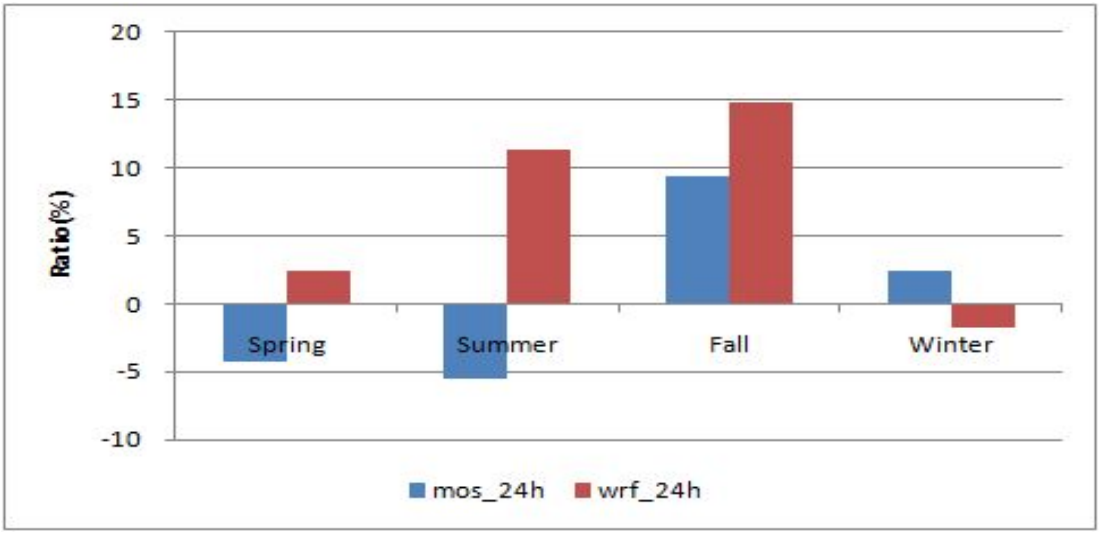


Fig. 4.23. Comparison of seasonal wind speed ratio of 24h forecast(06UTC)

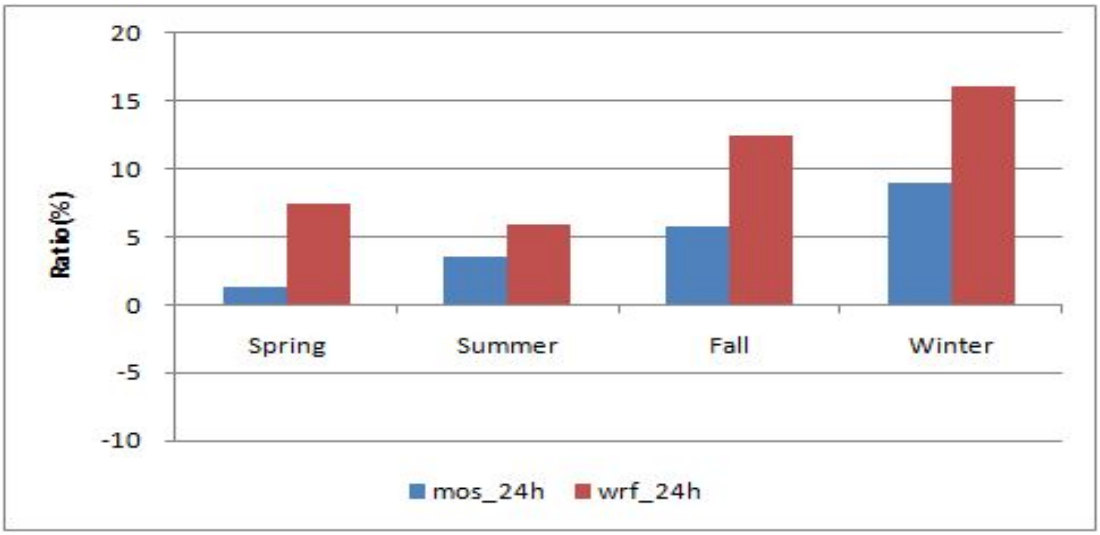


Fig. 4.24. Comparison of seasonal wind speed ratio of 24h forecast(18UTC)

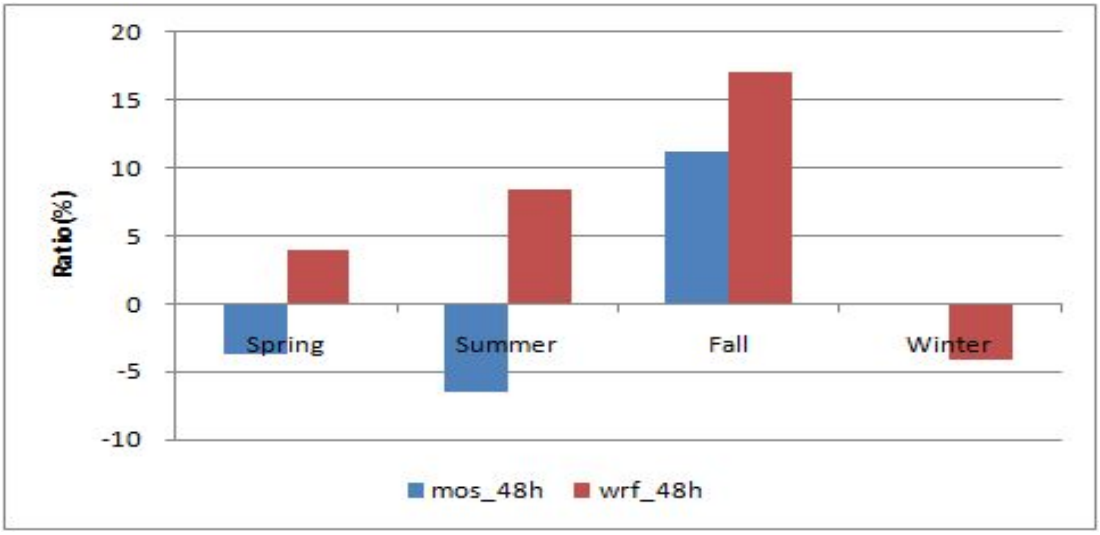


Fig. 4.25. Comparison of seasonal wind speed ratio of 48h forecast(06UTC)

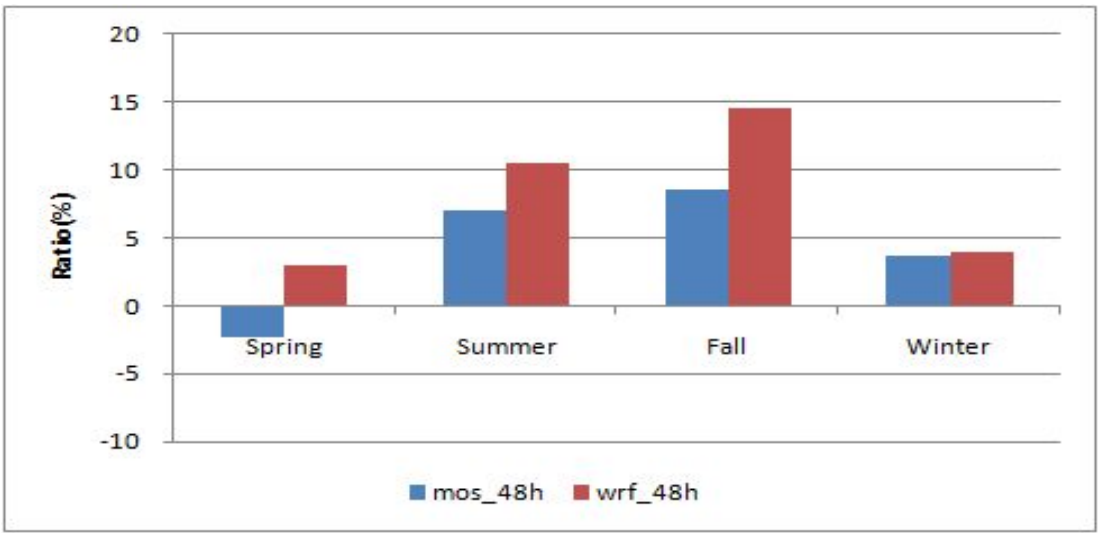


Fig. 4.26. Comparison of seasonal wind speed ratio of 48h forecast(18UTC)

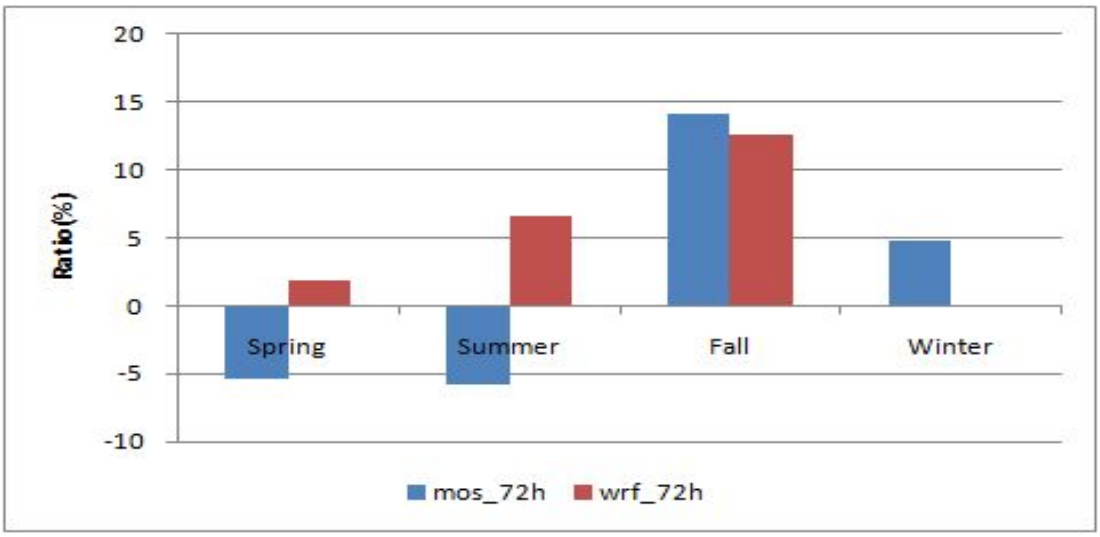


Fig. 4.27. Comparison of seasonal wind speed ratio of 72h forecast(06UTC)

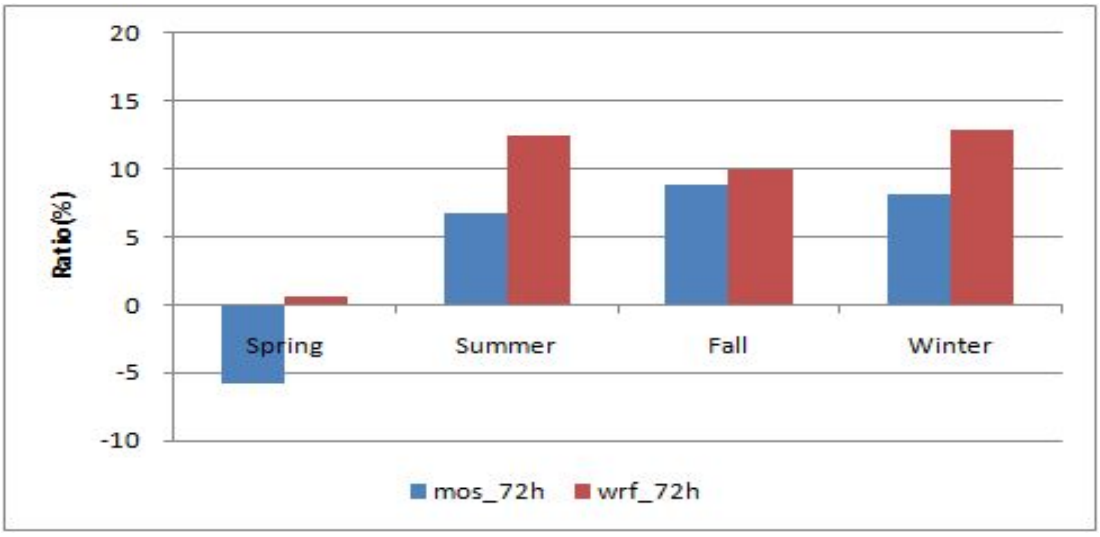


Fig. 4.28. Comparison of seasonal wind speed ratio of 72h forecast(18UTC)

Fig. 4.29. ~ 4.30. shows the ratio of wind speed comparison by wind direction and forecast time, respectively. In the outcome of 06UTC, between 0° ~ 215° wind speed difference between WRF model and observation were larger than another wind direction section. Meanwhile, in the outcome of 18UTC, between 215° ~ 360° wind speed difference was larger than another wind direction section. These results might be from the different main wind direction on daytime(06UTC) and nighttime (18UTC), but it need more research of wind forecasting on different wind direction by WRF model forecasting. In the outcome of MOS, 06UTC and 18UTC wind speed difference were, mostly smaller than WRF model's wind speed, but the difference between 280° ~ 360° wind direction showed the typically large underestimate. it need more analysis on the wind speed forecasting through wind direction, and also it need re-calculation of MOS forecast equation by wind direction.

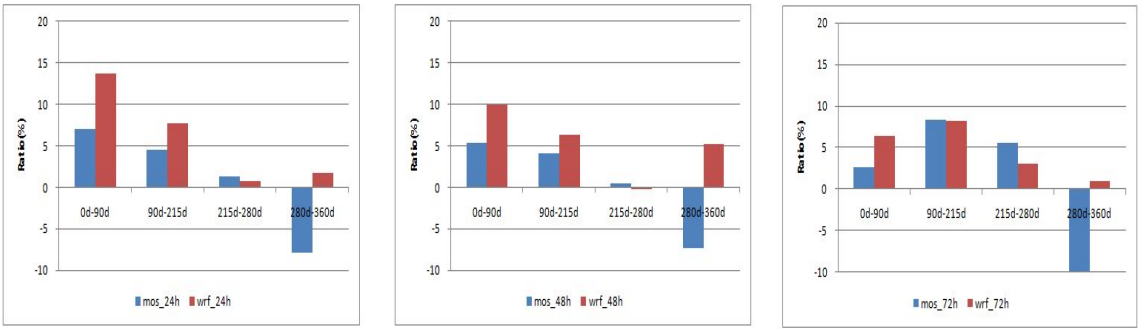


Fig. 4.29. Comparison of wind speed ratio by wind direction(06UTC)

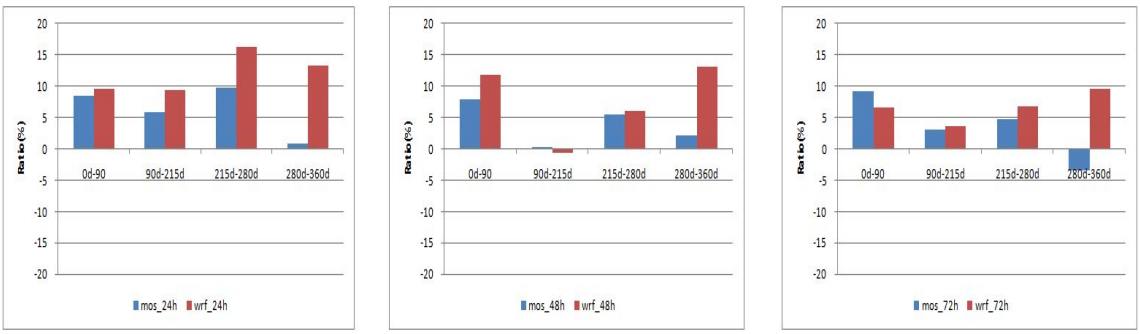


Fig. 4.30. Comparison of wind speed ratio by wind direction(18UTC)

4.9. Comparison of seasonal wind energy

Fig. 4.29 ~ 4.34 shows the ratio between calculated wind energy from observed wind speed to calculated wind energy from forecast wind speed by WRF and MOS forecast equation at 06UTC and 18UTC by forecast time (24h, 48h and 72h). In the outcome of 06UTC 24h forecast, the differences between the amount of wind energy calculated by the observed wind speed and the amount of wind energy predicted by WRF model was significantly great more than 40.4% ~ 53.9% in summer and fall. Yet in spring and winter, the differences between the amount of wind energy predicted in WRF model and the amount of wind energy calculated from the observed wind energy were less than 7.8%(spring) and -5.3%(winter), respectively. The difference of MOS was -12.8%, -16.7%, 32.6% and 7.4% during spring, summer, fall and winter, respectively. In the outcome of 18UTC 24h forecast, difference by WRF was greater than MOS through all seasons. Especially, in the case of WRF model forecast, greater errors were 44.8% ~ 59.4% during fall and winter. Meanwhile, the difference of MOS was not significant (approximately 4.3% ~ 30.6%) during seasons.

In the outcome of 06UTC 48h forecast, WRF forecast showed tendency to overestimate about 29.0% ~ 63.9% during summer and fall. But in the case of spring and winter, the difference between WRF forecast and the observed wind energy was not great(less than ±13%). In the case of MOS, the predicted values have tendency to underestimate compare to the observed wind energy in spring and summer, but the difference was not significant (-11.3% ~ -19.5%) during spring and winter, respectively. In the 18UTC 48h WRF forecast, the difference between the predicted values and the observed values were not great in spring and winter about 9.8 ~ 12.8%. However, in summer and fall, WRF forecast showed difference of 39.5 ~ 53.3% and MOS forecast showed difference -7.0%, 25.9%, 29.9% and 12.2% during spring,

summer, fall and winter, respectively.

In the outcome of 06UTC 72h forecast, the difference by WRF forecast and MOS forecast were not great in spring and winter however, in summer and fall the WRF forecast showed significant errors about 22.2% ~ 45.2%. Especially, in fall MOS forecast outcome showed greater difference(51.4%) than forecast outcome by WRF model. In the outcome of 18UTC 72h forecast, the difference between the predicted value by WRF model and the observed value showed insignificantly different. In summer, fall, and winter, the predicted value by MOS showed smaller difference than the predicted value of WRF model.

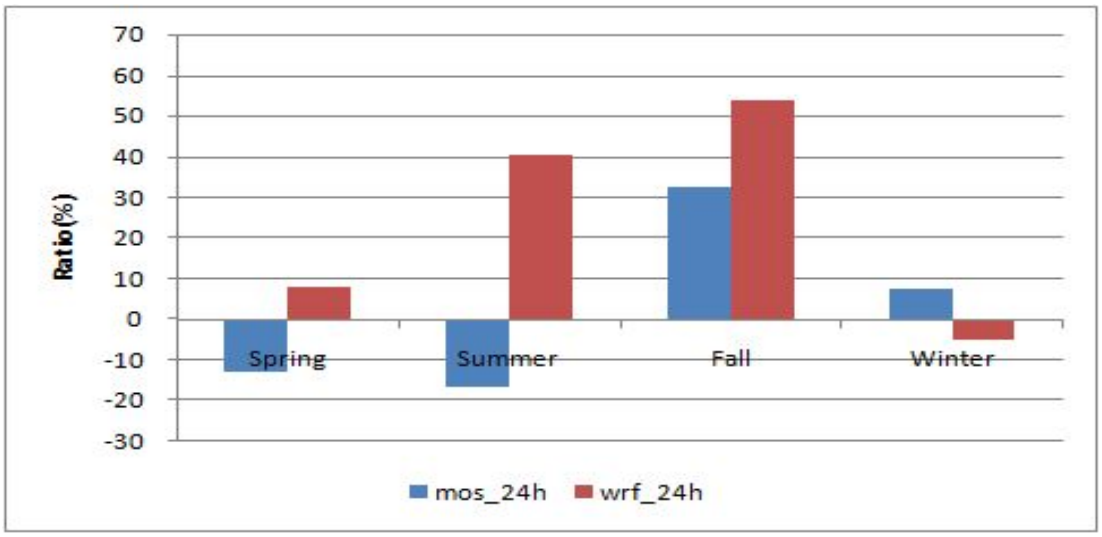


Fig. 4.31. Comparison of seasonal wind energy ratio of 24h forecast(06UTC)

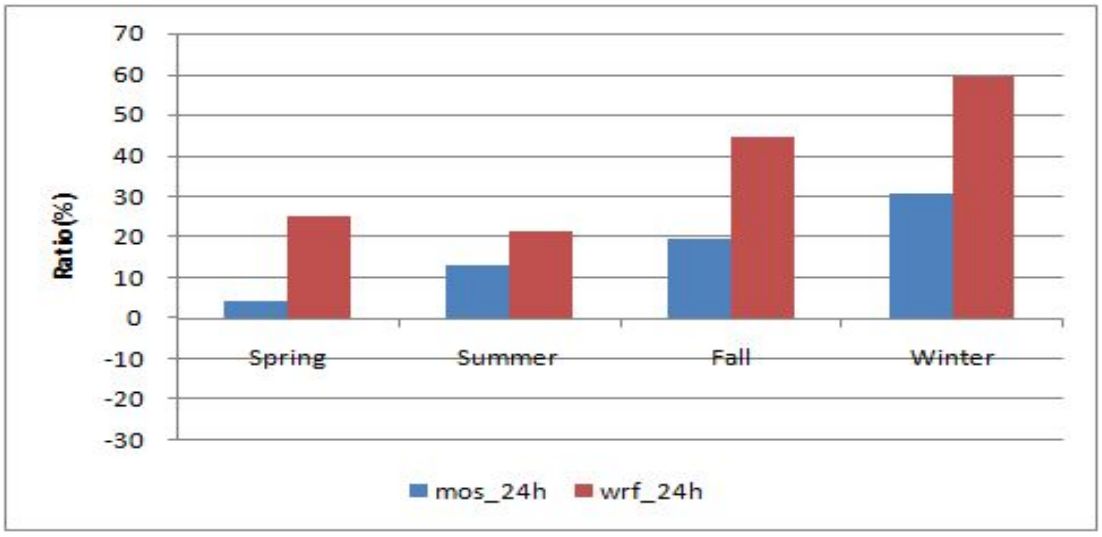


Fig. 4.32. Comparison of seasonal wind energy ratio of 24h forecast(18UTC)

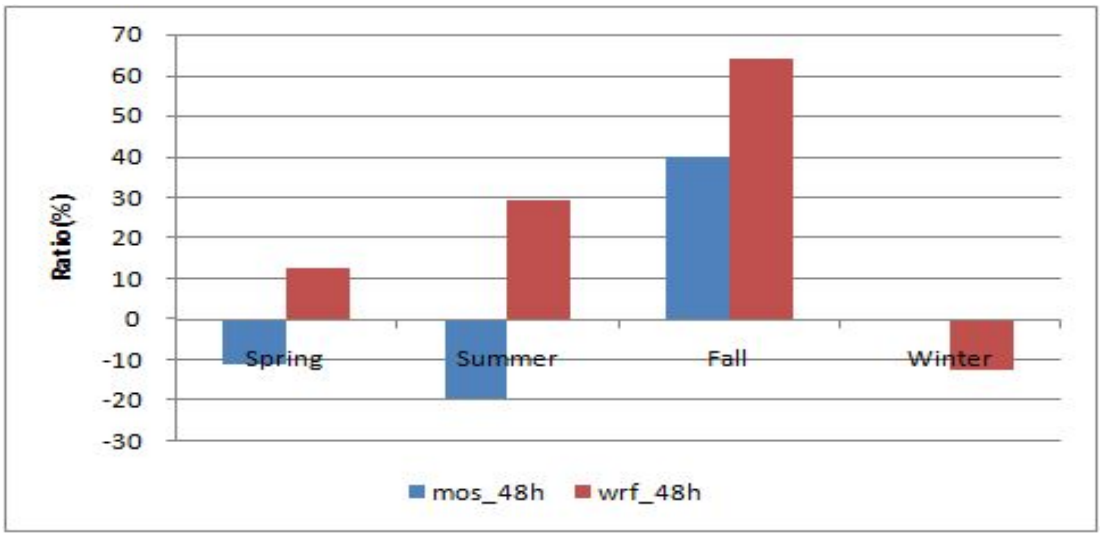


Fig. 4.33. Comparison of seasonal wind energy ratio of 48h forecast(06UTC)

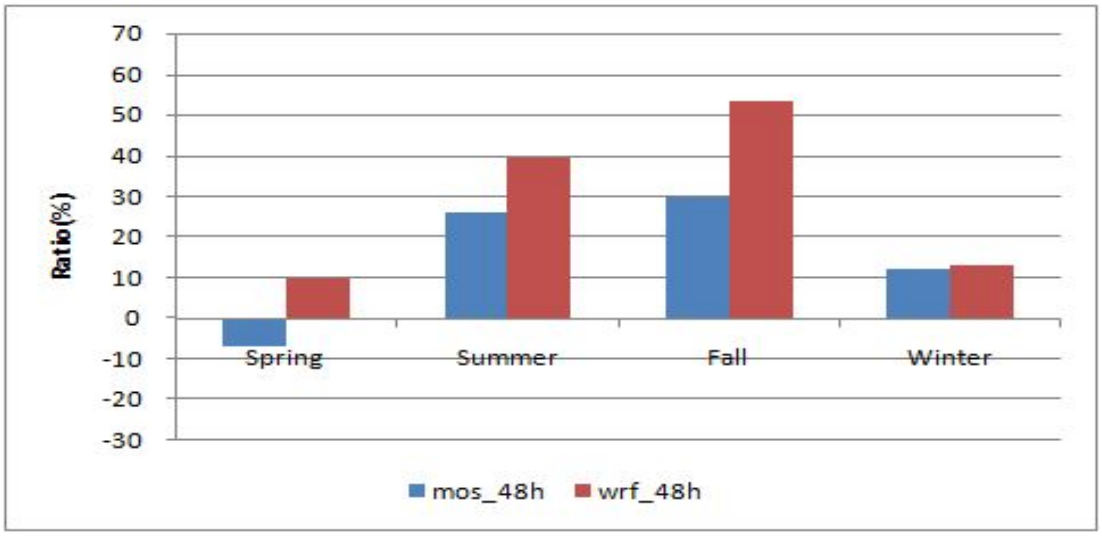


Fig. 4.34. Comparison of seasonal wind energy ratio of 48h forecast(18UTC)

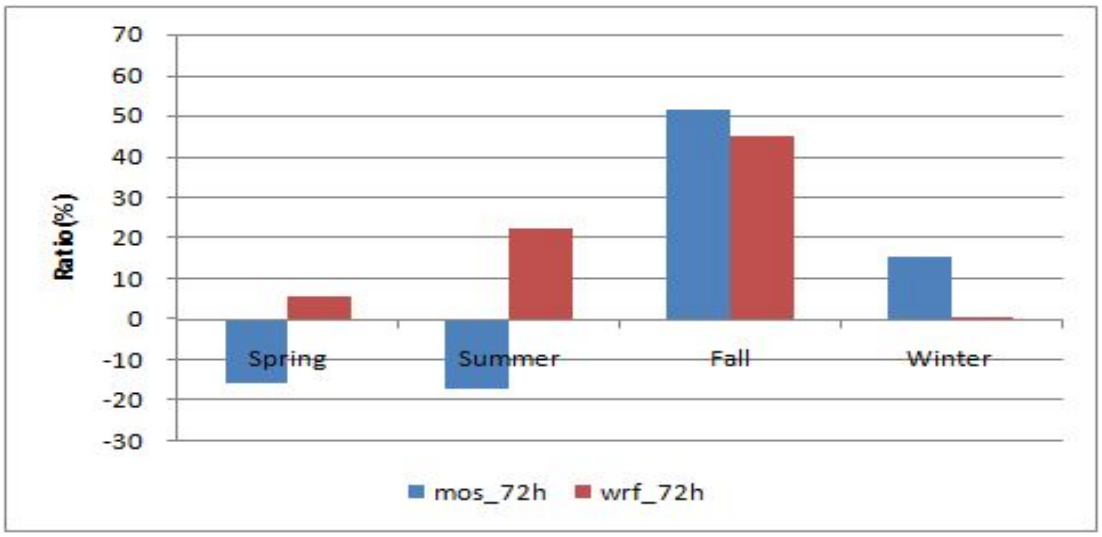


Fig. 4.35. Comparison of seasonal wind energy ratio of 72h forecast(06UTC)

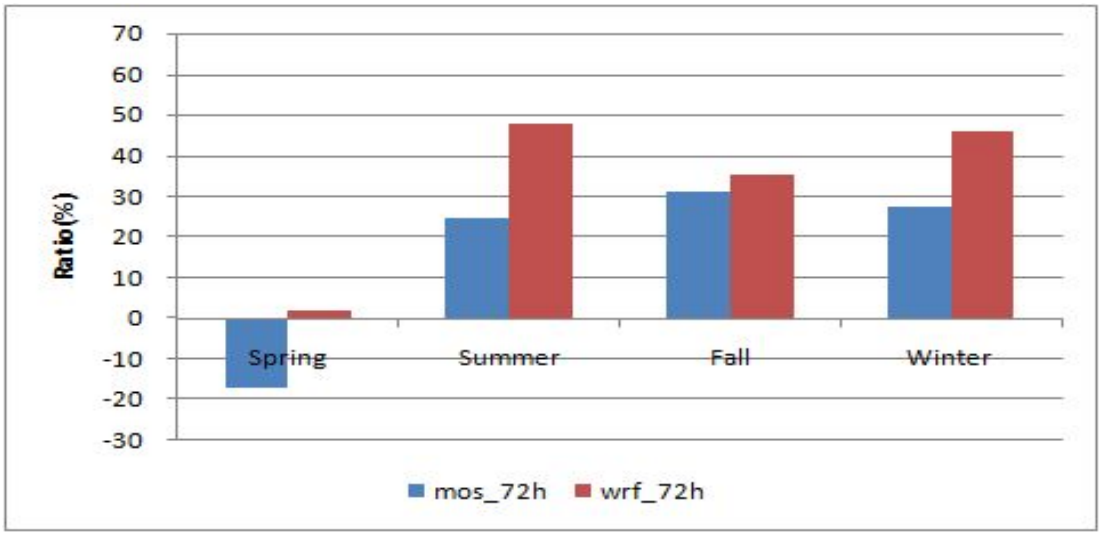


Fig. 4.36. Comparison of seasonal wind energy ratio of 72h forecast(18UTC)

# Ⅴ. Conclusions

Wind power plays an important role in supplying sustainable electricity and shows significant growth for the past few years. And recently electricity generated by wind turbine at wind farm has become an important part of various energy sources in national level. However, since forecasting of electricity from wind turbine at wind farm is determined by accurate forecasting of wind speed. But it is not easy to get the accurate wind speed after several days.

In this study, MOS forecast equation was developed to improve wind speed and wind power forecasting with WRF model output data. It is well known about MOS equation can make more accurate forecast wind speed at the point of model grid points. To evaluate the performance of MOS forecast equation I compared one year data set and two years data set of WRF model, respectively. When apply just one year data set on calculating of BIAS and RMSE of MOS forecast were increased both forecasting time(06UTC and 18UTC) during summer and winter seasons but, RMSE was not much different with comparison of two years data set. It means that more model output data using is effectively work to reduce the bias of wind speed forecasting through the MOS method.

Also, wind energy calculated from the predicted wind speed from WRF model and MOS forecast equation. The result 24h forecast result using two years numerical model output data, in case of 06UTC by WRF model were over estimated during spring(7.8%), summer(40.4%) and fall(53.9%) and under estimated during winter(-5.3%) compare to wind power energy computed in the observed wind speed. And as wind power energy by MOS were underestimated during spring(-12.8%), summer(-16.7%) and overestimated of fall(32.6%) and winter(7.4%). In case of 18UTC by WRF model wind power

energy forecast were over estimated during spring(24.9%), summer(21.3%), fall(44.8%) and winter(59.4%). And as wind power energy by MOS was overestimated during spring(4.3%), summer(12.9%), fall(19.4%) and winter(30.6%). Even though apply the MOS forecast equation, over than 30%(06UTC, fall) of wind power energy difference was appear.

# Ⅵ. Reference


[1] Ko, K. N., Kim, K. B., Huh, J. C., "A Study on Long-term Variation in Wind Energy", J.Korean Solar Energy Society, 2007. 11

[2] Physical Approach to Short-Term Wind Power Prediction, Springer-Verlag Berlin Heidelberg 2006.

[3] Breeze, P. (2004), "The Future of Global Offshore Wind Power: The technology, economics and impact of wind power generation", Reuters Business Insight.

[4] Ko, K. N., Kim, K. B., Huh, J. C., "A Study on Long-term Variations in Wind Characteristics in Cheju Island, Korea", SET2008-7th International Conference on Sustainable Energy Technologies; Seoul, Korea. 24-27 August, 2008

[5] Ko, K. N., Kim, K. B., Huh, J. C., "Characteristics of Wind Energy for Long-term Period (10 years) at Seoguang Site on Jeju Island", J.Korean Solar Energy Society Vol 28, No. 3, 2008

[6] Ko, K. N., Kim, K. B., Huh, J. C., "Analysis of Annual System Operating Characteristics at Hangwon Wind Farm on Jeju Island", The Korean Solar Energy Society, Vol 28, No. 2, 2008

[7] Kim, K. H. "Characteristics of Wind Energy for Long-term Period (10 years) at Seoguang Site on Jeju Island", KIER, 1999.

[8] Meibom P, Svendsen T, Sørensen B. "Trading wind in a hydro-dominated power pool system". International Journal of Sustainable Development 1999.

[9] Roulston MS, Kaplan DT, Hardenberg J, Smith LA. "Using medium-range weather forecasts to improve the value of wind energy production". Renewable Energy 2003, 602.

[10] Beyer, H.G., D. Heinemann, H. Mellinghoff, K. Mönnich, and H.-P. Waldl: "Forecast of Regional Power Output of Wind Turbines". In Proceedings of the European Wind Energy Conference, Nice, France, 1-5 March, 1999.

[11] G. Giebel, J. Badger, I. Martí Perez, P. Louka, G. Kallos, A. M. Palomares, C. Lac, G. Descombes: "Short-term Forecasting Using Advanced Physical Modelling - The Results of the Anemos Project, Results from mesoscale, microscale and CFD modeling". In Proceedings of the European Wind

Energy Conference, Athens, Greece, 27 Feb.- Mar. 2006.

[12] Lange, M., Focken, U.: "Physical Approach to Short-Term Wind Power Prediction", Springer 2006.

[13] Wicker, L. J., and W. C. Skamarock, "Time splitting methods for elastic models using forward time schemes", Mon. Wea. Rev., 130, 2088-2097, 2002.

[14] Meibom P, Svendsen T, Sørensen B. "Trading wind in a hydro-dominated power pool system". International Journal of Sustainable Development , 1999.

[15] Landberg L. "Short-term prediction of local wind conditions". Journal of Wind Engineering and Industrial Aerodynamics, 2001.

[16] Nielsen TS, Madsen H. "WPPT - a tool for wind power prediction. In: Wind power for the 21st Century", Kassel, Germany, 2000.

[17] Sa´nchez I. "Short-term prediction of wind energy production". International Journal of Forecasting, 2006.

[18] Marti I, San Isidro MJ, Cabezo´n D, Loureiro Y, Villanueva J, Cantero E, et al. "Wind power prediction in complex Terrain: from the synoptic scale to the local scale. In: the science of making torque from wind", Delft, The Netherlands, 2004.

[19] Focken U, Lange M, Mo¨nnich K, Waldl HP, Beyer HG, Luig "A. Short-term prediction of the aggregated power output of wind farms - a statistical analysis of the reduction of the prediction error by spatial smoothing effects". Journal of Wind Engineering and Industrial Aerodynamics 02.

[20] Rohrig K, Hoppe-Kilpper M, Ernst B, Schlo¨ gl F. "Online-monitoring and prediction of wind power in German transmission system operation centres". In: World wind energy conference, Cape Town, South Africa, 2003.

[21] Pinson P, Ranchin T, Kariniotakis G. "Short-term wind power prediction for offshore wind farms - Evaluation of fuzzy-neural network based models". In Global wind power conference, Chicago, Illinois, USA, 2004.

[22] Barbounis TG, Theocharis JB, Alexiadis MC, Dokopoulos PS. "Long-term wind speed and power forecasting using local recurrent neural network models". In: IEEE Transactions on Energy Conversion, 21, 2006.

[23] Bailey B, Brower MC, Zack J. "Short-term wind forecasting - Development and application of a mesoscale model". In: European wind energy

conference, Nice, France, 1999

[24] Glahn, H. R. and Lowry, D. A. "The Use of Model Output Statistics (MOS) in Objective Weather Forecasting", Techniques Development Laboratory, National Weather Service, NOAA, Silver Spring, Md. 20910

[25] Dallavalle, J. P., Erickson, M. C., and Maloney, J. C. III, "Model Output Statistics(MOS) Guidance for Short-range projections", Meteorological Development Laboratory, Office of Science and Technology, National Weather Service/NOAA, Silver Spring, Maryland

[26] Glahn, H. R. and Lowry, D. A. "The Use of Model Output Statistics (MOS) in Objective Weather Forecasting", Amer. Meteor.Soc., 796-801, 1976

[27] Glahn, H. R., and D. A. Lowry, "The use of Model Output Statistics (MOS) in objective weather forecasting". J. Appl. Meteor., **11**, 1202-1211, 1972

[28] Glahn, H. R., , and J. P. Dallavalle, "The new NWS MOS development and implementation systems". Preprints, 16th Conference on Probability and Statistics in the Atmospheric Sciences, Orlando, FL, Amer. Meteor. Soc., 78-81, 2002

[29] Her, S., Y., "Feasibility Study for Wind Characteristics Analysis by using WRF Meteorological Prediction Data". Multidisciplinary Graduate School Program for Wind Energy Graduate School Jeju National University. 2012.

[30] Wind Turbine Power Performance Testing using Nacelle Transfer Function, J.Korean Solar Energy Society, 2013(in press).

# Ⅶ. Appendix

## A.1. MOS equation of 06UTC at Spring.

Position = Sungsan(point), Ftime = + 000 h, Total freedom = 170, Radj = 40.83

| P_ID | Pname | Coefficient | STD_error | T-Value | P-Value | VIF | SD | MEAN |
|---|---|---|---|---|---|---|---|---|
| 0 | INTERCEPT | 2.98314 | | | | | | |
| 1 | WS80m | 0.57392 | 0.0528 | 10.8773 | 0.0000 | 1.0000 | 13.1730 | 7.4058 |

Position = Sungsan(point), Ftime = + 001 h, Total freedom = 168, Radj = 55.17

| P_ID | Pname | Coefficient | STD_error | T-Value | P-Value | VIF | SD | MEAN |
|---|---|---|---|---|---|---|---|---|
| 0 | INTERCEPT | 1.78301 | | | | | | |
| 1 | WS80m | 0.79186 | 0.0549 | 14.4121 | 0.0000 | 1.0000 | 12.8355 | 7.4840 |

Position = Sungsan(point), Ftime = + 002 h, Total freedom = 173, Radj = 61.23

| P_ID | Pname | Coefficient | STD_error | T-Value | P-Value | VIF | SD | MEAN |
|---|---|---|---|---|---|---|---|---|
| 0 | INTERCEPT | 1.02167 | | | | | | |
| 1 | WS80m | 0.86296 | 0.0521 | 16.5610 | 0.0000 | 1.0000 | 13.9478 | 7.3914 |

Position = Sungsan(point), Ftime = + 003 h, Total freedom = 171, Radj = 51.49

| P_ID | Pname | Coefficient | STD_error | T-Value | P-Value | VIF | SD | MEAN |
|---|---|---|---|---|---|---|---|---|
| 0 | INTERCEPT | 1.58114 | | | | | | |
| 1 | WS80m | 0.75034 | 0.0555 | 13.5106 | 0.0000 | 1.0000 | 13.8443 | 6.9622 |

Position = Sungsan(point), Ftime = + 004 h, Total freedom = 170, Radj = 45.60

| P_ID | Pname | Coefficient | STD_error | T-Value | P-Value | VIF | SD | MEAN |
|---|---|---|---|---|---|---|---|---|
| 0 | INTERCEPT | 1.84622 | | | | | | |
| 1 | WS80m | 0.72739 | 0.0607 | 11.9786 | 0.0000 | 1.0000 | 12.5457 | 6.8731 |

Position = Sungsan(point), Ftime = + 005 h, Total freedom = 175, Radj = 45.67

| P_ID | Pname | Coefficient | STD_error | T-Value | P-Value | VIF | SD | MEAN |
|---|---|---|---|---|---|---|---|---|
| 0 | INTERCEPT | 2.07012 | | | | | | |
| 1 | WS80m | 0.70009 | 0.0575 | 12.1689 | 0.0000 | 1.0000 | 13.0533 | 7.1449 |

Position = Sungsan(point), Ftime = + 006 h, Total freedom = 175, Radj = 36.76

| P_ID | Pname | Coefficient | STD_error | T-Value | P-Value | VIF | SD | MEAN |
|---|---|---|---|---|---|---|---|---|
| 0 | INTERCEPT | 2.54517 | | | | | | |
| 1 | WS80m | 0.60241 | 0.0594 | 10.1362 | 0.0000 | 1.0000 | 12.5410 | 7.0085 |

Position = Sungsan(point), Ftime = + 007 h, Total freedom = 177, Radj = 37.06

| P_ID | Pname | Coefficient | STD_error | T-Value | P-Value | VIF | SD | MEAN |
|---|---|---|---|---|---|---|---|---|
| 0 | INTERCEPT | 2.55744 | | | | | | |
| 1 | WS80m | 0.59259 | 0.0578 | 10.2569 | 0.0000 | 1.0000 | 13.1909 | 7.0758 |

Position = Sungsan(point), Ftime = + 008 h, Total freedom = 178, Radj = 41.45

| P_ID | Pname | Coefficient | STD_error | T-Value | P-Value | VIF | SD | MEAN |
|---|---|---|---|---|---|---|---|---|
| 0 | INTERCEPT | 2.35810 | | | | | | |
| 1 | WS80m | 0.60147 | 0.0534 | 11.2708 | 0.0000 | 1.0000 | 12.5762 | 7.0274 |

Position = Sungsan(point), Ftime = + 009 h, Total freedom = 177, Radj = 45.56

| P_ID | Pname | Coefficient | STD_error | T-Value | P-Value | VIF | SD | MEAN |
|---|---|---|---|---|---|---|---|---|
| 0 | INTERCEPT | 2.42102 | | | | | | |
| 1 | WS80m | 0.62079 | 0.0508 | 12.2126 | 0.0000 | 1.0000 | 12.0925 | 7.0753 |

Position = Sungsan(point), Ftime = + 010 h, Total freedom = 175, Radj = 28.61

| P_ID | Pname | Coefficient | STD_error | T-Value | P-Value | VIF | SD | MEAN |
|---|---|---|---|---|---|---|---|---|
| 0 | INTERCEPT | 3.21317 | | | | | | |
| 1 | WS80m | 0.50564 | 0.0600 | 8.4336 | 0.0000 | 1.0000 | 11.3488 | 6.8812 |

Position = Sungsan(point), Ftime = + 011 h, Total freedom = 177, Radj = 41.86

| P_ID | Pname | Coefficient | STD_error | T-Value | P-Value | VIF | SD | MEAN |
|---|---|---|---|---|---|---|---|---|
| 0 | INTERCEPT | 2.96479 | | | | | | |
| 1 | WS80m | 0.59085 | 0.0521 | 11.3337 | 0.0000 | 1.0000 | 12.9486 | 7.2916 |

Position = Sungsan(point), Ftime = + 012 h, Total freedom = 177, Radj = 47.83

| P_ID | Pname | Coefficient | STD_error | T-Value | P-Value | VIF | SD | MEAN |
|---|---|---|---|---|---|---|---|---|
| 0 | INTERCEPT | 2.47741 | | | | | | |
| 1 | WS80m | 0.64185 | 0.0502 | 12.7784 | 0.0000 | 1.0000 | 13.4659 | 7.1933 |

Position = Sungsan(point), Ftime = + 013 h, Total freedom = 173, Radj = 45.54

| P_ID | Pname | Coefficient | STD_error | T-Value | P-Value | VIF | SD | MEAN |
|---|---|---|---|---|---|---|---|---|
| 0 | INTERCEPT | 2.28993 | | | | | | |
| 1 | WS80m | 0.65084 | 0.0539 | 12.0684 | 0.0000 | 1.0000 | 12.9040 | 7.0552 |

Position = Sungsan(point), Ftime = + 014 h, Total freedom = 174, Radj = 44.20

| P_ID | Pname | Coefficient | STD_error | T-Value | P-Value | VIF | SD | MEAN |
|---|---|---|---|---|---|---|---|---|
| 0 | INTERCEPT | 2.04227 | | | | | | |
| 1 | WS80m | 0.68990 | 0.0586 | 11.7820 | 0.0000 | 1.0000 | 12.6500 | 7.0829 |

Position = Sungsan(point), Ftime = + 015 h, Total freedom = 175, Radj = 38.14

| P_ID | Pname | Coefficient | STD_error | T-Value | P-Value | VIF | SD | MEAN |
|---|---|---|---|---|---|---|---|---|
| 0 | INTERCEPT | 2.49387 | | | | | | |
| 1 | WS80m | 0.60631 | 0.0581 | 10.4353 | 0.0000 | 1.0000 | 11.2738 | 6.9614 |

Position = Sungsan(point), Ftime = + 016 h, Total freedom = 177, Radj = 39.72

| P_ID | Pname | Coefficient | STD_error | T-Value | P-Value | VIF | SD | MEAN |
|---|---|---|---|---|---|---|---|---|
| 0 | INTERCEPT | 2.27159 | | | | | | |
| 1 | WS80m | 0.66339 | 0.0612 | 10.8458 | 0.0000 | 1.0000 | 12.7907 | 7.1140 |

Position = Sungsan(point), Ftime = + 017 h, Total freedom = 174, Radj = 29.54

| P_ID | Pname | Coefficient | STD_error | T-Value | P-Value | VIF | SD | MEAN |
|---|---|---|---|---|---|---|---|---|
| 0 | INTERCEPT | 3.03148 | | | | | | |
| 1 | WS80m | 0.57352 | 0.0667 | 8.5997 | 0.0000 | 1.0000 | 12.0242 | 6.9789 |

Position = Sungsan(point), Ftime = + 018 h, Total freedom = 177, Radj = 46.65

| P_ID | Pname | Coefficient | STD_error | T-Value | P-Value | VIF | SD | MEAN |
|---|---|---|---|---|---|---|---|---|
| 0 | INTERCEPT | 1.85333 | | | | | | |
| 1 | WS80m | 0.77743 | 0.0623 | 12.4812 | 0.0000 | 1.0000 | 13.9796 | 7.3708 |

Position = Sungsan(point), Ftime = + 019 h, Total freedom = 177, Radj = 49.34

| P_ID | Pname | Coefficient | STD_error | T-Value | P-Value | VIF | SD | MEAN |
|---|---|---|---|---|---|---|---|---|
| 0 | INTERCEPT | 2.05873 | | | | | | |
| 1 | WS80m | 0.72690 | 0.0552 | 13.1679 | 0.0000 | 1.0000 | 13.1939 | 7.4135 |

---

Position = Sungsan(point), Ftime = + 020 h, Total freedom = 175, Radj = 53.77

---

| P_ID | Pname | Coefficient | STD_error | T-Value | P-Value | VIF | SD | MEAN |
|---|---|---|---|---|---|---|---|---|
| 0 | INTERCEPT | 1.67699 | | | | | | |
| 1 | WS80m | 0.75761 | 0.0530 | 14.3015 | 0.0000 | 1.0000 | 13.3262 | 7.5188 |

---

Position = Sungsan(point), Ftime = + 021 h, Total freedom = 174, Radj = 53.08

---

| P_ID | Pname | Coefficient | STD_error | T-Value | P-Value | VIF | SD | MEAN |
|---|---|---|---|---|---|---|---|---|
| 0 | INTERCEPT | 1.53742 | | | | | | |
| 1 | WS80m | 0.76155 | 0.0541 | 14.0659 | 0.0000 | 1.0000 | 12.3394 | 7.5560 |

---

Position = Sungsan(point), Ftime = + 022 h, Total freedom = 174, Radj = 45.92

---

| P_ID | Pname | Coefficient | STD_error | T-Value | P-Value | VIF | SD | MEAN |
|---|---|---|---|---|---|---|---|---|
| 0 | INTERCEPT | 1.53043 | | | | | | |
| 1 | WS80m | 0.75345 | 0.0618 | 12.1972 | 0.0000 | 1.0000 | 12.5865 | 7.5966 |

---

Position = Sungsan(point), Ftime = + 023 h, Total freedom = 172, Radj = 44.81

---

| P_ID | Pname | Coefficient | STD_error | T-Value | P-Value | VIF | SD | MEAN |
|---|---|---|---|---|---|---|---|---|
| 0 | INTERCEPT | 2.05349 | | | | | | |
| 1 | WS80m | 0.67514 | 0.0569 | 11.8590 | 0.0000 | 1.0000 | 10.8227 | 7.3792 |

---

Position = Sungsan(point), Ftime = + 024 h, Total freedom = 171, Radj = 46.71

---

| P_ID | Pname | Coefficient | STD_error | T-Value | P-Value | VIF | SD | MEAN |
|---|---|---|---|---|---|---|---|---|
| 0 | INTERCEPT | 1.40167 | | | | | | |
| 1 | WS80m | 0.75484 | 0.0614 | 12.2840 | 0.0000 | 1.0000 | 13.0723 | 7.4192 |

---

Position = Sungsan(point), Ftime = + 025 h, Total freedom = 168, Radj = 46.04

---

| P_ID | Pname | Coefficient | STD_error | T-Value | P-Value | VIF | SD | MEAN |
|---|---|---|---|---|---|---|---|---|
| 0 | INTERCEPT | 1.55101 | | | | | | |
| 1 | WS80m | 0.76343 | 0.0635 | 12.0133 | 0.0000 | 1.0000 | 12.5859 | 7.4639 |

---

Position = Sungsan(point), Ftime = + 026 h, Total freedom = 173, Radj = 41.11

---

| P_ID | Pname | Coefficient | STD_error | T-Value | P-Value | VIF | SD | MEAN |
|---|---|---|---|---|---|---|---|---|
| 0 | INTERCEPT | 1.87002 | | | | | | |
| 1 | WS80m | 0.74758 | 0.0677 | 11.0352 | 0.0000 | 1.0000 | 13.3819 | 7.4017 |

---

Position = Sungsan(point), Ftime = + 027 h, Total freedom = 171, Radj = 45.35

---

| P_ID | Pname | Coefficient | STD_error | T-Value | P-Value | VIF | SD | MEAN |
|---|---|---|---|---|---|---|---|---|
| 0 | INTERCEPT | 1.49571 | | | | | | |
| 1 | WS80m | 0.77192 | 0.0646 | 11.9541 | 0.0000 | 1.0000 | 13.5761 | 6.9483 |

---

Position = Sungsan(point), Ftime = + 028 h, Total freedom = 171, Radj = 35.12

---

| P_ID | Pname | Coefficient | STD_error | T-Value | P-Value | VIF | SD | MEAN |
|---|---|---|---|---|---|---|---|---|
| 0 | INTERCEPT | 2.27260 | | | | | | |
| 1 | WS80m | 0.68615 | 0.0709 | 9.6719 | 0.0000 | 1.0000 | 12.4941 | 6.8628 |

---

Position = Sungsan(point), Ftime = + 029 h, Total freedom = 176, Radj = 34.22

---

| P_ID | Pname | Coefficient | STD_error | T-Value | P-Value | VIF | SD | MEAN |
|---|---|---|---|---|---|---|---|---|
| 0 | INTERCEPT | 2.42074 | | | | | | |
| 1 | WS80m | 0.65218 | 0.0678 | 9.6213 | 0.0000 | 1.0000 | 13.0196 | 7.1288 |

---

Position = Sungsan(point), Ftime = + 030 h, Total freedom = 176, Radj = 30.43

---

| P_ID | Pname | Coefficient | STD_error | T-Value | P-Value | VIF | SD | MEAN |
|---|---|---|---|---|---|---|---|---|
| 0 | INTERCEPT | 2.76106 | | | | | | |

1 WS80m 0.57124 0.0647 8.8315 0.0000 1.0000 12.4752 7.0141

---

Position = Sungsan(point), Ftime = + 031 h, Total freedom = 177, Radj = 21.04

---

| P_ID | Pname | Coefficient | STD_error | T-Value | P-Value | VIF | SD | MEAN |
|---|---|---|---|---|---|---|---|---|
| 0 | INTERCEPT | 3.38070 | | | | | | |
| 1 | WS80m | 0.48502 | 0.0699 | 6.9396 | 0.0000 | 1.0000 | 12.8034 | 7.0472 |

---

Position = Sungsan(point), Ftime = + 032 h, Total freedom = 178, Radj = 28.56

---

| P_ID | Pname | Coefficient | STD_error | T-Value | P-Value | VIF | SD | MEAN |
|---|---|---|---|---|---|---|---|---|
| 0 | INTERCEPT | 2.80241 | | | | | | |
| 1 | WS80m | 0.54872 | 0.0646 | 8.4956 | 0.0000 | 1.0000 | 12.1547 | 7.0095 |

---

Position = Sungsan(point), Ftime = + 033 h, Total freedom = 177, Radj = 32.19

---

| P_ID | Pname | Coefficient | STD_error | T-Value | P-Value | VIF | SD | MEAN |
|---|---|---|---|---|---|---|---|---|
| 0 | INTERCEPT | 2.78626 | | | | | | |
| 1 | WS80m | 0.55888 | 0.0606 | 9.2204 | 0.0000 | 1.0000 | 11.9599 | 7.0112 |

---

Position = Sungsan(point), Ftime = + 034 h, Total freedom = 175, Radj = 25.29

---

| P_ID | Pname | Coefficient | STD_error | T-Value | P-Value | VIF | SD | MEAN |
|---|---|---|---|---|---|---|---|---|
| 0 | INTERCEPT | 3.25471 | | | | | | |
| 1 | WS80m | 0.48040 | 0.0619 | 7.7618 | 0.0000 | 1.0000 | 11.1895 | 6.8676 |

---

Position = Sungsan(point), Ftime = + 035 h, Total freedom = 177, Radj = 36.21

---

| P_ID | Pname | Coefficient | STD_error | T-Value | P-Value | VIF | SD | MEAN |
|---|---|---|---|---|---|---|---|---|
| 0 | INTERCEPT | 2.77443 | | | | | | |
| 1 | WS80m | 0.59179 | 0.0587 | 10.0732 | 0.0000 | 1.0000 | 12.8103 | 7.2539 |

---

Position = Sungsan(point), Ftime = + 036 h, Total freedom = 177, Radj = 32.88

---

| P_ID | Pname | Coefficient | STD_error | T-Value | P-Value | VIF | SD | MEAN |
|---|---|---|---|---|---|---|---|---|
| 0 | INTERCEPT | 2.82456 | | | | | | |
| 1 | WS80m | 0.59935 | 0.0640 | 9.3650 | 0.0000 | 1.0000 | 13.4153 | 7.1809 |

---

Position = Sungsan(point), Ftime = + 037 h, Total freedom = 173, Radj = 26.52

---

| P_ID | Pname | Coefficient | STD_error | T-Value | P-Value | VIF | SD | MEAN |
|---|---|---|---|---|---|---|---|---|
| 0 | INTERCEPT | 3.12054 | | | | | | |
| 1 | WS80m | 0.53165 | 0.0668 | 7.9645 | 0.0000 | 1.0000 | 12.8647 | 7.0098 |

---

Position = Sungsan(point), Ftime = + 038 h, Total freedom = 174, Radj = 32.45

---

| P_ID | Pname | Coefficient | STD_error | T-Value | P-Value | VIF | SD | MEAN |
|---|---|---|---|---|---|---|---|---|
| 0 | INTERCEPT | 2.76796 | | | | | | |
| 1 | WS80m | 0.58224 | 0.0633 | 9.1974 | 0.0000 | 1.0000 | 12.7155 | 7.0509 |

---

Position = Sungsan(point), Ftime = + 039 h, Total freedom = 175, Radj = 33.25

---

| P_ID | Pname | Coefficient | STD_error | T-Value | P-Value | VIF | SD | MEAN |
|---|---|---|---|---|---|---|---|---|
| 0 | INTERCEPT | 2.80083 | | | | | | |
| 1 | WS80m | 0.56871 | 0.0606 | 9.3899 | 0.0000 | 1.0000 | 11.3570 | 6.9449 |

---

Position = Sungsan(point), Ftime = + 040 h, Total freedom = 177, Radj = 29.91

---

| P_ID | Pname | Coefficient | STD_error | T-Value | P-Value | VIF | SD | MEAN |
|---|---|---|---|---|---|---|---|---|
| 0 | INTERCEPT | 2.70897 | | | | | | |
| 1 | WS80m | 0.60365 | 0.0690 | 8.7475 | 0.0000 | 1.0000 | 12.8298 | 7.0719 |

---

Position = Sungsan(point), Ftime = + 041 h, Total freedom = 174, Radj = 31.80

---

| P_ID | Pname | Coefficient | STD_error | T-Value | P-Value | VIF | SD | MEAN |
|---|---|---|---|---|---|---|---|---|

0 INTERCEPT 2.83187
1 WS80m 0.60679 0.0670 9.0618 0.0000 1.0000 11.8675 6.8771

---

Position = Sungsan(point), Ftime = + 042 h, Total freedom = 177, Radj = 40.95

---

P_ID Pname Coefficient STD_error T-Value P-Value VIF SD MEAN
0 INTERCEPT 2.40795
1 WS80m 0.69245 0.0623 11.1233 0.0000 1.0000 13.9407 7.3073

---

Position = Sungsan(point), Ftime = + 043 h, Total freedom = 177, Radj = 55.74

---

P_ID Pname Coefficient STD_error T-Value P-Value VIF SD MEAN
0 INTERCEPT 1.59464
1 WS80m 0.78214 0.0523 14.9626 0.0000 1.0000 13.0753 7.3713

---

Position = Sungsan(point), Ftime = + 044 h, Total freedom = 176, Radj = 46.87

---

P_ID Pname Coefficient STD_error T-Value P-Value VIF SD MEAN
0 INTERCEPT 1.90206
1 WS80m 0.72429 0.0579 12.4999 0.0000 1.0000 12.9780 7.4836

---

Position = Sungsan(point), Ftime = + 045 h, Total freedom = 175, Radj = 42.29

---

P_ID Pname Coefficient STD_error T-Value P-Value VIF SD MEAN
0 INTERCEPT 1.75456
1 WS80m 0.72650 0.0639 11.3686 0.0000 1.0000 12.1977 7.5176

---

Position = Sungsan(point), Ftime = + 046 h, Total freedom = 175, Radj = 35.52

---

P_ID Pname Coefficient STD_error T-Value P-Value VIF SD MEAN
0 INTERCEPT 2.57828
1 WS80m 0.61472 0.0623 9.8690 0.0000 1.0000 12.6758 7.4903

---

Position = Sungsan(point), Ftime = + 047 h, Total freedom = 173, Radj = 35.60

---

P_ID Pname Coefficient STD_error T-Value P-Value VIF SD MEAN
0 INTERCEPT 2.45001
1 WS80m 0.61184 0.0622 9.8295 0.0000 1.0000 10.5973 7.3138

---

Position = Sungsan(point), Ftime = + 048 h, Total freedom = 172, Radj = 39.59

---

P_ID Pname Coefficient STD_error T-Value P-Value VIF SD MEAN
0 INTERCEPT 1.87002
1 WS80m 0.68959 0.0647 10.6643 0.0000 1.0000 13.0677 7.3185

---

Position = Sungsan(point), Ftime = + 049 h, Total freedom = 169, Radj = 37.89

---

P_ID Pname Coefficient STD_error T-Value P-Value VIF SD MEAN
0 INTERCEPT 2.62383
1 WS80m 0.61245 0.0600 10.2039 0.0000 1.0000 12.6464 7.3341

---

Position = Sungsan(point), Ftime = + 050 h, Total freedom = 173, Radj = 24.95

---

P_ID Pname Coefficient STD_error T-Value P-Value VIF SD MEAN
0 INTERCEPT 3.55158
1 WS80m 0.49200 0.0643 7.6502 0.0000 1.0000 13.8419 7.2431

---

Position = Sungsan(point), Ftime = + 051 h, Total freedom = 171, Radj = 29.42

---

P_ID Pname Coefficient STD_error T-Value P-Value VIF SD MEAN
0 INTERCEPT 2.84754
1 WS80m 0.54351 0.0639 8.5021 0.0000 1.0000 13.5657 6.7762

---

Position = Sungsan(point), Ftime = + 052 h, Total freedom = 171, Radj = 34.20

---

| P_ID | Pname | Coefficient | STD_error | T-Value | P-Value | VIF | SD | MEAN |
|---|---|---|---|---|---|---|---|---|
| 0 | INTERCEPT | 2.75179 | | | | | | |
| 1 | WS80m | 0.56228 | 0.0593 | 9.4808 | 0.0000 | 1.0000 | 12.3392 | 6.6936 |

Position = Sungsan(point), Ftime = + 053 h, Total freedom = 176, Radj = 31.02

| P_ID | Pname | Coefficient | STD_error | T-Value | P-Value | VIF | SD | MEAN |
|---|---|---|---|---|---|---|---|---|
| 0 | INTERCEPT | 2.73985 | | | | | | |
| 1 | WS80m | 0.58826 | 0.0657 | 8.9515 | 0.0000 | 1.0000 | 13.4049 | 7.0169 |

Position = Sungsan(point), Ftime = + 054 h, Total freedom = 176, Radj = 28.50

| P_ID | Pname | Coefficient | STD_error | T-Value | P-Value | VIF | SD | MEAN |
|---|---|---|---|---|---|---|---|---|
| 0 | INTERCEPT | 2.87939 | | | | | | |
| 1 | WS80m | 0.53918 | 0.0639 | 8.4346 | 0.0000 | 1.0000 | 13.0136 | 6.9186 |

Position = Sungsan(point), Ftime = + 055 h, Total freedom = 176, Radj = 24.39

| P_ID | Pname | Coefficient | STD_error | T-Value | P-Value | VIF | SD | MEAN |
|---|---|---|---|---|---|---|---|---|
| 0 | INTERCEPT | 3.08801 | | | | | | |
| 1 | WS80m | 0.50342 | 0.0662 | 7.6000 | 0.0000 | 1.0000 | 13.0014 | 6.8774 |

Position = Sungsan(point), Ftime = + 056 h, Total freedom = 177, Radj = 17.03

| P_ID | Pname | Coefficient | STD_error | T-Value | P-Value | VIF | SD | MEAN |
|---|---|---|---|---|---|---|---|---|
| 0 | INTERCEPT | 3.82359 | | | | | | |
| 1 | WS80m | 0.39652 | 0.0649 | 6.1106 | 0.0000 | 1.0000 | 12.1443 | 6.8174 |

Position = Sungsan(point), Ftime = + 057 h, Total freedom = 176, Radj = 18.18

| P_ID | Pname | Coefficient | STD_error | T-Value | P-Value | VIF | SD | MEAN |
|---|---|---|---|---|---|---|---|---|
| 0 | INTERCEPT | 3.72093 | | | | | | |
| 1 | WS80m | 0.39801 | 0.0628 | 6.3330 | 0.0000 | 1.0000 | 11.8869 | 6.8254 |

Position = Sungsan(point), Ftime = + 058 h, Total freedom = 174, Radj = 15.38

| P_ID | Pname | Coefficient | STD_error | T-Value | P-Value | VIF | SD | MEAN |
|---|---|---|---|---|---|---|---|---|
| 0 | INTERCEPT | 3.92365 | | | | | | |
| 1 | WS80m | 0.38362 | 0.0672 | 5.7122 | 0.0000 | 1.0000 | 11.1539 | 6.6697 |

Position = Sungsan(point), Ftime = + 059 h, Total freedom = 176, Radj = 22.79

| P_ID | Pname | Coefficient | STD_error | T-Value | P-Value | VIF | SD | MEAN |
|---|---|---|---|---|---|---|---|---|
| 0 | INTERCEPT | 3.64568 | | | | | | |
| 1 | WS80m | 0.46935 | 0.0645 | 7.2776 | 0.0000 | 1.0000 | 12.9031 | 7.0537 |

Position = Sungsan(point), Ftime = + 060 h, Total freedom = 177, Radj = 30.63

| P_ID | Pname | Coefficient | STD_error | T-Value | P-Value | VIF | SD | MEAN |
|---|---|---|---|---|---|---|---|---|
| 0 | INTERCEPT | 2.91272 | | | | | | |
| 1 | WS80m | 0.56805 | 0.0638 | 8.8976 | 0.0000 | 1.0000 | 13.4549 | 7.0393 |

Position = Sungsan(point), Ftime = + 061 h, Total freedom = 173, Radj = 26.61

| P_ID | Pname | Coefficient | STD_error | T-Value | P-Value | VIF | SD | MEAN |
|---|---|---|---|---|---|---|---|---|
| 0 | INTERCEPT | 3.04243 | | | | | | |
| 1 | WS80m | 0.52553 | 0.0658 | 7.9826 | 0.0000 | 1.0000 | 12.6191 | 6.8632 |

Position = Sungsan(point), Ftime = + 062 h, Total freedom = 174, Radj = 35.83

| P_ID | Pname | Coefficient | STD_error | T-Value | P-Value | VIF | SD | MEAN |
|---|---|---|---|---|---|---|---|---|
| 0 | INTERCEPT | 2.51890 | | | | | | |
| 1 | WS80m | 0.59614 | 0.0602 | 9.9084 | 0.0000 | 1.0000 | 12.7177 | 6.9051 |

Position = Sungsan(point), Ftime = + 063 h, Total freedom = 175, Radj = 21.03

| P_ID | Pname | Coefficient | STD_error | T-Value | P-Value | VIF | SD | MEAN |
|---|---|---|---|---|---|---|---|---|
| 0 | INTERCEPT | 3.63679 | | | | | | |
| 1 | WS80m | 0.42594 | 0.0617 | 6.8991 | 0.0000 | 1.0000 | 11.2371 | 6.8210 |

Position = Sungsan(point), Ftime = + 064 h, Total freedom = 177, Radj = 27.67

| P_ID | Pname | Coefficient | STD_error | T-Value | P-Value | VIF | SD | MEAN |
|---|---|---|---|---|---|---|---|---|
| 0 | INTERCEPT | 3.17586 | | | | | | |
| 1 | WS80m | 0.50583 | 0.0610 | 8.2883 | 0.0000 | 1.0000 | 12.8852 | 6.9787 |

Position = Sungsan(point), Ftime = + 065 h, Total freedom = 174, Radj = 23.48

| P_ID | Pname | Coefficient | STD_error | T-Value | P-Value | VIF | SD | MEAN |
|---|---|---|---|---|---|---|---|---|
| 0 | INTERCEPT | 3.42547 | | | | | | |
| 1 | WS80m | 0.49298 | 0.0668 | 7.3747 | 0.0000 | 1.0000 | 11.9592 | 6.8251 |

Position = Sungsan(point), Ftime = + 066 h, Total freedom = 177, Radj = 31.73

| P_ID | Pname | Coefficient | STD_error | T-Value | P-Value | VIF | SD | MEAN |
|---|---|---|---|---|---|---|---|---|
| 0 | INTERCEPT | 3.05285 | | | | | | |
| 1 | WS80m | 0.57644 | 0.0632 | 9.1253 | 0.0000 | 1.0000 | 13.7531 | 7.2697 |

Position = Sungsan(point), Ftime = + 067 h, Total freedom = 178, Radj = 39.59

| P_ID | Pname | Coefficient | STD_error | T-Value | P-Value | VIF | SD | MEAN |
|---|---|---|---|---|---|---|---|---|
| 0 | INTERCEPT | 2.96330 | | | | | | |
| 1 | WS80m | 0.58492 | 0.0539 | 10.8468 | 0.0000 | 1.0000 | 13.2199 | 7.3877 |

Position = Sungsan(point), Ftime = + 068 h, Total freedom = 175, Radj = 34.51

| P_ID | Pname | Coefficient | STD_error | T-Value | P-Value | VIF | SD | MEAN |
|---|---|---|---|---|---|---|---|---|
| 0 | INTERCEPT | 2.79559 | | | | | | |
| 1 | WS80m | 0.57227 | 0.0593 | 9.6550 | 0.0000 | 1.0000 | 12.6307 | 7.4080 |

Position = Sungsan(point), Ftime = + 069 h, Total freedom = 174, Radj = 47.35

| P_ID | Pname | Coefficient | STD_error | T-Value | P-Value | VIF | SD | MEAN |
|---|---|---|---|---|---|---|---|---|
| 0 | INTERCEPT | 1.96941 | | | | | | |
| 1 | WS80m | 0.68969 | 0.0550 | 12.5496 | 0.0000 | 1.0000 | 11.8612 | 7.4417 |

Position = Sungsan(point), Ftime = + 070 h, Total freedom = 174, Radj = 35.03

| P_ID | Pname | Coefficient | STD_error | T-Value | P-Value | VIF | SD | MEAN |
|---|---|---|---|---|---|---|---|---|
| 0 | INTERCEPT | 2.36530 | | | | | | |
| 1 | WS80m | 0.64502 | 0.0662 | 9.7378 | 0.0000 | 1.0000 | 12.5089 | 7.4651 |

Position = Sungsan(point), Ftime = + 071 h, Total freedom = 172, Radj = 25.52

| P_ID | Pname | Coefficient | STD_error | T-Value | P-Value | VIF | SD | MEAN |
|---|---|---|---|---|---|---|---|---|
| 0 | INTERCEPT | 3.27581 | | | | | | |
| 1 | WS80m | 0.50264 | 0.0649 | 7.7422 | 0.0000 | 1.0000 | 10.5161 | 7.2769 |

Position = Sungsan(point), Ftime = + 072 h, Total freedom = 171, Radj = 33.80

| P_ID | Pname | Coefficient | STD_error | T-Value | P-Value | VIF | SD | MEAN |
|---|---|---|---|---|---|---|---|---|
| 0 | INTERCEPT | 2.81436 | | | | | | |
| 1 | WS80m | 0.56372 | 0.0600 | 9.3978 | 0.0000 | 1.0000 | 12.9852 | 7.2901 |

## A.2. MOS equation of 18UTC at Spring.

Position = Sungsan(point), Ftime = + 000 h, Total freedom = 177, Radj = 39.49

| P_ID | Pname | Coefficient | STD_error | T-Value | P-Value | VIF | SD | MEAN |
|---|---|---|---|---|---|---|---|---|
| 0 | INTERCEPT | 2.48208 | | | | | | |
| 1 | WS80m | 0.52412 | 0.0486 | 10.7941 | 0.0000 | 1.0000 | 11.2198 | 6.9118 |

Position = Sungsan(point), Ftime = + 001 h, Total freedom = 179, Radj = 40.40

| P_ID | Pname | Coefficient | STD_error | T-Value | P-Value | VIF | SD | MEAN |
|---|---|---|---|---|---|---|---|---|
| 0 | INTERCEPT | 2.25768 | | | | | | |
| 1 | WS80m | 0.62601 | 0.0566 | 11.0601 | 0.0000 | 1.0000 | 12.6629 | 7.3233 |

Position = Sungsan(point), Ftime = + 002 h, Total freedom = 180, Radj = 39.71

| P_ID | Pname | Coefficient | STD_error | T-Value | P-Value | VIF | SD | MEAN |
|---|---|---|---|---|---|---|---|---|
| 0 | INTERCEPT | 2.25711 | | | | | | |
| 1 | WS80m | 0.63257 | 0.0579 | 10.9346 | 0.0000 | 1.0000 | 13.3430 | 7.2459 |

Position = Sungsan(point), Ftime = + 003 h, Total freedom = 176, Radj = 38.22

| P_ID | Pname | Coefficient | STD_error | T-Value | P-Value | VIF | SD | MEAN |
|---|---|---|---|---|---|---|---|---|
| 0 | INTERCEPT | 2.15886 | | | | | | |
| 1 | WS80m | 0.62140 | 0.0593 | 10.4835 | 0.0000 | 1.0000 | 12.8989 | 7.1192 |

Position = Sungsan(point), Ftime = + 004 h, Total freedom = 177, Radj = 47.97

| P_ID | Pname | Coefficient | STD_error | T-Value | P-Value | VIF | SD | MEAN |
|---|---|---|---|---|---|---|---|---|
| 0 | INTERCEPT | 1.53555 | | | | | | |
| 1 | WS80m | 0.70703 | 0.0552 | 12.8138 | 0.0000 | 1.0000 | 12.7169 | 7.1219 |

Position = Sungsan(point), Ftime = + 005 h, Total freedom = 178, Radj = 41.64

| P_ID | Pname | Coefficient | STD_error | T-Value | P-Value | VIF | SD | MEAN |
|---|---|---|---|---|---|---|---|---|
| 0 | INTERCEPT | 2.08179 | | | | | | |
| 1 | WS80m | 0.65565 | 0.0580 | 11.3140 | 0.0000 | 1.0000 | 11.1633 | 7.0156 |

Position = Sungsan(point), Ftime = + 006 h, Total freedom = 180, Radj = 51.68

| P_ID | Pname | Coefficient | STD_error | T-Value | P-Value | VIF | SD | MEAN |
|---|---|---|---|---|---|---|---|---|
| 0 | INTERCEPT | 1.44393 | | | | | | |
| 1 | WS80m | 0.75498 | 0.0543 | 13.9107 | 0.0000 | 1.0000 | 12.6220 | 7.1249 |

Position = Sungsan(point), Ftime = + 007 h, Total freedom = 177, Radj = 39.86

| P_ID | Pname | Coefficient | STD_error | T-Value | P-Value | VIF | SD | MEAN |
|---|---|---|---|---|---|---|---|---|
| 0 | INTERCEPT | 2.10113 | | | | | | |
| 1 | WS80m | 0.65545 | 0.0603 | 10.8780 | 0.0000 | 1.0000 | 11.8930 | 6.9978 |

Position = Sungsan(point), Ftime = + 008 h, Total freedom = 180, Radj = 56.31

| P_ID | Pname | Coefficient | STD_error | T-Value | P-Value | VIF | SD | MEAN |
|---|---|---|---|---|---|---|---|---|
| 0 | INTERCEPT | 0.83764 | | | | | | |
| 1 | WS80m | 0.84549 | 0.0554 | 15.2645 | 0.0000 | 1.0000 | 13.7946 | 7.3503 |

Position = Sungsan(point), Ftime = + 009 h, Total freedom = 180, Radj = 56.51

| P_ID | Pname | Coefficient | STD_error | T-Value | P-Value | VIF | SD | MEAN |
|---|---|---|---|---|---|---|---|---|
| 0 | INTERCEPT | 1.15103 | | | | | | |
| 1 | WS80m | 0.81173 | 0.0530 | 15.3247 | 0.0000 | 1.0000 | 13.1671 | 7.4271 |

Position = Sungsan(point), Ftime = + 010 h, Total freedom = 178, Radj = 48.43

| P_ID | Pname | Coefficient | STD_error | T-Value | P-Value | VIF | SD | MEAN |
|---|---|---|---|---|---|---|---|---|
| 0 | INTERCEPT | 1.36536 | | | | | | |
| 1 | WS80m | 0.78952 | 0.0609 | 12.9683 | 0.0000 | 1.0000 | 13.1704 | 7.5039 |

Position = Sungsan(point), Ftime = + 011 h, Total freedom = 177, Radj = 57.88

| P_ID | Pname | Coefficient | STD_error | T-Value | P-Value | VIF | SD | MEAN |
|---|---|---|---|---|---|---|---|---|
| 0 | INTERCEPT | 1.12685 | | | | | | |
| 1 | WS80m | 0.82639 | 0.0529 | 15.6282 | 0.0000 | 1.0000 | 12.2631 | 7.5348 |

Position = Sungsan(point), Ftime = + 012 h, Total freedom = 177, Radj = 50.43

| P_ID | Pname | Coefficient | STD_error | T-Value | P-Value | VIF | SD | MEAN |
|---|---|---|---|---|---|---|---|---|
| 0 | INTERCEPT | 1.87609 | | | | | | |
| 1 | WS80m | 0.71921 | 0.0534 | 13.4569 | 0.0000 | 1.0000 | 12.7171 | 7.5680 |

Position = Sungsan(point), Ftime = + 013 h, Total freedom = 175, Radj = 37.00

| P_ID | Pname | Coefficient | STD_error | T-Value | P-Value | VIF | SD | MEAN |
|---|---|---|---|---|---|---|---|---|
| 0 | INTERCEPT | 2.95653 | | | | | | |
| 1 | WS80m | 0.57681 | 0.0566 | 10.1875 | 0.0000 | 1.0000 | 10.9024 | 7.3608 |

Position = Sungsan(point), Ftime = + 014 h, Total freedom = 174, Radj = 50.51

| P_ID | Pname | Coefficient | STD_error | T-Value | P-Value | VIF | SD | MEAN |
|---|---|---|---|---|---|---|---|---|
| 0 | INTERCEPT | 1.89303 | | | | | | |
| 1 | WS80m | 0.74429 | 0.0557 | 13.3648 | 0.0000 | 1.0000 | 13.0359 | 7.3851 |

Position = Sungsan(point), Ftime = + 015 h, Total freedom = 171, Radj = 49.75

| P_ID | Pname | Coefficient | STD_error | T-Value | P-Value | VIF | SD | MEAN |
|---|---|---|---|---|---|---|---|---|
| 0 | INTERCEPT | 2.23751 | | | | | | |
| 1 | WS80m | 0.76138 | 0.0583 | 13.0497 | 0.0000 | 1.0000 | 12.5501 | 7.3948 |

Position = Sungsan(point), Ftime = + 016 h, Total freedom = 176, Radj = 38.28

| P_ID | Pname | Coefficient | STD_error | T-Value | P-Value | VIF | SD | MEAN |
|---|---|---|---|---|---|---|---|---|
| 0 | INTERCEPT | 2.47094 | | | | | | |
| 1 | WS80m | 0.71890 | 0.0685 | 10.4964 | 0.0000 | 1.0000 | 13.4821 | 7.3186 |

Position = Sungsan(point), Ftime = + 017 h, Total freedom = 174, Radj = 30.93

| P_ID | Pname | Coefficient | STD_error | T-Value | P-Value | VIF | SD | MEAN |
|---|---|---|---|---|---|---|---|---|
| 0 | INTERCEPT | 2.49580 | | | | | | |
| 1 | WS80m | 0.64885 | 0.0730 | 8.8831 | 0.0000 | 1.0000 | 13.3944 | 6.8994 |

Position = Sungsan(point), Ftime = + 018 h, Total freedom = 174, Radj = 37.32

| P_ID | Pname | Coefficient | STD_error | T-Value | P-Value | VIF | SD | MEAN |
|---|---|---|---|---|---|---|---|---|
| 0 | INTERCEPT | 1.97719 | | | | | | |
| 1 | WS80m | 0.69931 | 0.0684 | 10.2283 | 0.0000 | 1.0000 | 12.3189 | 6.8326 |

Position = Sungsan(point), Ftime = + 019 h, Total freedom = 179, Radj = 38.45

| P_ID | Pname | Coefficient | STD_error | T-Value | P-Value | VIF | SD | MEAN |
|---|---|---|---|---|---|---|---|---|
| 0 | INTERCEPT | 2.42594 | | | | | | |
| 1 | WS80m | 0.64347 | 0.0606 | 10.6218 | 0.0000 | 1.0000 | 12.9271 | 7.1200 |

Position = Sungsan(point), Ftime = + 020 h, Total freedom = 179, Radj = 35.85

| P_ID | Pname | Coefficient | STD_error | T-Value | P-Value | VIF | SD | MEAN |
|---|---|---|---|---|---|---|---|---|
| 0 | INTERCEPT | 2.31264 | | | | | | |
| 1 | WS80m | 0.64585 | 0.0643 | 10.0506 | 0.0000 | 1.0000 | 12.7263 | 7.0211 |

Position = Sungsan(point), Ftime = + 021 h, Total freedom = 179, Radj = 24.29

| P_ID | Pname | Coefficient | STD_error | T-Value | P-Value | VIF | SD | MEAN |
|---|---|---|---|---|---|---|---|---|
| 0 | INTERCEPT | 3.11437 | | | | | | |
| 1 | WS80m | 0.52755 | 0.0690 | 7.6438 | 0.0000 | 1.0000 | 12.8647 | 7.0100 |

Position = Sungsan(point), Ftime = + 022 h, Total freedom = 180, Radj = 30.43

| P_ID | Pname | Coefficient | STD_error | T-Value | P-Value | VIF | SD | MEAN |
|---|---|---|---|---|---|---|---|---|
| 0 | INTERCEPT | 3.03304 | | | | | | |
| 1 | WS80m | 0.53656 | 0.0601 | 8.9290 | 0.0000 | 1.0000 | 12.2204 | 6.9729 |

Position = Sungsan(point), Ftime = + 023 h, Total freedom = 179, Radj = 30.93

| P_ID | Pname | Coefficient | STD_error | T-Value | P-Value | VIF | SD | MEAN |
|---|---|---|---|---|---|---|---|---|
| 0 | INTERCEPT | 3.29157 | | | | | | |
| 1 | WS80m | 0.51508 | 0.0572 | 9.0079 | 0.0000 | 1.0000 | 11.8973 | 6.9856 |

Position = Sungsan(point), Ftime = + 024 h, Total freedom = 177, Radj = 26.61

| P_ID | Pname | Coefficient | STD_error | T-Value | P-Value | VIF | SD | MEAN |
|---|---|---|---|---|---|---|---|---|
| 0 | INTERCEPT | 3.58820 | | | | | | |
| 1 | WS80m | 0.46126 | 0.0571 | 8.0725 | 0.0000 | 1.0000 | 11.1861 | 6.8303 |

Position = Sungsan(point), Ftime = + 025 h, Total freedom = 179, Radj = 34.22

| P_ID | Pname | Coefficient | STD_error | T-Value | P-Value | VIF | SD | MEAN |
|---|---|---|---|---|---|---|---|---|
| 0 | INTERCEPT | 3.05573 | | | | | | |
| 1 | WS80m | 0.56809 | 0.0586 | 9.7016 | 0.0000 | 1.0000 | 12.9026 | 7.2317 |

Position = Sungsan(point), Ftime = + 026 h, Total freedom = 180, Radj = 44.85

| P_ID | Pname | Coefficient | STD_error | T-Value | P-Value | VIF | SD | MEAN |
|---|---|---|---|---|---|---|---|---|
| 0 | INTERCEPT | 2.29735 | | | | | | |
| 1 | WS80m | 0.67337 | 0.0555 | 12.1402 | 0.0000 | 1.0000 | 13.3334 | 7.1464 |

Position = Sungsan(point), Ftime = + 027 h, Total freedom = 176, Radj = 42.47

| P_ID | Pname | Coefficient | STD_error | T-Value | P-Value | VIF | SD | MEAN |
|---|---|---|---|---|---|---|---|---|
| 0 | INTERCEPT | 2.22848 | | | | | | |
| 1 | WS80m | 0.67696 | 0.0592 | 11.4428 | 0.0000 | 1.0000 | 12.9134 | 7.0249 |

Position = Sungsan(point), Ftime = + 028 h, Total freedom = 177, Radj = 29.01

| P_ID | Pname | Coefficient | STD_error | T-Value | P-Value | VIF | SD | MEAN |
|---|---|---|---|---|---|---|---|---|
| 0 | INTERCEPT | 3.06877 | | | | | | |
| 1 | WS80m | 0.58110 | 0.0679 | 8.5641 | 0.0000 | 1.0000 | 12.7685 | 7.0680 |

Position = Sungsan(point), Ftime = + 029 h, Total freedom = 178, Radj = 28.07

| P_ID | Pname | Coefficient | STD_error | T-Value | P-Value | VIF | SD | MEAN |
|---|---|---|---|---|---|---|---|---|
| 0 | INTERCEPT | 3.37538 | | | | | | |
| 1 | WS80m | 0.52588 | 0.0626 | 8.3945 | 0.0000 | 1.0000 | 11.3224 | 6.9475 |

Position = Sungsan(point), Ftime = + 030 h, Total freedom = 180, Radj = 31.16

| P_ID | Pname | Coefficient | STD_error | T-Value | P-Value | VIF | SD | MEAN |
|---|---|---|---|---|---|---|---|---|
| 0 | INTERCEPT | 2.95275 | | | | | | |
| 1 | WS80m | 0.59055 | 0.0650 | 9.0811 | 0.0000 | 1.0000 | 12.7444 | 7.1017 |

Position = Sungsan(point), Ftime = + 031 h, Total freedom = 177, Radj = 21.94

| P_ID | Pname | Coefficient | STD_error | T-Value | P-Value | VIF | SD | MEAN |
|---|---|---|---|---|---|---|---|---|
| 0 | INTERCEPT | 3.31086 | | | | | | |
| 1 | WS80m | 0.50404 | 0.0707 | 7.1248 | 0.0000 | 1.0000 | 11.8371 | 6.9191 |

Position = Sungsan(point), Ftime = + 032 h, Total freedom = 180, Radj = 41.63

| P_ID | Pname | Coefficient | STD_error | T-Value | P-Value | VIF | SD | MEAN |
|---|---|---|---|---|---|---|---|---|
| 0 | INTERCEPT | 1.75605 | | | | | | |
| 1 | WS80m | 0.74664 | 0.0656 | 11.3743 | 0.0000 | 1.0000 | 13.8587 | 7.3287 |

Position = Sungsan(point), Ftime = + 033 h, Total freedom = 180, Radj = 40.12

| P_ID | Pname | Coefficient | STD_error | T-Value | P-Value | VIF | SD | MEAN |
|---|---|---|---|---|---|---|---|---|
| 0 | INTERCEPT | 2.10973 | | | | | | |
| 1 | WS80m | 0.66880 | 0.0607 | 11.0265 | 0.0000 | 1.0000 | 13.2469 | 7.3702 |

Position = Sungsan(point), Ftime = + 034 h, Total freedom = 178, Radj = 34.01

| P_ID | Pname | Coefficient | STD_error | T-Value | P-Value | VIF | SD | MEAN |
|---|---|---|---|---|---|---|---|---|
| 0 | INTERCEPT | 2.62219 | | | | | | |
| 1 | WS80m | 0.60734 | 0.0631 | 9.6309 | 0.0000 | 1.0000 | 13.1187 | 7.4480 |

Position = Sungsan(point), Ftime = + 035 h, Total freedom = 177, Radj = 44.09

| P_ID | Pname | Coefficient | STD_error | T-Value | P-Value | VIF | SD | MEAN |
|---|---|---|---|---|---|---|---|---|
| 0 | INTERCEPT | 1.95871 | | | | | | |
| 1 | WS80m | 0.68115 | 0.0575 | 11.8556 | 0.0000 | 1.0000 | 12.3167 | 7.4994 |

Position = Sungsan(point), Ftime = + 036 h, Total freedom = 177, Radj = 38.78

| P_ID | Pname | Coefficient | STD_error | T-Value | P-Value | VIF | SD | MEAN |
|---|---|---|---|---|---|---|---|---|
| 0 | INTERCEPT | 2.58051 | | | | | | |
| 1 | WS80m | 0.61686 | 0.0580 | 10.6354 | 0.0000 | 1.0000 | 12.7555 | 7.5073 |

Position = Sungsan(point), Ftime = + 037 h, Total freedom = 175, Radj = 33.69

| P_ID | Pname | Coefficient | STD_error | T-Value | P-Value | VIF | SD | MEAN |
|---|---|---|---|---|---|---|---|---|
| 0 | INTERCEPT | 3.11851 | | | | | | |
| 1 | WS80m | 0.54134 | 0.0571 | 9.4831 | 0.0000 | 1.0000 | 10.7297 | 7.3273 |

Position = Sungsan(point), Ftime = + 038 h, Total freedom = 174, Radj = 35.47

| P_ID | Pname | Coefficient | STD_error | T-Value | P-Value | VIF | SD | MEAN |
|---|---|---|---|---|---|---|---|---|
| 0 | INTERCEPT | 2.94327 | | | | | | |
| 1 | WS80m | 0.58966 | 0.0600 | 9.8299 | 0.0000 | 1.0000 | 13.0286 | 7.3440 |

Position = Sungsan(point), Ftime = + 039 h, Total freedom = 171, Radj = 31.34

| P_ID | Pname | Coefficient | STD_error | T-Value | P-Value | VIF | SD | MEAN |
|---|---|---|---|---|---|---|---|---|
| 0 | INTERCEPT | 3.35035 | | | | | | |
| 1 | WS80m | 0.57126 | 0.0643 | 8.8910 | 0.0000 | 1.0000 | 12.4919 | 7.3674 |

Position = Sungsan(point), Ftime = + 040 h, Total freedom = 176, Radj = 28.33

| P_ID | Pname | Coefficient | STD_error | T-Value | P-Value | VIF | SD | MEAN |
|---|---|---|---|---|---|---|---|---|
| 0 | INTERCEPT | 3.27261 | | | | | | |
| 1 | WS80m | 0.56858 | 0.0677 | 8.3999 | 0.0000 | 1.0000 | 13.5087 | 7.2938 |

Position = Sungsan(point), Ftime = + 041 h, Total freedom = 174, Radj = 24.96

| P_ID | Pname | Coefficient | STD_error | T-Value | P-Value | VIF | SD | MEAN |
|---|---|---|---|---|---|---|---|---|
| 0 | INTERCEPT | 3.03076 | | | | | | |
| 1 | WS80m | 0.52390 | 0.0683 | 7.6730 | 0.0000 | 1.0000 | 13.4965 | 6.8520 |

Position = Sungsan(point), Ftime = + 042 h, Total freedom = 174, Radj = 32.53

| P_ID | Pname | Coefficient | STD_error | T-Value | P-Value | VIF | SD | MEAN |
|---|---|---|---|---|---|---|---|---|
| 0 | INTERCEPT | 2.72889 | | | | | | |
| 1 | WS80m | 0.54724 | 0.0594 | 9.2142 | 0.0000 | 1.0000 | 12.2582 | 6.7777 |

---

Position = Sungsan(point), Ftime = + 043 h, Total freedom = 179, Radj = 28.77

---

| P_ID | Pname | Coefficient | STD_error | T-Value | P-Value | VIF | SD | MEAN |
|---|---|---|---|---|---|---|---|---|
| 0 | INTERCEPT | 3.05545 | | | | | | |
| 1 | WS80m | 0.52978 | 0.0619 | 8.5613 | 0.0000 | 1.0000 | 13.3206 | 7.0989 |

---

Position = Sungsan(point), Ftime = + 044 h, Total freedom = 179, Radj = 28.45

---

| P_ID | Pname | Coefficient | STD_error | T-Value | P-Value | VIF | SD | MEAN |
|---|---|---|---|---|---|---|---|---|
| 0 | INTERCEPT | 3.16377 | | | | | | |
| 1 | WS80m | 0.50548 | 0.0595 | 8.4951 | 0.0000 | 1.0000 | 12.7796 | 6.9667 |

---

Position = Sungsan(point), Ftime = + 045 h, Total freedom = 179, Radj = 22.94

---

| P_ID | Pname | Coefficient | STD_error | T-Value | P-Value | VIF | SD | MEAN |
|---|---|---|---|---|---|---|---|---|
| 0 | INTERCEPT | 3.18062 | | | | | | |
| 1 | WS80m | 0.49018 | 0.0665 | 7.3674 | 0.0000 | 1.0000 | 12.7257 | 6.9517 |

---

Position = Sungsan(point), Ftime = + 046 h, Total freedom = 180, Radj = 17.51

---

| P_ID | Pname | Coefficient | STD_error | T-Value | P-Value | VIF | SD | MEAN |
|---|---|---|---|---|---|---|---|---|
| 0 | INTERCEPT | 3.94786 | | | | | | |
| 1 | WS80m | 0.39466 | 0.0630 | 6.2607 | 0.0000 | 1.0000 | 12.0765 | 6.9149 |

---

Position = Sungsan(point), Ftime = + 047 h, Total freedom = 179, Radj = 28.75

---

| P_ID | Pname | Coefficient | STD_error | T-Value | P-Value | VIF | SD | MEAN |
|---|---|---|---|---|---|---|---|---|
| 0 | INTERCEPT | 3.00851 | | | | | | |
| 1 | WS80m | 0.52562 | 0.0614 | 8.5575 | 0.0000 | 1.0000 | 11.8754 | 6.8956 |

---

Position = Sungsan(point), Ftime = + 048 h, Total freedom = 177, Radj = 24.59

---

| P_ID | Pname | Coefficient | STD_error | T-Value | P-Value | VIF | SD | MEAN |
|---|---|---|---|---|---|---|---|---|
| 0 | INTERCEPT | 3.40755 | | | | | | |
| 1 | WS80m | 0.47153 | 0.0615 | 7.6629 | 0.0000 | 1.0000 | 11.1758 | 6.7197 |

---

Position = Sungsan(point), Ftime = + 049 h, Total freedom = 179, Radj = 32.41

---

| P_ID | Pname | Coefficient | STD_error | T-Value | P-Value | VIF | SD | MEAN |
|---|---|---|---|---|---|---|---|---|
| 0 | INTERCEPT | 2.79644 | | | | | | |
| 1 | WS80m | 0.60607 | 0.0650 | 9.3180 | 0.0000 | 1.0000 | 12.9852 | 7.1089 |

---

Position = Sungsan(point), Ftime = + 050 h, Total freedom = 180, Radj = 34.73

---

| P_ID | Pname | Coefficient | STD_error | T-Value | P-Value | VIF | SD | MEAN |
|---|---|---|---|---|---|---|---|---|
| 0 | INTERCEPT | 2.36320 | | | | | | |
| 1 | WS80m | 0.63266 | 0.0643 | 9.8381 | 0.0000 | 1.0000 | 13.5405 | 7.0812 |

---

Position = Sungsan(point), Ftime = + 051 h, Total freedom = 176, Radj = 17.23

---

| P_ID | Pname | Coefficient | STD_error | T-Value | P-Value | VIF | SD | MEAN |
|---|---|---|---|---|---|---|---|---|
| 0 | INTERCEPT | 3.65899 | | | | | | |
| 1 | WS80m | 0.44432 | 0.0724 | 6.1346 | 0.0000 | 1.0000 | 12.8726 | 6.9209 |

---

Position = Sungsan(point), Ftime = + 052 h, Total freedom = 177, Radj = 18.32

---

| P_ID | Pname | Coefficient | STD_error | T-Value | P-Value | VIF | SD | MEAN |
|---|---|---|---|---|---|---|---|---|
| 0 | INTERCEPT | 3.78745 | | | | | | |
| 1 | WS80m | 0.43427 | 0.0681 | 6.3805 | 0.0000 | 1.0000 | 12.8434 | 6.9787 |

---

Position = Sungsan(point), Ftime = + 053 h, Total freedom = 178, Radj = 17.67

---

| P_ID | Pname | Coefficient | STD_error | T-Value | P-Value | VIF | SD | MEAN |
|---|---|---|---|---|---|---|---|---|
| 0 | INTERCEPT | 4.12948 | | | | | | |

1 WS80m 0.38730 0.0619 6.2604 0.0000 1.0000 11.2441 6.8603

---

Position = Sungsan(point), Ftime = + 054 h, Total freedom = 180, Radj = 25.77

---

| P_ID | Pname | Coefficient | STD_error | T-Value | P-Value | VIF | SD | MEAN |
|---|---|---|---|---|---|---|---|---|
| 0 | INTERCEPT | 3.45522 | | | | | | |
| 1 | WS80m | 0.49135 | 0.0617 | 7.9682 | 0.0000 | 1.0000 | 12.7236 | 6.9934 |

---

Position = Sungsan(point), Ftime = + 055 h, Total freedom = 177, Radj = 27.25

---

| P_ID | Pname | Coefficient | STD_error | T-Value | P-Value | VIF | SD | MEAN |
|---|---|---|---|---|---|---|---|---|
| 0 | INTERCEPT | 3.05511 | | | | | | |
| 1 | WS80m | 0.50556 | 0.0616 | 8.2031 | 0.0000 | 1.0000 | 11.8815 | 6.8225 |

---

Position = Sungsan(point), Ftime = + 056 h, Total freedom = 180, Radj = 32.24

---

| P_ID | Pname | Coefficient | STD_error | T-Value | P-Value | VIF | SD | MEAN |
|---|---|---|---|---|---|---|---|---|
| 0 | INTERCEPT | 2.46116 | | | | | | |
| 1 | WS80m | 0.63402 | 0.0681 | 9.3086 | 0.0000 | 1.0000 | 13.8969 | 7.2635 |

---

Position = Sungsan(point), Ftime = + 057 h, Total freedom = 180, Radj = 42.32

---

| P_ID | Pname | Coefficient | STD_error | T-Value | P-Value | VIF | SD | MEAN |
|---|---|---|---|---|---|---|---|---|
| 0 | INTERCEPT | 1.81033 | | | | | | |
| 1 | WS80m | 0.69343 | 0.0601 | 11.5366 | 0.0000 | 1.0000 | 13.3040 | 7.3155 |

---

Position = Sungsan(point), Ftime = + 058 h, Total freedom = 179, Radj = 36.54

---

| P_ID | Pname | Coefficient | STD_error | T-Value | P-Value | VIF | SD | MEAN |
|---|---|---|---|---|---|---|---|---|
| 0 | INTERCEPT | 2.18783 | | | | | | |
| 1 | WS80m | 0.64801 | 0.0635 | 10.2013 | 0.0000 | 1.0000 | 13.0629 | 7.4072 |

---

Position = Sungsan(point), Ftime = + 059 h, Total freedom = 178, Radj = 36.43

---

| P_ID | Pname | Coefficient | STD_error | T-Value | P-Value | VIF | SD | MEAN |
|---|---|---|---|---|---|---|---|---|
| 0 | INTERCEPT | 2.16800 | | | | | | |
| 1 | WS80m | 0.65344 | 0.0644 | 10.1491 | 0.0000 | 1.0000 | 12.2553 | 7.4458 |

---

Position = Sungsan(point), Ftime = + 060 h, Total freedom = 178, Radj = 36.97

---

| P_ID | Pname | Coefficient | STD_error | T-Value | P-Value | VIF | SD | MEAN |
|---|---|---|---|---|---|---|---|---|
| 0 | INTERCEPT | 2.48297 | | | | | | |
| 1 | WS80m | 0.62935 | 0.0613 | 10.2671 | 0.0000 | 1.0000 | 12.5896 | 7.4575 |

---

Position = Sungsan(point), Ftime = + 061 h, Total freedom = 176, Radj = 26.48

---

| P_ID | Pname | Coefficient | STD_error | T-Value | P-Value | VIF | SD | MEAN |
|---|---|---|---|---|---|---|---|---|
| 0 | INTERCEPT | 3.57235 | | | | | | |
| 1 | WS80m | 0.47048 | 0.0586 | 8.0246 | 0.0000 | 1.0000 | 10.5915 | 7.2768 |

---

Position = Sungsan(point), Ftime = + 062 h, Total freedom = 175, Radj = 32.57

---

| P_ID | Pname | Coefficient | STD_error | T-Value | P-Value | VIF | SD | MEAN |
|---|---|---|---|---|---|---|---|---|
| 0 | INTERCEPT | 2.87528 | | | | | | |
| 1 | WS80m | 0.56740 | 0.0613 | 9.2489 | 0.0000 | 1.0000 | 12.8078 | 7.2761 |

---

Position = Sungsan(point), Ftime = + 063 h, Total freedom = 172, Radj = 34.19

---

| P_ID | Pname | Coefficient | STD_error | T-Value | P-Value | VIF | SD | MEAN |
|---|---|---|---|---|---|---|---|---|
| 0 | INTERCEPT | 3.08895 | | | | | | |
| 1 | WS80m | 0.56509 | 0.0594 | 9.5059 | 0.0000 | 1.0000 | 12.4279 | 7.2896 |

---

Position = Sungsan(point), Ftime = + 064 h, Total freedom = 176, Radj = 22.60

---

| P_ID | Pname | Coefficient | STD_error | T-Value | P-Value | VIF | SD | MEAN |
|---|---|---|---|---|---|---|---|---|

0 INTERCEPT 3.69683
1 WS80m 0.49329 0.0682 7.2374 0.0000 1.0000 13.5544 7.1808

---

Position = Sungsan(point), Ftime = + 065 h, Total freedom = 174, Radj = 30.41

---

P_ID Pname Coefficient STD_error T-Value P-Value VIF SD MEAN
0 INTERCEPT 2.47510
1 WS80m 0.58172 0.0663 8.7779 0.0000 1.0000 13.5870 6.7360

---

Position = Sungsan(point), Ftime = + 066 h, Total freedom = 174, Radj = 26.76

---

P_ID Pname Coefficient STD_error T-Value P-Value VIF SD MEAN
0 INTERCEPT 2.55545
1 WS80m 0.55298 0.0688 8.0353 0.0000 1.0000 12.2800 6.6640

---

Position = Sungsan(point), Ftime = + 067 h, Total freedom = 179, Radj = 22.53

---

P_ID Pname Coefficient STD_error T-Value P-Value VIF SD MEAN
0 INTERCEPT 3.32121
1 WS80m 0.49706 0.0682 7.2845 0.0000 1.0000 13.4438 7.0161

---

Position = Sungsan(point), Ftime = + 068 h, Total freedom = 179, Radj = 19.64

---

P_ID Pname Coefficient STD_error T-Value P-Value VIF SD MEAN
0 INTERCEPT 3.59862
1 WS80m 0.43213 0.0646 6.6895 0.0000 1.0000 12.7583 6.8572

---

Position = Sungsan(point), Ftime = + 069 h, Total freedom = 179, Radj = 16.87

---

P_ID Pname Coefficient STD_error T-Value P-Value VIF SD MEAN
0 INTERCEPT 3.89369
1 WS80m 0.38757 0.0634 6.1105 0.0000 1.0000 12.7312 6.8339

---

Position = Sungsan(point), Ftime = + 070 h, Total freedom = 180, Radj = 17.63

---

P_ID Pname Coefficient STD_error T-Value P-Value VIF SD MEAN
0 INTERCEPT 3.97044
1 WS80m 0.37600 0.0598 6.2863 0.0000 1.0000 12.0842 6.7856

---

Position = Sungsan(point), Ftime = + 071 h, Total freedom = 179, Radj = 21.26

---

P_ID Pname Coefficient STD_error T-Value P-Value VIF SD MEAN
0 INTERCEPT 3.92949
1 WS80m 0.39426 0.0561 7.0237 0.0000 1.0000 11.8971 6.8556

---

Position = Sungsan(point), Ftime = + 072 h, Total freedom = 177, Radj = 18.30

---

P_ID Pname Coefficient STD_error T-Value P-Value VIF SD MEAN
0 INTERCEPT 3.95811
1 WS80m 0.36299 0.0569 6.3758 0.0000 1.0000 11.3532 6.6511

# 감사의 글

이 논문을 완성하기까지 많은 지도와 격려를 해주신 허종철 교수님께 감사의 말씀을 드립니다. 특히, 풍력이 무엇이고, 이를 기상과 어떻게 연관시켜 이해해야 하는지에 대한 개념을 깨우치게 해주신 교수님 감사합니다. 풍력이라는 학문 자체로써의 호기심을 가지게 해주시고, 풍력발전과의 관계에 대해 많은 것을 배울 수 있었습니다.

밤 늦은 시간까지 연구에 몰두하시면서 늘 격려를 해주신 고경남 교수님 감사합니다. 교수님께서 말씀하신 기본에 충실한 연구자가 될 수 있도록 더욱 정진하겠습니다.

지난 대학원생활 동안 공학이라는 새로운 분야에 도전한 저에게 풍성한 공학적 사고와 수준 높은 지식을 일깨워 주신 권기린 교수님, 김귀식 교수님, 현명택 교수님, 정동원 교수님, 박윤철 교수님께 감사의 말씀을 드립니다.

논문의 질을 보다 높일 수 있도록 많은 질타와 토론을 이끌어주신 문일주 교수님, 김동호 박사님 감사합니다. 이 논문을 바탕으로 보다 성장한 연구자가 될 수 있도록 노력하겠습니다.

오랜 벗이자 마음의 길잡이 역할을 해주신 김경보 박사님, 박사님의 격려가 이곳까지 올 수 있는 큰 힘이 되었습니다. 감사합니다.

늦은 밤까지 연구에 몰두하며 실험실을 집 삼은 수영, 수많은 자료 부탁에도 즉시 도와준 현우 고맙습니다. 자주 찾아가지 못했지만 늘 반갑게 맞아준 실험실 후배님들 늘 감사했습니다.

직장과 학업을 병행하면서 조금은 직장에 소홀한 부분도 많았었는데 묵묵히 지켜봐주시고, 따뜻한 미소를 보내주신 박훈 과장님, 과장님의 배려가 있어 이 논문이 결실을 볼 수 있었습니다. 감사합니다.

한결같이 '잘 할 수 있을꺼야...' 긍정의 힘을 실어준 수치모델관리관실 직원 모두에게 감사드립니다. 이제는 좀 더 본연의 업무를 충실히 하도록 하겠습니다.

수 많은 주말과, 밤을 빼앗겨도 언제나 격려와 따뜻한 마음으로 든든한 지원을 해준 나의 사랑하는 아내 김옥현, 사랑하는 딸 민채, 민서 고마워 그리고 사랑해.

2013. 6. 27. 늦은밤